UNDERSTANDING STRUCTURE-MECHANICAL PROPERTY RELATIONSHIP OF BREAST CANCER CELLS

Li Qingsen

(B.Eng & M.Eng., HUST)

A THESIS SUBMITTED

FOR THE DEGREE OF DOCTOR OF PHILOSOPHY

DEPARTMENT OF MECHANICAL ENGINEERING

NATIONAL UNIVERSITY OF SINGAPORE

2009

Acknowledgements

Table of Contents

Summary

Cancer has long been one of the leading causes of death in the industrial world. The main reason for its high mortality is due to inefficient early detection which results in the spread of cancer cells to other distant sites in the body, via a process known as metastasis. Since metastasis involves invasive and physical movements of cancer cells through the extra-cellular matrix and circulation system, cell mechanics has been extended to study cancer from a mechanistic perspective in order to better understand the pathophysiology of cancer. The potential applications of cell mechanics study on cancer not only include early cancer detection and diagnosis, but also better understanding of the underlying mechanisms of cancer metastasis and these can lead to better strategies in treating cancer.

In view of the different physiological states cancer cells can undergo including being adherent and in suspension, we studied cancer cells in these two conditions. Firstly, A microfluidic device was designed to mimic cancer cells traversing capillaries and investigate their overall mechanical behavior and the role of nucleus in large deformation. Secondly, to further understand the structure-property relationship of cancer cells, micropipette was used to specifically probe the near surface mechanical properties , which was related to the underlying actin cortex, of suspended breast cancer cells. AFM indentation was used to probe the near surface mechanical properties of adherent breast cancer cells. The nucleus as an important structural component was first characterized in the context of cancer cells in this study. The corresponding cytoskeletal (actin) and nuclear structure was then investigated using confocal microscopy. Elastic moduli of both cell surface (including cytoskeleton) and isolated nucleus of non-malignant breast epithelial cells (MCF-10A) were twice

higher than their malignant counterparts (MCF-7), which was due to the change in corresponding structures. The similar elastic modulus of the isolated nuclei and that of the cell suggests that other than cytoskeleton, nucleus also contributes to the overall cellular mechanical properties.

This study gives us a better understanding about the structure-property relationship of cell mechanics in the context of cancer cells. It demonstrates that besides cytoskeleton, nucleus also contributes to cancer cell mechanics. The potential application of cancer cell and nuclear mechanics is that it can possibly serve as another biomarker for cancer detection and diagnosis.

List of Tables

List of Figures

List of Symbols

CD — AFM cantilever deflection

D — Initial diameter of the cell

E — Young's modulus

EI — Elongation index

F — Indentation force

g — Gravitational acceleration

G — Shear modulus

h — Height difference

l — Elongated length of a deformed cell in the microchannel

L — Distance travelled by the cell

L_P — Projection length

k — Spring constant of AFM cantilever

R — Radius of the spherical bead

RID — Relative indentation depth

RID_0 — X coordinates of the contact point

Chapter 1 Introduction

Cancer has long been a life threatening disease with high mortality. The main reason for its high mortality is due to the inefficient early detection which results in the spread of cancer cells and the formation of new tumors in the other distant sites in the body. This process called metastasis involves invasive and physical movements of cancer cells through the extra-cellular matrix and circulation system, therefore cell mechanics has been applied to study cancer from a mechanistic perspective in order to better understand the pathophysiology of cancer. Understanding of cancer cell mechanics not only can help early cancer detection and diagnosis, but also give insight of the underlying mechanisms of cancer metastasis, which can lead to better strategies in treating cancer.

In this chapter, we will first explain the close connections between cancer metastasis and cell mechanics. In view of the importance of structure-property relationship of cancer cell mechanics, we will then review the components and structures of cells including cytoskeleton, nucleus and their connections. To take a step further, we will specifically review the nuclear structure of cancer cells and its deviation from normal nucleus. Finally, we will discuss besides cytoskeleton why we study nuclear mechanics in the context of cancer cells. Though the contribution of cytoskeleton to cell mechanics has been extensively studied, but not for nucleus, we believe that nucleus also plays an important role in overall cancer cell mechanics, especially in the context of cancer metastasis.

1.1 Cancer and metastasis

Cancer is a class of diseases characterized by the unrestricted proliferation of abnormal cells and their ability to invade healthy body tissues and destroy them (limLee and Lim 2007). Cancer has long been one of the leading causes of death in the world and is presently responsible for about 25% of all deaths (Jemal, Murray et al. 2005). It is estimated that there will be about 15 million new cancer cases annually by 2020 worldwide (Lee and Lim 2007). For example, breast cancer is most common for female, as one in every eight woman develops breast cancer at some stage of their lives, and it causes about 15% of cancer deaths in women (Jemal, Murray et al. 2005).

The reason for the high mortality of cancer is the lack of early detection which results in its spread to other distant sites in the body, via a process known as metastasis, which is the major cause of cancer related death. In the case of breast cancer diagnosis, the conventional mammogram has a size detection limit of only 3mm (Simon, Ibrahim et al. 2002), while other standard examinations for clinical diagnosis, like palpation, ultrasonography and needle biopsy, do not detect abnormal cell growth efficiently until they have become malignant or have metastasized (Du, Cheng et al. 2007). Early detection of cancer before metastasis can make cancer easier to be treated successfully by excision since it is only restricted within a local region of the body. On the other hand, the chance for treating cancer which has metastasized is much lower.

Metastasis, which is responsible for about 90% of death due to solid tumors (Gupta and Massague 2006), is a process involving the dissemination of cancer cells from a primary tumor to other sites in the body leading to the formation of new tumors at

those sites (Chambers, Groom et al. 2002). The metastasis process consists of several important steps as illustrated in Fig. 1.1:
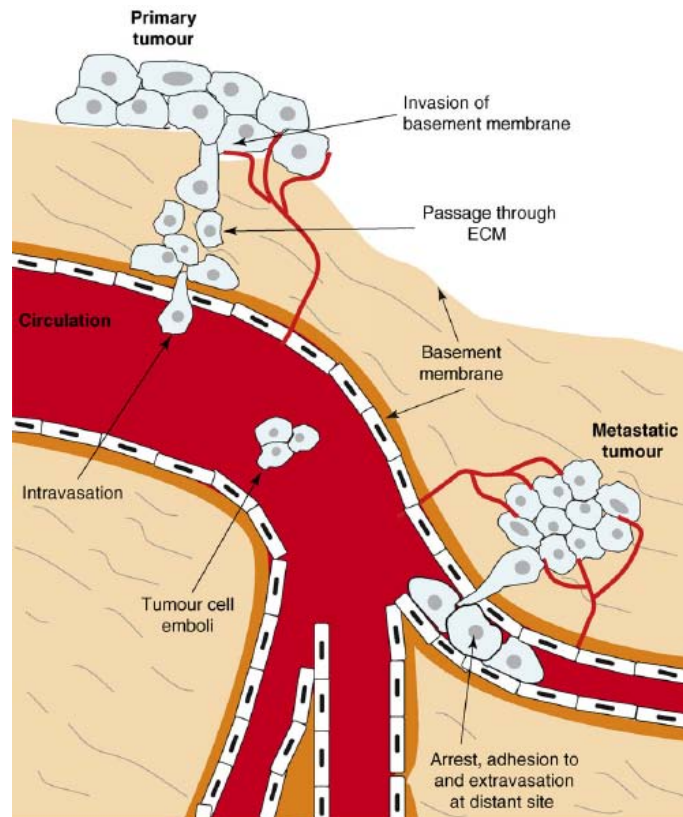
Fig. 1.1 Schematic diagram of cancer metastasis process showing the spread of cancer cells from a primary tumor to a distant site (Lee and Lim 2007).

1. Intravasation: cancer cells leave the primary tumor and enter into the circulatory system by infiltrating into the blood vessel directly or through the lymphatic system.

2. Transportation and arrest: cancer cells that survive in the blood vessel travel to other parts of the body until they are arrested in a particular region of the circulatory system.

3. Extravasation: cancer cells invade into the surrounding tissue from the blood vessel where they are arrested.

4. Growth of new tumor: cancer cells survive in the new environment and initiate micrometastasis and then grow into new tumor accompanied by the development of new blood capillaries (angiogenesis).

As we can see in the whole process of cancer metastasis, there is evidently a strong relation with mechanics. As cancer cells break away from the primary tumor, migrate through the extra-cellular matrix (ECM), infiltrate into the blood vessel, flow along in the blood stream, get arrested in a new position within the circulatory system, squeeze into the tissue and form a new tumor, they constantly exert mechanical force to the surrounding tissues or undergoes deformation when subjected to physiological flow conditions. Mechanics dominates the whole process, especially as cancer cells need to traverse through narrow blood capillaries and endothelial barriers in the circulatory system or tissue.

In order to effectively combat against cancer, we not only have to find better and reliable methods for early detection, but also better understand the underlying mechanisms of cancer metastasis in order to develop new strategies to treat cancer. It is therefore necessary to investigate the disease from different aspects, and in our case we will do so from a mechanistic perspective due to its importance in cancer metastasis.

1.2 Importance of mechanics in cancer metastasis

The details of the metastasis process still remains largely unknown and is currently a hot topic for many researchers from different fields (Ding, Sunamura et al. 2001).

The mechanical behavior of cancer cells is important as mechanical factors are known to play an important role in influencing the metastatic process (Chambers, Groom et

al. 2002). Mechanical factors such as elasticity, cell adhesion and rheology affect the initial outcome of cancer cells after they have detached from a primary tumor site. For example, when normal cells become cancerous and metastatic, they are known to possess an increased propensity to migrate across the basal membrane and the endothelium to make their way into the circulatory system. Also, the efficient arrest of most circulating cancer cells at a secondary site is dependent on the relative sizes of the cancer cells and capillaries (Chambers, Groom et al. 2002). Altered genetic composition and protein expression in cancers are responsible for changes in intracellular structural and cellular deformability (Fuchs and Weber 1994; Suresh, Spatz et al. 2005). This not only affects cell motility, adhesion and interaction but also cell growth and division (Chen, Mrksich et al. 1997; Boudreau and Bissell 1998; Huang and Ingber 1999; Alberts, Johnson et al. 2002; Lodish, Berk et al. 2003).

The arrest of cancer cells in the circulatory system is thought to be an essential step in metastasis. Some researchers proposed that this arrest is mainly due to mechanical entrapment of tumor cells in the microvasculature (Sugarbaker 1981; Barberaguillem, Alonsovarona et al. 1989; Morris, Macdonald et al. 1993; Cameron, Schmidt et al. 2000; Ding, Sunamura et al. 2001; Mook, Van Marle et al. 2003). On the other hand, it is also reported that this process can be mediated by the inducible adhesion between cancer cells and specific endothelium (Enns, Gassmann et al. 2004; Gassmann, Enns et al. 2004; Krishnan, Bane et al. 2005).

Ding et al. used *in vivo* microscopy to study the early events of liver metastasis. They confirmed that mechanical entrapment of a solid tumor cell promoted liver metastasis while no detectable adhesion molecules were involved. At the same time, they also found that lymphoma cells promoted liver metastasis through the arrest of P-selectin,

an adhesion molecule-mediated pathway (Ding, Sunamura et al. 2001). In addition, Hart et al. proposed that mechanical entrapment of cancer cells in capillaries and the organ-determined modulation of tumor growth are two mechanisms that regulate the specificity of metastatic patterns of transplantable rodent tumors (Hart 1982).

An interesting phenomena observed by Gabor showed that mechanical trauma can induce a state of dormancy in cancer cells (Gabor and Weiss 1985). This offers a possible explanation for situations in which metastasis occurred years after an apparent successful primary tumor treatment (Chambers, Groom et al. 2002). This also indicates that mechanical deformation or entrapment may affect the outcome of those types of metastasis.

However, other studies have shown that mechanical factors alone are not the only ones that affect the metastasis process (Cameron, Schmidt et al. 2000). Generally, three mechanisms called mechanical, specific adhesion and organ-determined modulation ("seed and soil") all seem to contribute to this process and the mechanisms may be different for each specific type of cancer. However, the relative contribution of the three mechanisms may vary for different types of tumor (Kieran and Longenecker 1983). And mechanical entrapment may play an important role in contributing to the initial step.

As cancer metastasis is a complex process of a mechanical nature involving interactions of cancer cells with their surroundings, it is important to study metastasis from a mechanical point of view since this may shed light to understand the underlying mechanism. Cell mechanics, which investigates how cells sense, respond to and generate mechanical forces involved in different cellular functions, is of great

importance in understanding physiology and pathology. At the cellular level, we first

need to understand the structure-property relation of cells.

1.3 Structure and mechanical properties of cancer cells

Before we attempt to understand the structure-property relationship of cancer cells,

we will first take a look at the structure of a eukaryotic cell.
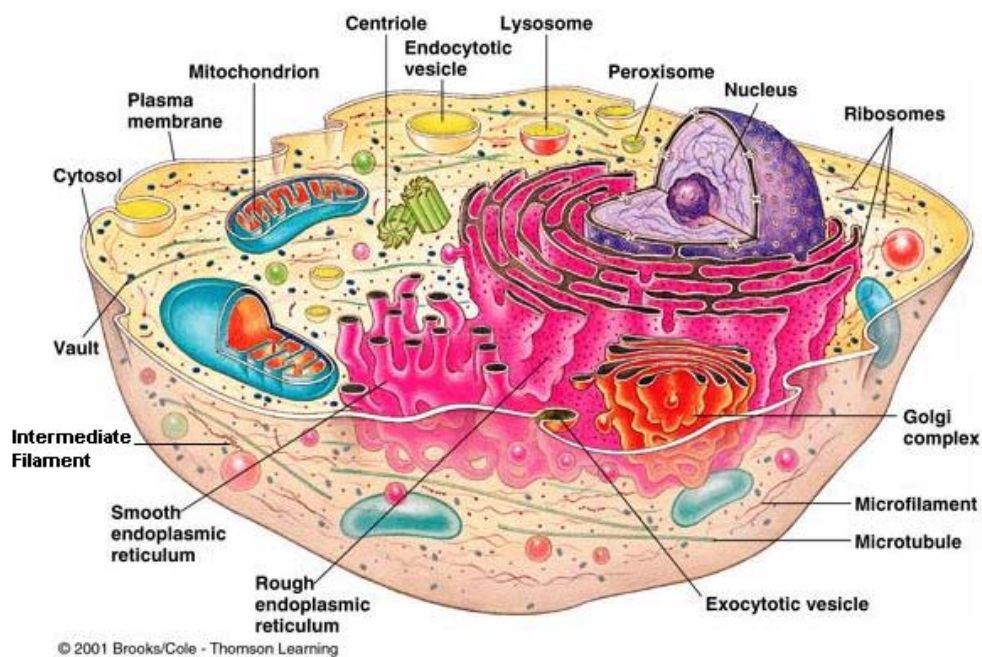
Fig. 1.2 Schematic diagram of the structure of a eukaryotic cell (adapted from http://www.colorado.edu/kines/Class/IPHY3430-200/image/ShHP40201.jpg).

A cell, as the basic unit of life, is composed of a mass of organelles with different

functions enclosed by the plasma membrane. From an engineering point of view, the

cell can be treated as a delicately "designed" machine with complicated functional

materials. The structural components of this "machine" are the plasma membrane and

the underlying cytoskeleton. The plasma membrane is a semi-permeable lipid bilayer

which surrounds the whole cell and separates it from the extracellular environment.

The cytoskeleton, which consists of microfilaments, intermediate filaments and

microtubules, is a dynamic structure which maintains the integrity of the cell and

enables its motility. It plays important roles in cellular division and any form of communication with the environment. Fig. 1.2 shows the complex organization of functional and structural components of a eukaryotic cell.

We take a close look at the structural components and their organization inside the cell. As shown in Fig. 1.3, the integrity of the cell, which can respond to mechanical stresses appropriately, is based on a large network of physically connected structural components starting from the ECM, via adhesion molecules and cytoskeleton to the nucleus (Houben, Ramaekers et al. 2007). This physical connection may serve as a channel to transmit the mechanical signals (stress and strain) received by the adhesion molecule from outside of the cell directly to the nucleus and regulate gene expression, via the process called mechanotransduction. Moreover, nucleus plays a pivotal role in regulating the cytoskeletal and adhesion structures in the cell by connections between nuclear structure and cytoskeleton through linker protein like Nesprins and SUN-proteins (Houben, Ramaekers et al. 2007).
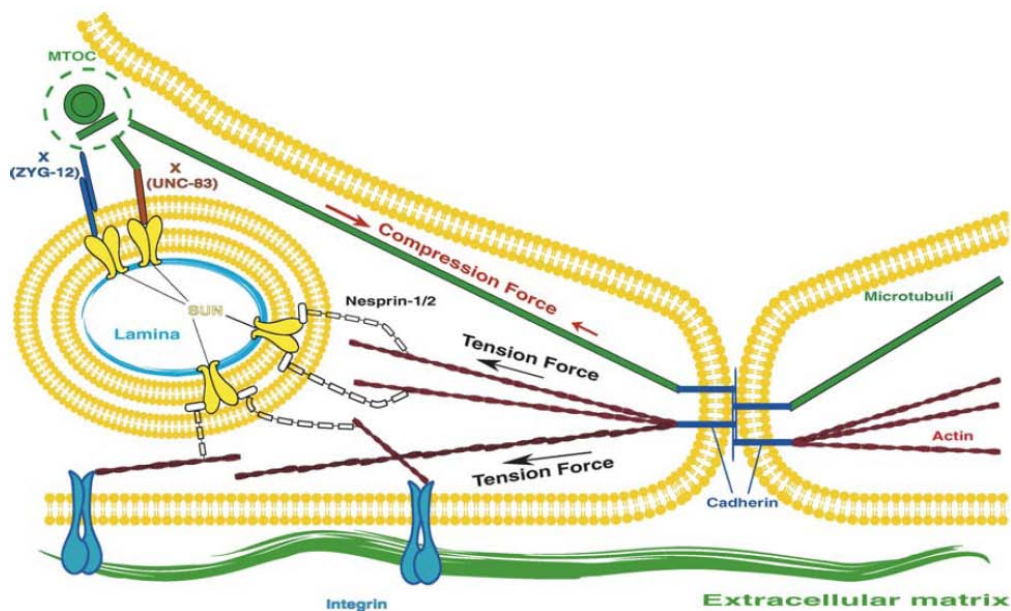
Fig. 1.3 Schematic diagram of the integral network of a cell responding to mechanical loading (Houben, Ramaekers et al. 2007).

Mechanical properties of cancer cells have been studied using different biomechanical techniques like micropipette aspiration, atomic force microscopy (AFM) and optical stretcher, and it was found that most cancer cells are more deformable than their corresponding normal cells (Ward, Li et al. 1991; Thoumine and Ott 1997; Lekka, Laidler et al. 1999; Lekka, Lekki et al. 1999; Park, Koch et al. 2005; Suresh, Spatz et al. 2005). Moreover, there seems to be a direct correlation between an increase in deformability and the progression of a transformed phenotype from a non-malignant cell line into a malignant, and metastatic cell line, which can effectively be used as a biomarker to detect cancer (Ward, Li et al. 1991; Guck, Schinkinger et al. 2005).

Some evidence has shown that the change in the deformability of cells as they transform from being non-malignant to malignant is the result of a change in the concentration and structure of cytoskeleton, which may also affect metastasis when cancer cells migrate through the ECM and endothelial barriers (Ward, Li et al. 1991; Thoumine and Ott 1997; Guck, Schinkinger et al. 2005; Suresh, Spatz et al. 2005; Suresh 2007). As a cell progresses to the cancerous state, the amount of F-actin is reduced, which is also accompanied by a reconstruction in cytoskeleton . In fact, cytoskeletal changes can result in changes in the overall mechanical property of the cell and also changes in their cellular functions (Lincoln, Erickson et al. 2004). However, the underlying molecular mechanism causing this cytoskeletal change is not fully understood. Moreover, the change in structure and mechanical property of nucleus and its contribution to cell mechanics during malignant transformation is not well studied.

1.4 Nuclear structure of cancer cells

The nucleus is a major component of eukaryotic cells, which contains the chromosomes — the secret of life. Also, it is a site of major metabolic activities, including DNA replication, gene transcription, RNA processing and ribosome subunit maturation and assembly.

Moreover, structure and mechanical properties of the nucleus plays an important role in the overall cellular mechanical behavior and mechanotransduction, and one pathway shows that mechanical stress may regulate gene expression through direct physical connections starting from the ECM, via adhesion molecules and cytoskeleton to the nucleus (Vaziri, Lee et al. 2006). Therefore, any change in the nuclear structure can cause impaired nuclear mechanics and alter the mechanotransduction pathway leading to some diseases like Emery-Dreifuss muscular dystrophy (Lammerding and Lee 2005; Lammerding, Fong et al. 2006). So, the mechanical property of the nucleus is an important factor in the mechanotransduction pathway as it determines the nuclear shape and its response to external mechanical stimulus, which may in turn regulate the transport action and the expression of nucleic acids and consequently affecting cellular function.

Nucleus is separated from cytoplasm by a nuclear envelope. As shown in Fig. 1.4 (Stuurman, Heins et al. 1998), the nuclear envelope consists of an inner nuclear membrane (INM), an outer nuclear membrane (ONM, an extension of rough endoplasmic reticulum (ER)) and nuclear lamina (Prokocimer, Margalit et al. 2006). INM and ONM join at the nuclear pore complexes (NPC), which allow for nuclear-cytoplasmic transport. The nuclear lamina, which lies beneath the INM, is a dense network of lamins (lamin A/C and lamin B) plus lamin-associated proteins, which

plays an important role in supporting the nuclear structure, and also in organizing the nuclear envelope and chromatin (Vaziri and Mofrad 2007).
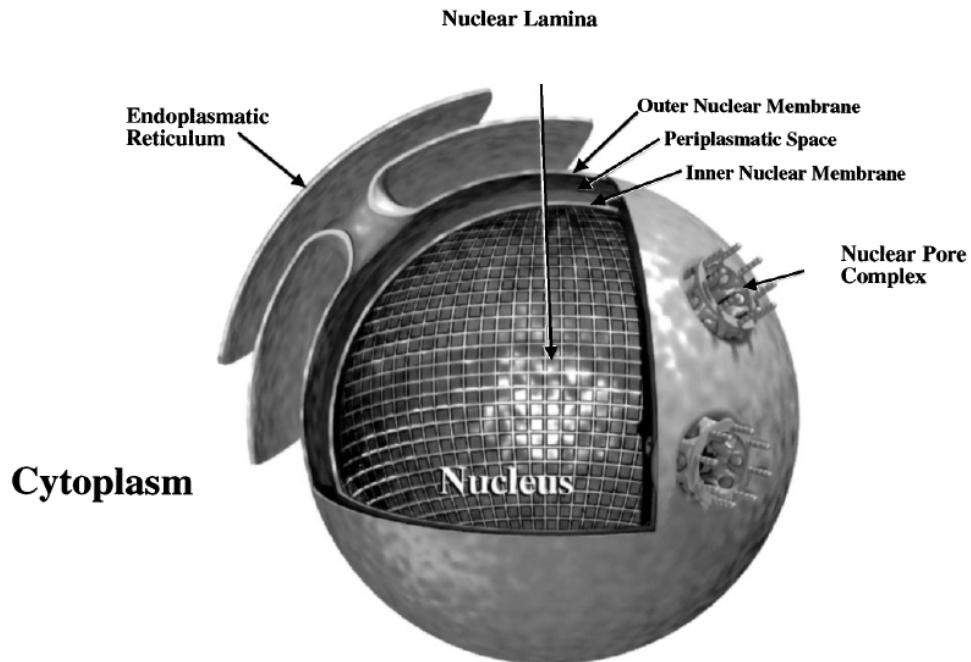
Fig. 1.4 Schematic diagram of the structure of a nucleus (Stuurman, Heins et al. 1998).

In the case of cancer cells, there is a dramatic change occurring in the nuclear architecture as they become malignant (Davie, Samuel et al. 1999; Spencer and Davie 2000). Some of the existing studies have already shown characteristic differences in nuclear architectures of cancer cells compared with normal cells as shown in Fig. 1.5, which affect nuclear size and shape and chromatin texture as shown in table 1.1. Changes in the nuclear structure and its corresponding mechanical property may reveal insights into the process of malignant transformation and may provide a basis for the development of new diagnostic tools and therapeutics (Zink, Fischer et al. 2004) .
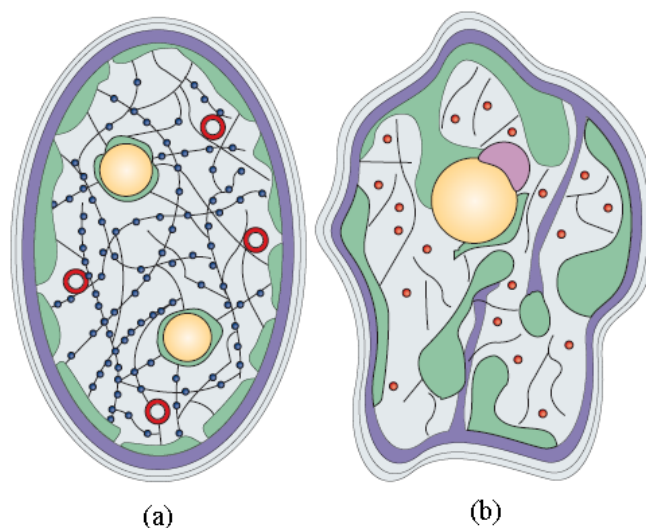
Fig. 1.5 Nuclear structures of (a) normal and (b) cancer cells (purple: lamina; green: heterochromatin; yellow: nucleoli) (Zink, Fischer et al. 2004).

Table 1.1 List showing some differences between the nucleus of normal and cancer cells

	Normal cells	Cancer cells
Nuclear shape	Regular and ellipsoid shape	Irregular and begin to fold
Heterochromatin	Fine layer	Coarse aggregate
Nucleoli	Smaller size or less, Number(1~3)	Larger size or increase in number

In the nuclear architecture, nuclear lamina is involved in many nuclear activities which are implicated in tumor formation including transcriptional activation, heterochromatin organization, senescence and apoptosis (Moss, Krivosheyev et al. 1999). Deviation of the nuclear lamins and their associated proteins are thought to be an additional event involved in malignant transformation and tumor progression, which can be a potential novel targets for anti-cancer drug development (Prokocimer, Margalit et al. 2006). As we know, lamina, which compose of lamin A/C and lamin B, is the main structural component used to support and determine the nuclear shape and integrity (Dahl, Kahn et al. 2004; Lammerding, Schulze et al. 2004; Broers, Kuijpers

et al. 2005; Dahl, Scaffidi et al. 2006; Lammerding, Fong et al. 2006; Scaffidi and Misteli 2006; Stewart, Roux et al. 2007). In tumor cells, the main changes are aberrant localization and reduction in expression of lamins A/C, which are frequently correlated with cancer aggressiveness, proliferation rate and differentiation state. Lamin A/C has been found to be reduced in some skin cancers (basal cell and squamous cell) (Venables, McLean et al. 2001; Oguchi, Sagara et al. 2002), gastrointestinal tract neoplasms including adenocarcinoma of stomach and colon, lung cancer (Kaufmann, Mabry et al. 1991; Broers, Raymond et al. 1993), testicular germ cell tumors (Machiels, Ramaekers et al. 1997) and cancerous prostate tissues (Coradeghini, Barboro et al. 2006). Especially, it is also reduced in breast cancer (Moss, Krivosheyev et al. 1999). Consequently, we hypothesize that the mechanical properties of the cancer cell nucleus may change. One study showed that the nucleus of small-cell lung carcinoma is susceptible to crushing during biopsy possibly due to lack of proteins encoded by the lamin A/C gene (Zink, Fischer et al. 2004). However, no quantitative studies have been performed.

A method established by Beale in 1860 and used as a "gold standard" for detecting cancer is to examine unstained cell structure and look out for any variation in nuclear size and shape (Zink, Fischer et al. 2004). In our case, the possible change in mechanical properties of the nucleus can be a quantitative and more accurate method to help detect cancer. In addition, more detailed information on the mechanical properties of the nucleus is needed to understand its role in mechanotransduction and the structure-property relationship of the cancer cells as this may give insight on the process of malignant transformation.

1.5 Why study nuclear mechanics besides cytoskeleton in the context of cancer metastasis?

Cytoskeletal structure, especially actin network, has been extensively studied and has been shown to play a crucial role in contributing to cell mechanics in different cell lines (Rotsch and Radmacher 2000; Nagayama and Matsumoto 2008). In the context of cancer cells, optical stretcher experiments (Guck, Schinkinger et al. 2005) and computational modeling (Ananthakrishnan, Guck et al. 2006) suggest that the increased deformability during the transformation of cells from nonmalignant to malignant is due to the change in cytoskeletal structure, especially actin structure. However, the structure and mechanical property of internal organelles like nucleus and its contribution to cell deformability is not well understood.

It is crucial to understand nuclear structure as nucleus contributes to the overall mechanical properties of the cell indirectly through connecting to and regulating the cytoskeleton. As reviewed earlier, the nucleus plays a pivotal role in regulating the cytoskeletal and adhesion structures in the cell through connections between nuclear structure and cytoskeleton via linker protein like Nesprins and SUN-proteins (Houben, Ramaekers et al. 2007). It has been shown that alterations in the nuclear structure (lamina) consequently give rise to alterations in the cytoskeleton (Broers, Peeters et al. 2004). Studies have shown that there is a dramatic change occurring in the nuclear architectures as they transform from being normal to malignant cells (Holth, Chadee et al. 1998; Bosman 1999; Konety and Getzenberg 1999; Zink, Fischer et al. 2004; Prokocimer, Margalit et al. 2006). So it is possible that the change in the cytoskeletal structure, which is thought to be responsible to the change in

mechanical properties as cells transform from being non-malignant to malignant, is due to the nuclear structural changes in cancer cells.

In addition, the nuclear structure and mechanical property might have direct contribution to cellular mechanical properties. As the nucleus is the stiffest and the largest organelle inside the cell (Dahl, Ribeiro et al. 2008), it is reasonable to assume that it may directly contribute to mechanical behavior of the cell in some situations as we know that the cell is a complex and heterogeneous material. As a major structural component in the cell, the nucleus occupies nearly 10% of the entire cell volume and in the case of cancer cells it occupies even more (Sommoggy, Wiendl et al. 1975; Mihailovic, Dordevic et al. 1999). It was found that the nucleus of bovine capillary endothelial cells is 9 times stiffer than cytoplasm (Maniotis, Chen et al. 1997), and the elasticity and viscosity of neutrophil nucleus is 10 times larger than that of cytoplasm (Dong, Skalak et al. 1991). Endothelial nucleus has an elastic modulus 10 times larger than the cytoplasm (Caille, Thoumine et al. 2002). Nuclei of articular chondrocytes are 3-4 times stiffer and nearly twice as viscous as the cytoplasm (Guilak, Tedrow et al. 2000). Therefore, the nucleus may play an important role in situations when a cell undergoes large compression, in which internal organelles like nucleus may dominate its mechanical behavior. In fact, some studies have shown that the nucleus may be the main contributor to the heterogeneity of the cell and may be a major compression-bearing component of the cell (Caille, Thoumine et al. 2002; Zink, Fischer et al. 2004; Deguchi, Maeda et al. 2005), and also plays an important role in the maintenance of cellular strength (Houben, Ramaekers et al. 2007).

In the context of cancer metastasis, cancer cells (HT-1080, with a diameter of near 20μm) undergo extremely large deformation as they pass through small capillaries

with a diameter of around 3 to 8µm (Yamauchi, Yang et al. 2005). Under such conditions of large deformation, the heterogeneity exhibited by internal organelles like nucleus may become the main factor in contributing to the overall mechanical behavior of the cell. Based on the techniques used for the mechanical testing of cancer cells and the theory used to interpret the data, most of the current studies (Ward, Li et al. 1991; Thoumine and Ott 1997; Lekka, Laidler et al. 1999; Lekka, Lekki et al. 1999; Park, Koch et al. 2005) have been carried out in the region of small deformation and the cells have been treated as a homogenous material with elastic or viscoelastic properties. In those studies, it is reasonable to assume that when cells undergo small compression or stretching in physiological conditions, the near surface cytoskeletal structure of the cell plays a major role in determining their mechanical properties. However, they may not be applicable to cells undergoing large deformation and to the situations where heterogeneity or non-linear behavior of the cells may play a major role.

Therefore, the structure and mechanical properties of the nucleus may contribute to the overall mechanical behavior indirectly by regulating the cytoskeleton and also directly by contributing to the heterogeneity of the cell which can be revealed at large deformation conditions. Thus more than cytoskeleton, it is of great importance to investigate the structure and mechanical properties of the cancer cell nucleus in terms of its contribution to cell mechanics in the context of cancer metastasis. However, few studies have been done on the nuclear structure and mechanical property and its contribution to cell mechanics, and none has been done in the context of cancer cells.

1.6 Objectives and scope of work

Since cancer cell mechanics is very important for understanding the mechanistic mechanism of cancer metastasis, which can also be used as a biomarker for better cancer detection and diagnosis, it is crucial to investigate the structure-property relationship of cancer cells. Cytoskeleton has been recognized as one of the most important structures in contribution to cell mechanics, but besides that we are going to study nuclear mechanics as we believe it is also a major contributor to cell mechanics especially in the context of cancer metastasis.

The structure and mechanical property of the nucleus is very important not only for understanding its role in regulating the whole cellular structure through connection with cytoskeleton, but also for its contribution to the heterogeneity of the cell as the nucleus is the largest and one of the stiffest organelles inside the cell. Moreover, the physical connections between nucleus and cytoskeleton indicate that nucleus may play an important role in mechanotransduction. Therefore, besides cytoskeleton it is also important to investigate the structure and mechanical properties of nucleus and its contribution to overall cancer cell mechanical behavior, which may also help in the understanding the mechanistic nature of cancer metastasis.

Our interest is in studying the structure and mechanical properties of cancer cells, especially nuclear mechanics and its role in contributing towards the structure of the cell and its overall mechanical behavior in metastasis. Since many studies showed that dramatic changes occur in the nuclear structure especially lamina of cancer cells compared to that of normal cells, we hypothesize that there is a corresponding change in the mechanical properties of the nucleus as the cells become malignant. Moreover, the nucleus may have a potential role in directly affecting the overall mechanical

behavior of the cancer cells especially while these cancer cells undergo large compression when they are entrapped or are passing through endothelial barrier and traversing capillaries during migration and metastasis.

Therefore, the aim of this project is to study the difference in the structure and mechanical property of non-malignant and malignant cells, which includes cytoskeleton and nucleus. Especially we will investigate nuclear structure and mechanical properties and understand its possible contribution to overall mechanical behavior of the cancer cells in the context of cancer metastasis.

Specifically this project aims to:

1. Model breast cancer cells traversing blood capillaries during hematogenous metastasis by flowing cancer cells through elastomeric microchannels, and investigate their cellular mechanical behavior and the role of nucleus in large deformation condition.

2. Quantify the near surface mechanical properties of malignant human breast epithelial cells (MCF-7) and non-malignant human breast epithelial cells (MCF-10A) in suspension using micropipette aspiration and investigate their underlying actin structure differences.

3. Investigate the structure and mechanical property of malignant human breast epithelial cells (MCF-7) and compare them with non-malignant human breast epithelial cells (MCF-10A) in adherent condition using atomic force microscopy and confocal microscopy.

4. Quantify the mechanical properties of the isolated nucleus of MCF-10A and MCF-7 using atomic force microscopy and examine their lamin A/C structures using confocal microscopy.

By carrying out the above, we hope to find out:

1. Whether there is any significant change in the mechanical property of the cell and its corresponding cytoskeletal structure as they become malignant, and

2. Whether there is any significant change in the mechanical property of the nucleus as cells become malignant and its relation to overall cellular mechanical properties.

In the next chapter, we will review previous work done on the mechanical properties of the cancer cells and cell nucleus and the techniques used in those studies.

Chapter 2 Literature Review

A variety of techniques from micro to nano scale have been developed and widely used to investigate cellular mechanical properties of different cell types.

In this chapter, we will first review the principles of different techniques including atomic force microscopy (AFM), micropipette aspiration, microfluidics. We will then review current studies on the mechanical properties of different types of cancer cells. Finally, we will review studies done on probing the mechanical properties of cell nucleus.

2.1 Methods

2.1.1 Micropipette aspiration

Micropipette aspiration has long been widely used as one of the prevailing experimental techniques to study the mechanical properties of individual single cells (Lim, Zhou et al. 2006 a). Fig. 2.1 shows the schematic diagram of the micropipette aspiration set-up. The apparatus consists essentially of a hydrostatic system with two reservoirs, a precision syringe pump for adjusting the water level in one of the reservoirs (variable reservoir) to bring about a suction pressure. Fine movement of the micropipette was controlled by a micromanipulator.

Basically, the technique involves exerting a hydrostatic suction pressure, ΔP, on the surface of a cell through a glass pipette of radius, R_p, and aspirating the cell into the pipette (Hochmuth 2000). By taking note of the aspirated length, L, the suction pressure used and the time taken, the time-dependent pressure-deformation

relationship can then be obtained and the mechanical properties of the cell determined (Zhou, Lim et al. 2005; Lim, Zhou et al. 2006 a)
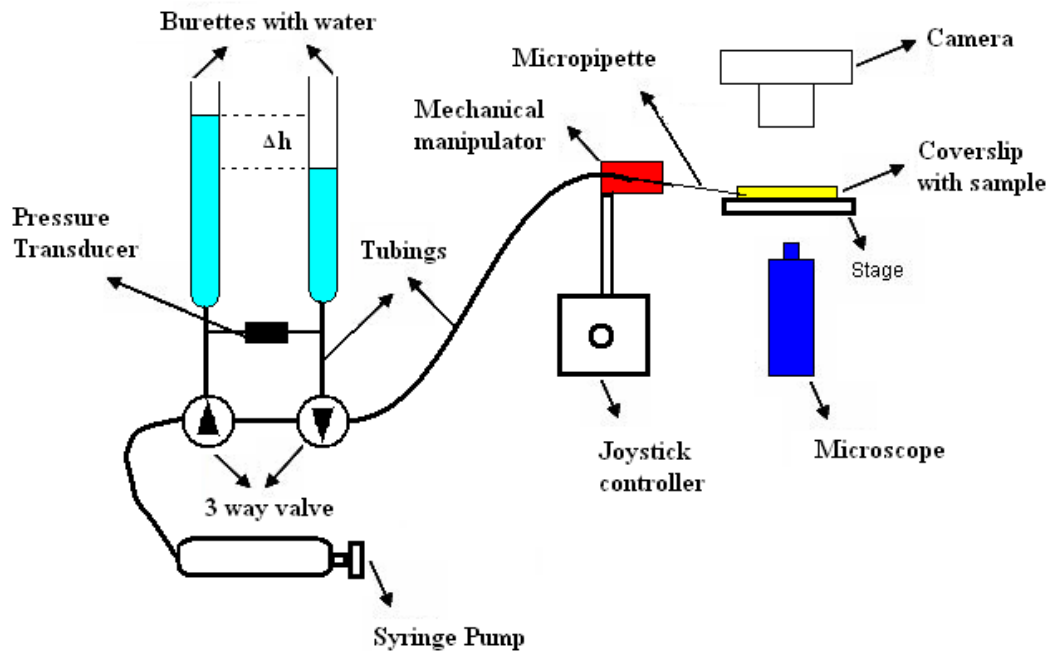
Fig. 2.1 Schematic diagram of the micropipette aspiration system set-up.

Many studies have been carried out using the micropipette aspiration technique to investigate the overall mechanical properties of different types of cells such as erythrocytes, chondrocytes, leukocytes and endothelial cells (Chien, Sung et al. 1978; Schmid-Schonbein, Sung et al. 1981; Sato, Levesque et al. 1987; Jones, Ting-Beall et al. 1999; Ohashi, Hagiwara et al. 2006; Trickey, Baaijens et al. 2006) and isolated nucleus (Dahl, Kahn et al. 2004; Dahl, Engler et al. 2005; Rowat, Lammerding et al. 2006).

Besides experimental studies, a series of mechanical models have been developed to interpret the data (see (Lim, Zhou et al. 2006 a) for detailed review). Moreover, computational simulations like finite element method have been developed to analyze

the results obtained using micropipette aspiration and investigate their structure-property relationship (Zhou, Lim et al. 2005; Vaziri and Mofrad 2007).

One study even showed that the aspiration of the cell elongates the nucleus which suggests that the nucleus deformation may be involved in mechanotransduction via the transfer of strain through the actin microfilaments and microtubules and contribute to the overall mechanics of the cell (Ohashi, Hagiwara et al. 2006).

2.1.2 Atomic force microscopy

Atomic force microscopy (AFM) is currently a very powerful tool used in biological research as it can probe biological samples in their physiological environment. As shown in Fig. 2.2, the working principle of the AFM is based on a very sensitive cantilever which can sense forces at the pico-Newton scale between atoms on the sample surface and atoms on the cantilever tip. The relative position of the sample and the tip is controlled by a computer-controlled piezoelectric stage, and the deflection of the cantilever, due to the interaction between the tip and sample, is in turn detected by a laser beam reflected by the cantilever and recorded using a photodiode detector. By scanning the surface of the sample, high resolution image down to the nano-scale can be obtained. Also, the interaction forces between the sample and the tip can be measured right down to the pico-Newton range, which makes the AFM suitable for investigating molecular interactions.
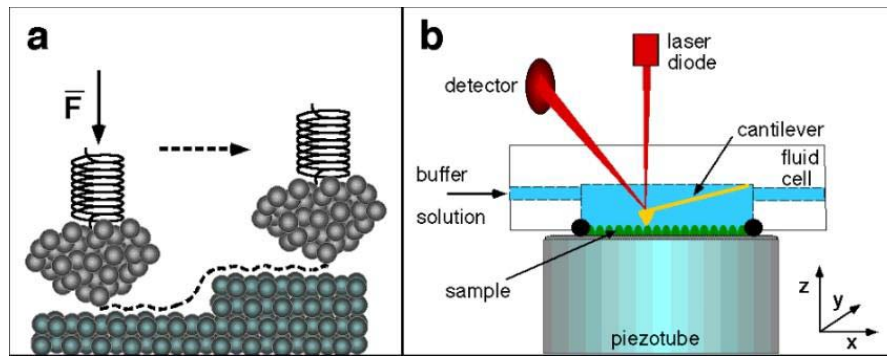
Fig. 2.2 Schematic diagram of the working principle of the AFM: (a) shows the interaction of the atoms between the AFM tip and sample surface; (b) shows the set up of an AFM system (http://www.mih.unibas.ch/Booklet/Booklet96/Chapter3/Chapter3.html).

AFM has been widely used in studies involving cell mechanics, like imaging and indentation and novel force measurement in molecular interaction.

2.1.2.1 AFM imaging of cells

The morphology of live cells (Henderson 1994; Hoh and Schoenenberger 1994; Legrimellec, Lesniewska et al. 1994; Hofmann, Rotsch et al. 1997; Braet, Seynaeve et al. 1998; Le Grimellec, Lesniewska et al. 1998; Bushell, Cahill et al. 1999; Tatsuo Ushiki 2000; Sinniah, Paauw et al. 2002; Braet and Wisse 2004; Pesen and Hoh 2005) or fixed cells (Legrimellec, Lesniewska et al. 1994; Pietrasanta, Schaper et al. 1994; Braet, Seynaeve et al. 1998; Weyn, Kalle et al. 1998; Sinniah, Paauw et al. 2002; Moloney, McDonnell et al. 2004; Pesen and Hoh 2005) and cellular dynamics (Ushiki, Hitomi et al. 1999; Chen, Wang et al. 2004; McNally and Ben Borgens 2004) can be investigated using the high resolution imaging capabilities of the AFM.

The major advantage of AFM compared with SEM is imaging under physiological aqueous condition without vacuum and the use of electrons. Although it is quite challenging due to the softness of the living cell, live cell imaging has been done on MDCK cells (polarized renal epithelial cells) (Hoh and Schoenenberger 1994;

Legrimellec, Lesniewska et al. 1994), chicken cardiocytes (Hofmann, Rotsch et al. 1997), colon carcinoma cells, skin fibroblasts and liver macrophages (Braet, Seynaeve et al. 1998), CV-1 kidney cells (Le Grimellec, Lesniewska et al. 1998), human fibroblast (Bushell, Cahill et al. 1999), Rabbit corneal fibroblasts, Chang conjunctival cells, and transformed human corneal epithelial cells (Sinniah, Paauw et al. 2002). High resolution images of cell cortex of bovine pulmonary artery endothelial cells was also achieved (Pesen and Hoh 2005). Improvements have been made to optimize the AFM imaging on live cells, including decreasing imaging force to 20 -25 pN with indentation less than 10 nm (Le Grimellec, Lesniewska et al. 1998) and activate substrate to promote good adhesion between cell and substrate (Bushell, Cahill et al. 1999). However, live cell imaging is comparatively difficult to carry out as the cell is very soft and usually does not adhere very well to the substrate. In light of this, Muys et al. proposed a technique which is known as "bioimprinttrade mark" to permanently capture a replica impression of biological cells by printing the cell onto Polydimethylsiloxane (PDMS) mold, and subsequently using the AFM to image the rigid medium of the PDMS mold. This method overcomes many difficulties used in conventional live cells imaging by transferring the cell topology onto a rigid medium and high resolution imaging of membrane morphological structures can be achieved (Muys, Alkaisi et al. 2006).

Another alternative method is to fix the cells using different concentration of paraformaldehyde and glutaraldehyde or their mix (Weyn, Kalle et al. 1998; Moloney, McDonnell et al. 2004). One of the optimized fixative was 4% PFA (Moloney, McDonnell et al. 2004). Fixed cells can be imaged under dry or wet condition. Dried cells after strong fixation have a flattening cytoplasm and loss of nuclear structure, but showed clear cytoskeleton. On the other hand, wet fixed cells showed an overall

'rounding' morphology and ill-defined structure (Weyn, Kalle et al. 1998). After removing the plasma membrane, the internal organelle of dried cells like mitochondria, cytoskeletal network, nucleus and even nucleoli can be imaged by AFM with high resolution (Pietrasanta, Schaper et al. 1994).

Generally, both live and fixed cell imaging have their own advantages. AFM image of living cells give morphology of the cells in their physiological condition, and reveal sub-membrane cytoskeletal elements (Hoh and Schoenenberger 1994; Braet, Seynaeve et al. 1998; Sinniah, Paauw et al. 2002), like stress fibers (Hofmann, Rotsch et al. 1997) and cell cortex (Pesen and Hoh 2005). The contrast in AFM imaging of live cells is contributed from the differences in local mechanical properties as plasma membrane deforms more than the underlying stiffer cytoskeletal filaments, which are in turn elevated and revealed in AFM image (Hoh and Schoenenberger 1994; Pesen and Hoh 2005). However, membrane structures, such as ruffles, lamellipodia, microvilli can only be clearly imaged for fixed cells (Hoh and Schoenenberger 1994). Dried cells were more easily and quickly imaged with better resolution than wet cells (live or wet fixed cells) (Weyn, Kalle et al. 1998). For example, Braet et al. used the AFM to investigate the surface and sub-membranous structures of live and fixed colon carcinoma cells (Braet, Seynaeve et al. 1998). AFM imaging of living cells revealed the presence of cytoskeleton, but detailed membrane structure can only be observed in the case of fixed cells.

Besides static morphological studies, dynamic cellular behavior can also be investigated using the AFM. Ushiki et al. combined the AFM with a fluid chamber system, which provides fresh culture medium at a regulated temperature, to examine the cellular dynamics of the cell motion in the long time range (Ushiki, Hitomi et al.

1999). Chen et al. used the AFM to investigate the ultrastructure of living human bladder cancer cells and the dynamic change of single cancerous cell division, which is expected to help elucidate the mechanism of malignant transformation of normal bladder cells (Chen, Wang et al. 2004). AFM is also used by McNally et al. to image the dynamic architectures of developing neurons, and 'real time' images of the death process of the neuron were captured after physically manipulating the cell (McNally and Ben Borgens 2004).

2.1.2.2 Measurements of cellular mechanical properties

AFM offers unique advantages for investigating cell mechanics as it offers high resolution imaging and the ability to obtain measurements of the localized mechanical properties. By combining imaging and indentation modalities, and relating the spatial distribution of cell mechanical properties to the structure of the underlying cytoskeleton, Costa et al. proposed using the elastography of cells obtained from AFM as a disease marker (Costa 2003; Costa 2006).

Typical AFM measurements include AFM indentation using a sharp tip (Rotsch, Braet et al. 1997; Rotsch, Jacobson et al. 1999; Lieber, Aubry et al. 2004) or a spherical probe (Mahaffy, Park et al. 2004; Smith, Tolloczko et al. 2005). Besides experimental studies, a lot of effort was put into interpreting the AFM indentation data. Costa used finite element model to investigate factors affecting AFM indentation such as depth, tip geometry, material nonlinearity and heterogeneity and derived the apparent elastic modulus as a function of those factors (Costa and Yin 1999).

They also tried to use an alternative "pointwise modulus" approach to examine the indentation for subcellular mechanics of human aortic endothelial cells. They found

that there are two sets of material properties for two different regions, with Young's

modulus of 5.6 ± 3.5 kPa for regions prominent with linear structures, and 1.5±0.76

kPa for adjacent regions (Costa, Sim et al. 2006).

Besides adherent cells, AFM can also be used to study non-adherent cells like passive

human leukocytes by mechanically immobilizing them in micro-fabricated wells

(Rosenbluth, Lam et al. 2006).

In addition to classical indentation modalities using a sharp tip, AFM was also used to

measure bulk mechanical properties of cells on the larger length scale instead of the

nano length scale by modifying the AFM tip from a sharp pyramid to a spherical bead

of a different size. Canetta et al. modified the AFM probe to stretch cells thereby

measuring their rheological properties (Canetta, Duperray et al. 2005). Lulevich et al.

used the microsphere-modified AFM probes to compress the cell and measure the

reaction force as shown in Fig. 2.3. The force and deformation curve showed a cubic

relationship at small deformation (< 30%) with multiple peaks at 30%-70%

deformation (Lulevich, Zink et al. 2006).
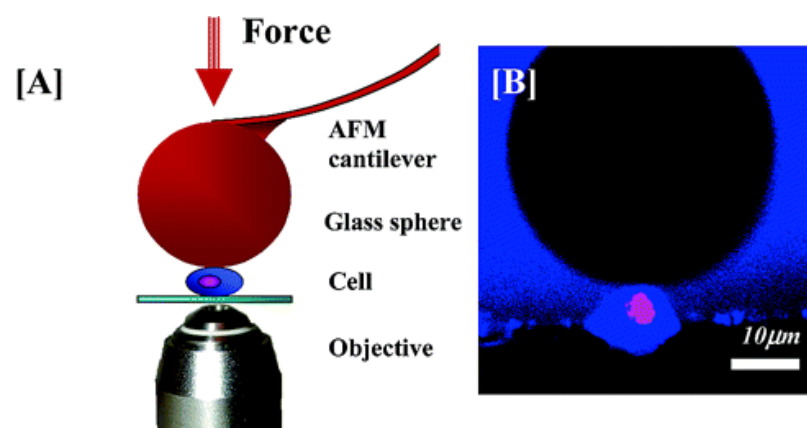
Fig. 2.3 (A) Schematic of the cell compression experiment using a microsphere-modified
AFM probe (B) Confocal image reveals the typical AFM probe position (Lulevich, Zink et al.
2006).

2.1.3 Microfluidics studies

Microfluidics is a novel *in vitro* method which can be used to mimic the flow behavior of cells in the micro-circulatory system.

Microfluidic devices has been used to study hemorheology and hemolysis, like the deformation dynamics of erythrocyte under high shear stress (Zhao, Antaki et al. 2006), the micro-rheology of erythrocytes as they pass through microchannels of dimensions similar to human blood capillaries (Sutton, Tracey et al. 1997) and the impact of impaired deformability of RBCs on the blood flow (Shevkoplyas, Yoshida et al. 2006). Blood diseases like malaria were also studied by using elastomeric microchannels (Fig. 2.4) which successfully mimicked the capillary blockage and "pitting" process of malaria infected RBCs (Shelby, White et al. 2003).
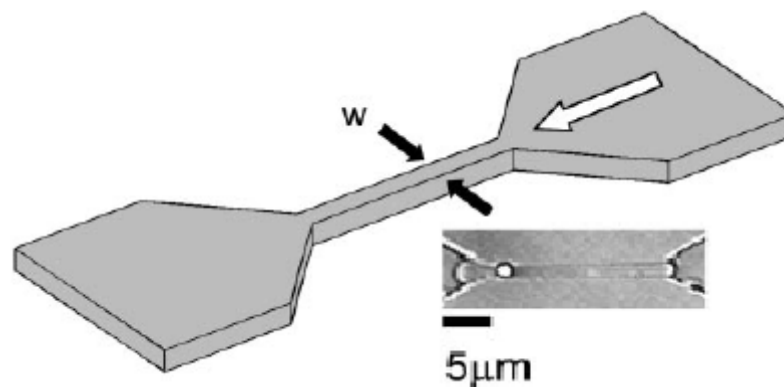
Fig. 2.4 Schematic diagram showing the geometry of the microchannel and a RBC passing through the channel (Shelby, White et al. 2003).

Chaw et al. used a microfluidic device to study the migratory and deformability capabilities of a single cancer cell. They showed that the cells were unable to migrate through a 3μm micro-gap, which suggested that the migratory capabilities might be governed by the deformability of the cells. Their experiment mimics in a way the

migration process of cancer cells through the endothelial barrier (Chaw, Manimaran et al. 2006).

In 2006, Lee et al. have designed an on-chip erythrocyte deformability test using microfluidics to distinguish cancerous blood from normal blood (Lee, Bang et al. 2007). They have defined useful parameters which are linked to the inherent deformability of the cancerous cells and plotted 2D and 3D graphs using these parameters. This proves to be effective as they can discriminate cancerous blood population from normal one with better sensitivity and reliability.

Based on constriction geometry, flow rate, cell deformability, a microfluidic application to separate the RBCs from the suspending plasma was also proposed (Faivre, Abkarian et al. 2006). Microfluidics was also successfully used to filter circulatory tumor cells (CTCs) from blood mixture based on the different physical size and deformability of RBCs and tumor cells (Chen, Zhang et al. 2006; Tan, Yobas et al. 2009).

2.2 Current studies

2.2.1 Mechanical properties of cancer cells

Mechanical properties of cancer cells have been studied using different biomechanical techniques like micropipette aspiration, atomic force microscopy (AFM) and optical stretcher, since it was found that most cancer cells are more deformable than their corresponding normal cells (Ward, Li et al. 1991; Thoumine and Ott 1997; Lekka, Laidler et al. 1999; Lekka, Lekki et al. 1999; Park, Koch et al. 2005; Suresh, Spatz et al. 2005). Moreover, there seems to be a direct correlation between an increase in deformability and the progression of a transformed phenotype from a non-malignant

cell line into a malignant, and metastatic cell line, which can effectively be used as a biomarker to detect cancer (Ward, Li et al. 1991; Guck, Schinkinger et al. 2005).

Some evidence has shown that the change in the deformability of cells as they transform from being non-malignant to malignant is the result of a change in the structure of cytoskeleton, which may also affect metastasis when cancer cells migrate through extracellular matrix and endothelial barriers (Ward, Li et al. 1991; Thoumine and Ott 1997; Suresh, Spatz et al. 2005). However, the reason causing this cytoskeletal change is not fully understood.

For example, Thoumine et al. used the micropipette aspiration technique to investigate the difference in mechanical properties of normal human dermal fibroblasts and SV40-transformed ones. They found that the apparent viscosity of transformed fibroblasts is 30% lower than that of normal fibroblasts, and transformed fibroblasts are more fragile than normal cells (Thoumine and Ott 1997). Ward et al. also used the same technique and found an increase in deformability as rat fibroblasts underwent transformation from non-malignant to malignant and metastatic cell line (Ward, Li et al. 1991).

However, using micropipette aspiration, Wu et al. found that the elastic coefficients of hepatocellular carcinoma cells (HCC) were significantly higher than those of hepatocytes, which indicates that hepatocytes are more deformable than HCC cells (Wu, Zhang et al. 2000). They also investigated the different effects of cytoskeleton perturbing agents (colchicines and cytochalasin D) on the viscoelastic properties of both cell lines, which suggests the difference in the cytoskeleton structure is responsible for different mechanical property and function in these two types of cells

(Wu, Zhang et al. 1997; Wu, Zhang et al. 2000; Wu, Zhang et al. 2001; Zhang, Long et al. 2002).

Besides studying drug effects, the role of p53 gene on deformability and metastasis of tumor cells were also investigated. Through micropipette experiments, it was found that murine erythroleukemia cells (MEL) transfected with wild-type *p53* gene are stiffer than MEL and those transfected with mutant *p53* genes, which suggested that they are more difficult to deform and migrate *in vivo* (Yao, Gu et al. 2003; Sun, Wang et al. 2004).

Lekka et al. used the AFM to measure the elastic properties of different types of cells in their culture condition including normal cells and cancerous ones, and found that the Young's modulus of normal cells was one order higher than cancerous ones (Lekka, Laidler et al. 1999). They also studied the effect of chitosan on the stiffness of non-malignant transitional ureter (HCV 29) and malignant transitional cell of urine bladder (T24). It was found that the treatment of chitosan can cause a decrease in the energy production of ATP and an increase in the Young's modulus values (Lekka, Laidler et al. 2001).

Lincoln et al. used the optical stretcher to characterize MCF-10, MCF-7 and modMCF-7 human breast epithelial cells and found that malignant cells can deform easier than non-malignant cells, and hence can be used as a marker for the diagnosis of cancer (Lincoln, Erickson et al. 2004; Wottawah, Schinkinger et al. 2005). Furthermore, Guck et al. demonstrated that the optical deformability is sensitive enough to distinguish between cells of different mechanical properties. Mechanical testing of MCF-10 (benign tumor), MCF-7 (adenocarcinoma, non-metastatic), MDA-MB-231 (Highly metastatic) breast cell lines showed that the deformability of cells

increases from non-malignant to malignant cells and also from non-metastatic to metastatic state, which indicates the mechanical properties of cells can be correlated to malignant transformation (Guck, Schinkinger et al. 2005). However, they only provided a measure of the relative cell stiffness by defining "stiffness" to be in terms of the ratio of the dimensions of major and minor axes of the cell prior to and during stretching. They found that human cancerous breast cell could stretch to about 5 times more than their non-cancerous counterparts (Lincoln, Erickson et al. 2004).

2.2.2 Mechanical properties of the cell nucleus

As the importance of nuclear structure and its function in cells, especially in understanding mechanotransduction becomes apparent, an increasing number of studies have been carried out to investigate the structure and mechanical properties of the nucleus. For example, Guilak et al. (Guilak 2000; Guilak, Tedrow et al. 2000) used the technique of micropipette aspiration to study the viscoelastic properties of mechanically and chemically isolated nuclei of articular chondrocytes. They found that isolated nucleus behaves similar to the cytoplasm in that it can be treated as a viscoelastic solid material, but the nucleus is 3-4 times stiffer and twice as viscous as the cytoplasm, which suggests that the nucleus may contribute mainly to the inhomogeneity of the apparent mechanical properties of the whole cell. Also, the mechanically isolated nucleus has a significantly higher equilibrium modulus than the chemically isolated nucleus. This may be due to the partial disruption of the nuclear matrix of the membrane by the chemical which was used to isolate the nucleus.

Micropipette aspiration was also used by Deguchi et al. to investigate the mechanical properties of the isolated endothelial nucleus under fluid shear stress, and was found to be significantly higher than that of the control nucleus in normal condition without

the presence of shear stress. Their results suggested that the structure of the nuclei had underwent remodeling due to the shear stress and the nucleus may be the main intracellular compression-bearing organelle (Deguchi, Maeda et al. 2005).

In addition, Knight et al. used confocal microscopy to examine the nucleus morphology of chondrocyte compressed in alginate constructs. They found that the deformation of the nucleus is less than the cell and the deformation is reduced significantly after 25 minutes (Knight, Bravenboer et al. 2002).

On the other hand, Tseng et al. used particle nanotracking to quantify the micro-organization and the viscoelastic properties of the nucleus in Swiss 3T3 fibroblasts. They also found that the intranuclear region is stiffer than the cytoplasm and more elastic than viscous, which shows a type of strong solid-like behavior (Tseng, Lee et al. 2004).

More information on nuclear mechanics is also needed to understand the force-induced changes in gene expression and the subsequent remodeling of the nuclear architecture in the context of cell development and disease. Dahl et al. used micropipette aspiration combined with fluorescent labeling to study the structure of protein-lamin B in an isolated nucleus, which are shown to contribute to the viscoelastic properties of the isolated nuclei. By comparing the unswollen with the swollen nuclei, they showed that chromatin is a primary force-bearing element in unswollen nuclei, whereas lamina sustained much of the load for swollen nuclei (Dahl, Engler et al. 2005). Mutations on *LMNA*, the gene encoding A type lamins, can cause a premature aging disease known as Hutchinson-Gilford progeria syndrome. Their results have shown that reduced deformability of the nucleus can cause misregulation of mechanosensitive gene expression (Dahl, Scaffidi et al. 2006).

Besides experimental studies, Vaziri et al. used finite element modeling to study the mechanics of the nucleus in a micropipette aspiration experiment. In their model, the nucleoplasm is treated as a viscoelastic Maxwell material. On the other hand, the nuclear envelope, which comprises three layers, is modeled in such a way that the inner (first layer of the nuclear envelope) and outer nuclear membranes (second layer) are treated as a modified Maxwell material and nuclear lamina (third layer) is treated as a linear elastic material. This computational model is validated by comparing with the experimental results from Guilak and Denguchi (Vaziri and Mofrad 2007). Using a similar computational model, they also studied the AFM indentation carried out on an isolated nucleus, and the role of individual nuclear elements, namely inner and outer membranes, nuclear lamina, and nucleoplasm, as well as the loading and experimental factors such as the indentation rate and the probe angle (Vaziri, Lee et al. 2006).

2.3 Summary

Standard techniques including AFM, micropipette aspiration and microfluidics have been used to investigate single cells or isolated nuclei. Although there have been many studies done to investigate the mechanical properties of cancer cells, there are relatively few studies carried out to investigate the structure and mechanical properties of the nucleus of cancer cell and its role in contributing to the cellular structure and mechanical behavior in the context of cancer cell mechanics and metastasis.

Hence, it is important to obtain the structure-property relationship of the nucleus and its contribution to the overall cellular structure and mechanical behavior.

Chapter 3 Microfluidics Study of Breast Cancer Cells in Suspension

3.1 Introduction

Metastasis is the predominant cause of death in cancer. To effectively treat cancer, the cancer cells must be detected at the earliest possible stage before it metastasizes to other parts of the body. Hence, cell stiffness is proposed as a biomarker which can allow us to identify cancerous cells with high sensitivity so that it can be diagnosed and treated early.

Moreover, understanding mechanical behavior of cancer cells may shed light on the mechanism of cancer metastasis. The mechanical behavior of cancer cells is important as mechanical factors are known to play an important role in influencing the metastatic process (Chambers, Groom et al. 2002). In the process of metastasis, cancer cells will undergo large deformation to traverse small capillaries and their deformability is an important factor. In another way, it is now known that the arrest of cancer cells at the site of target organs is essential for the success of metastasis. This trapping of cancer cells has been attributed to physical factors such as the relative sizes of cells and capillaries, the blood pressure in the organ and the deformability of the cells (Chambers, Groom et al. 2002; Yamauchi, Yang et al. 2005).

As reviewed earlier, prior work on breast cancer cells includes using a dual-beam optical stretcher to study the deformability of single suspended human epithelial breast cancer cell (Guck, Schinkinger et al. 2005). The cell was first trapped using the optical forces from two divergent laser beams which gave a zero net force and the cell was held stationary. The trapped cell was subsequently stretched along the laser beam axis when a higher laser power was applied. They found that cancerous MCF-7 breast epithelial cells deformed more than the normal MCF-10 breast epithelial cells.

Lincoln et al. had also used the optical stretcher to deform cells and their results showed that cancer cells stretched significantly five times more than normal cells and metastatic cancer cells could stretch up to twice as much as non-metastatic cancer cells (Lincoln, Erickson et al. 2004). This could mean that optical deformability could be used as a biomarker to differentiate cancer cells from healthy cells, and could even distinguish metastatic from non-metastatic cancer cells. Lincoln et al. later improvised the setup and combined both optical stretcher and microfluidic cell delivery system to give a novel microfluidic optical stretcher (Lincoln, Schinkinger et al. 2007). They then performed experiments on MCF-10A and modMCF-7 cells (cancerous breast epithelial cell which are highly metastatic) to study their time-dependent response to a constant stress. Their results showed that modMCF-7 cells displayed a higher relative axial strain than normal MCF-10A cells.

Although the optical stretcher has the ability to probe the mechanical properties of a single suspended cell as a whole, a drawback however is that the forces imposed on the cell by the laser is not sufficiently large enough to promote significant deformability which is necessary to simulate *in vivo* conditions encountered by migrating cancer cells (Suresh 2007). Moreover, the direct exposure to a laser beam and its effects on the cells is another limitation of the technique (Suresh 2007). Hence, there is a need to search for alternative techniques which can allow us to study the mechanical properties of single cells in physiological conditions. Microfluidic technology has emerged as an attractive alternative because it can provide an environment to mimic *in vivo* processes such as migration of cells through capillaries during metastasis and study the overall cell mechanical behavior as a whole.

In this chapter, in an attempt to compare the overall deformability of benign and cancerous breast epithelial cells under large deformation, we created an *in vitro* capillary-like microenvironment using microfluidics to mimic the behavior of breast cancer cells as they traversed the capillaries during metastasis. By taking quantitative measurements of several flow parameters such as entry time, elongation index and transit velocity, we seek to distinguish cancer cells from healthy cells based on their differences in deformability using microfluidics. Moreover, the importance of nuclei in the cellular mechanical behavior is demonstrated as cancer cells undergo large deformation. This chapter lays the foundation for further studies on the structure and mechanical properties of cancer cells and isolated nucleus.

3.2 Methods

3.2.1 Cell culture and preparation of cell samples

MCF-10A is a standard model non-cancerous human mammary epithelial cell and is derived from the benign breast tissue of a 36-year-old woman with fibrocystic disease. MCF-7 corresponds to a human adenocarcinoma cell line whereby the cell is cancerous and it is derived from the mammary gland of a 69-year-old female Caucasian. These are gifts from the A*STAR's Institute of Microelectronics (Singapore) and the life science institute, National University of Singapore (Singapore), respectively.

MCF-7 cell lines were cultured in DMEM (Dulbecco's Modified Eagle's Medium) supplemented with 10% fetal bovine serum (FBS) and 1% penicillin-streptomycin (Invitrogen, USA), while MCF-10A was cultured in MEGM (mammary epithelial growth medium). Both cell lines were maintained at 37 °C in a 95% air / 5% CO_2 incubator (SANYO, Japan). Cells were cultured until 80% confluent and subsequently

harvested using trypsin. They were then washed with their culture medium, centrifuged down and resuspended in their medium. Cells in a suspension state were then used for the microfluidics experiments.

3.2.2 Live nuclear labeling

For live nuclear labeling, cells were incubated with 1 µM Hoechst 33342 stain for 10 minutes at 37 °C, and then washed twice in PBS. After that, cells were harvested for microfluidics experiments using trypsin as described in section 3.2.1.

3.2.3 Microfluidics device fabrication

A silicon wafer master mould which consists of the design of the microfluidic channel was fabricated using electron beam and lithography techniques (Institute of Microelectronics, Singapore). Poly (dimethylsiloxane) (PDMS) was first pre-mixed with a curing agent (Sylgard 184, Dow Corning) in the ratio of 10:1 and then poured onto the silicon wafer master mould and degassed in a desiccator. After the PDMS has been cured at 80 °C for 2 hours, it is peeled off from the master and 2 holes were punched in each reservoir using a modified syringe tip (0.5 mm diameter) as shown in Fig. 3.1 The PDMS channels were subsequently bonded tightly onto glass coverslips using an air plasma machine (Harrick Plasma Cleaner, USA).
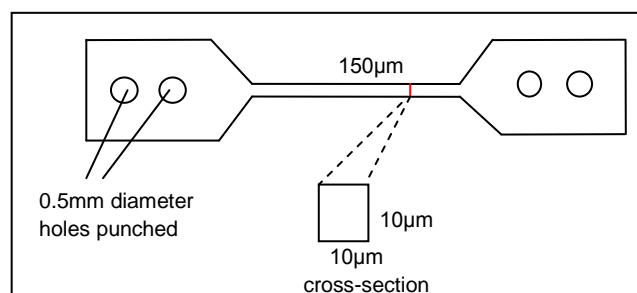
Fig. 3.1 The bonded PDMS microchannel is 150 μm in length and has a square cross section area of 10 μm × 10 μm.

3.2.4 Pressure differential system setup

The burette setup (Fig. 3.2) that was used to drive the cells through the channel was based on the working principles of a manometer. Briefly, the pressure generator setup involves the use of 2 identical burettes held at the same level with a retort stand. The burettes were filled with phosphate buffer solution (PBS) and the pressure generated in the microfluidic channels was governed by a simple mathematical equation:

$$\Delta P = \rho g h \qquad (3.1)$$

where ΔP is the pressure difference between the burettes, h is the height difference of PBS between the burettes, ρ is the density of $1\times$ PBS and g is the gravitational acceleration.
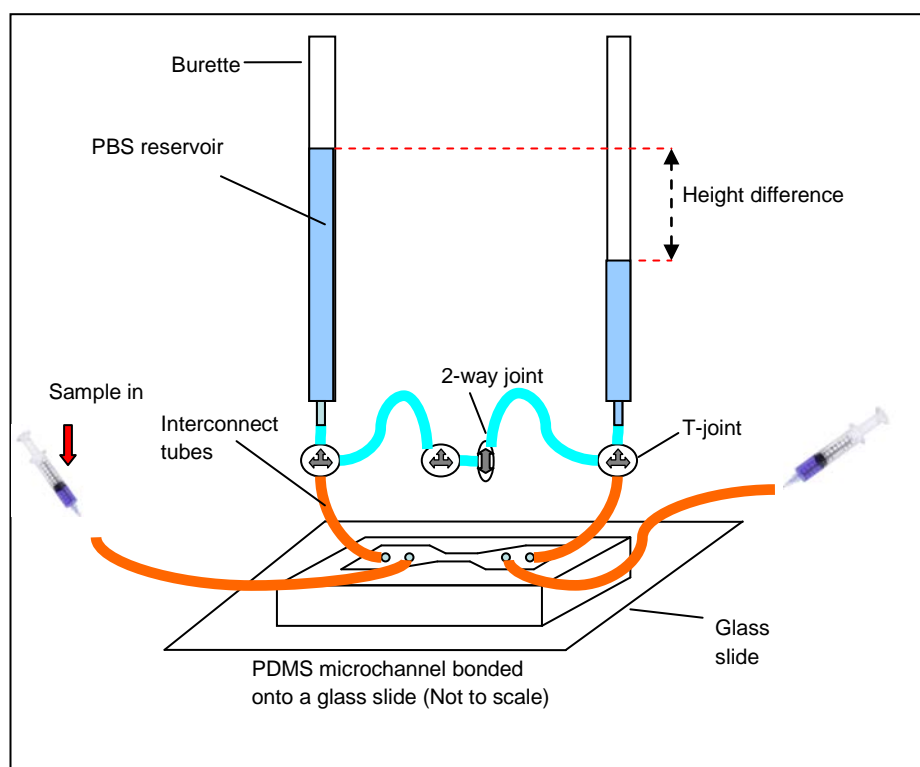
Fig. 3.2 Diagram of the PBS column-based microfluidic system.

The bonded PDMS microchannel was connected to the burette setup and syringes using interconnect tubes through the punched holes. It was then mounted onto the stage under an inverted light microscope with mercury lamp attached (Leica DC 500, Germany). The aperture setting was set at 40× throughout the course of this study to give us large field of vision and good resolution at the same time.

A high speed camera (Quantum 512SC, USA) was mounted onto the microscope and imaging software MetaMorph (Molecular Devices, Sunnyvale, CA, version 7.1) was used to capture and process the video images. Differential interference contrast (DIC) was selected to enable easy identification of cells passing through the channel.

Before the sample was injected into the microchannel, the PDMS reservoirs and microchannel were filled with a diluted solution of bovine serum albumin (BSA) (4% wt) at 37°C. It was then left to stand for 1 hour. The reservoir and the microchannel were coated with BSA to prevent any non-specific adsorption of the cells to the channel wall during the course of the experiment.

3.2.5 Cell flow parameters

Several parameters which may be useful for assessing the deformability of cells during metastasis have been defined. A tracking application in MetaMorph will be used to track the movement of the cell in real time as it squeezes into and through the microchannel. Based on the distance-to-origin profile plotted for each cell, the parameters can then be obtained from the graph. Listed below are short descriptions of the defined parameters.

3.2.5.1 Transit Velocity

Transit velocity (equation 3.2) is the average velocity of the cell when passing through the microchannel. It is calculated from the equation :

$$\text{Transit velocity } V_{transit} = L / t_{transit} \tag{3.2}$$

Where L is distance travelled by the cell and $t_{transit}$ is the time for the cell to travel the same distance L.

3.2.5.2 Entry time

Entry time (equation 3.3) is defined as the time taken for the cell to deform and enter the microchannel:

$$\text{Entry time } T_{entry} = T_f - T_i \tag{3.3}$$

where T_i is the time when the cell touches the microchannel before entering, and T_f is the time when the cell has just wholly deformed into the microchannel but has not transverse the channel yet.

3.2.5.3 Elongation index

Elongation index (equation 3.4) is the ratio of the elongated length of each deformed single cell in the microchannel (l) to the initial diameter of the cell before squeezing into the channel (D):

$$\text{Elongation index } EI = l / D \tag{3.4}$$

3.3 Results and discussion

MCF-7 and MCF-10A cells were driven to transverse through PDMS microchannels of 150 μm in length and square cross section area of 10 μm by 10 μm. The pressure difference used is a height of 5cm PBS (490.5Pa) and at room temperature of 22°C - 24°C.

3.3.1 Typical distance-to-origin cell profile

A distance-to-origin cell profile represents the distance travelled by the cell with time as it squeezes and flows through a microchannel. A typical profile would be similar to the one shown in Fig. 3.3 In this example, the MCF-7 cell has an entry time of 0.858 seconds. From the graph, this corresponds to a non-linear entry time region before 0.858 seconds and an eventual straight linear portion after the entry time. This means that the cell was travelling across the microchannel with a constant transit velocity after it has fully deformed into the channel.
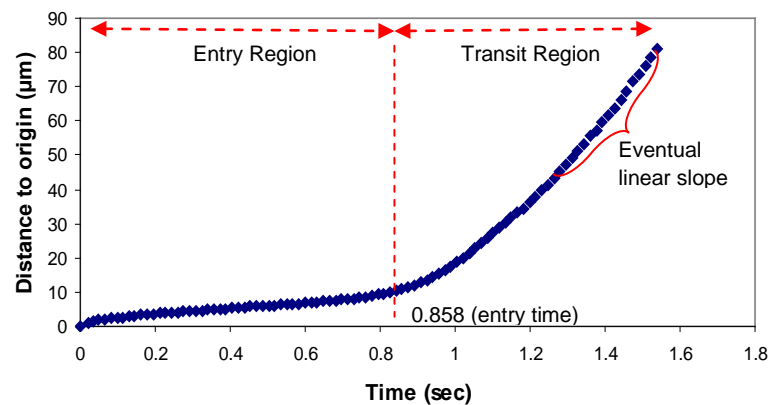
Fig. 3.3 Plot of a distance-to-origin profile of a single typical MCF-7 cell.

The profile can be further subdivided into two regions, the entry region and the region of transit across the microchannel for a more detailed analysis.

3.3.1.1 Entry time region
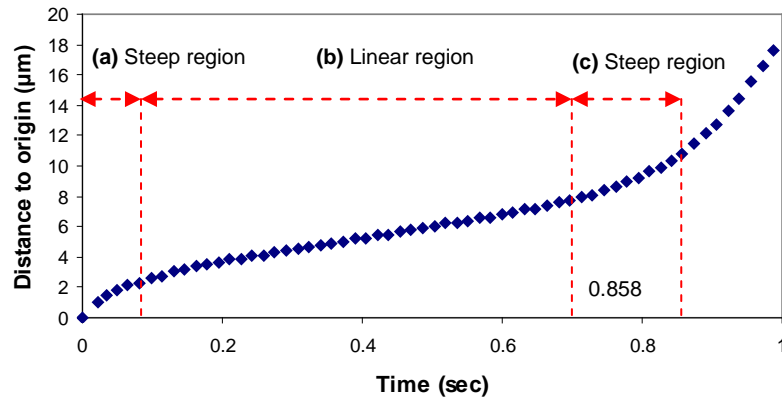
Fig. 3.4 Plot showing the entry time region of a single typical MCF-7 cell.
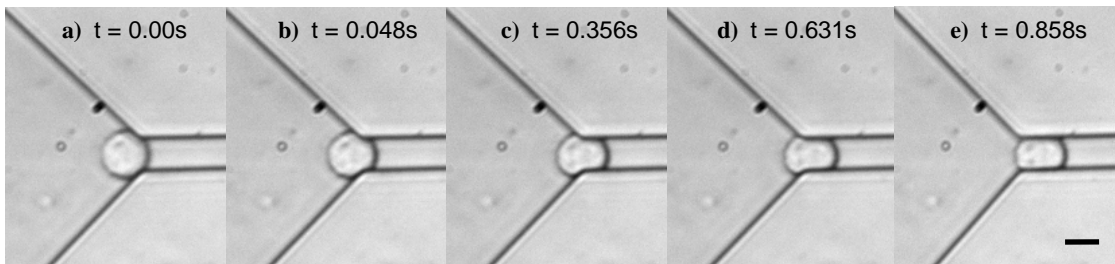
Fig. 3.5 Optical images showing the entry of a single MCF-7 cell into a $10\,\mu m$ by $10\,\mu m$ microchannel (Scale bar represents 10 µm).

Fig. 3.4 shows a magnified view of the period of cell entry and Fig. 3.5 shows the corresponding snap shots of the MCF-7 cell squeezing into the microchannel. When the cell first touches the channel as shown in Fig. 3.5 (a), the time is set to zero and this corresponds to the origin of the graph shown in Fig. 3.4.

From Fig. 3.4, we can see that the profile can be further divided into three distinct portions. Firstly, as the cell is squeezed into the microchannel as shown in Fig. 3.5 (a), the graph begins with a steep slope and this gradually decreases. This means that the cell initial entry velocity into the channel is the highest at the beginning but slows down as the cell attempts to squeeze into the channel. The entry velocity may slow down due to the increased resistance encountered by the cell. This initial non-linear

portion corresponds to the optical images shown in Fig. 3.5 (a) and (b).

This non-linear region lasts only for a short duration and it is followed immediately by a linear region with a gentler slope. This linear portion of the graph is also the longest in the entire entry-time region. This region matches the optical images in Fig. 3.5 (b) and (d) which showed the main part of the cell squeezing into the channel. This region of the graph may correspond to the nucleus possibly squeezing into the channel because the nucleus is known to be stiffer than the cytoplasm and will take a longer time to deform into the microchannel (Smith, Tolloczko et al. 2005; Vaziri and Mofrad 2007).

Lastly, the slope increases again at the final region, corresponding to an increased entry velocity at the end. This may be due to the remaining cytoplasm deforming into the microchannel after the nucleus has fully entered the channel. This final region is represented by Fig. 3.5 (d) to (e) and the instantaneous time at the position of the cell in Fig. 3.5 (e) corresponds to the entry time after the whole cell has fully deformed into the channel.

3.3.1.2 Linear region

$y = 131.85x - 123.3$
$R^2 = 0.9973$
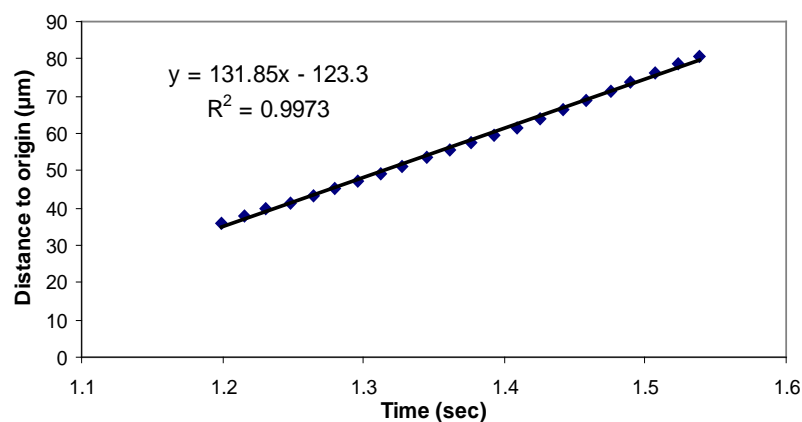
Fig. 3.6 Plot showing the transit region of a typical MCF-7 cell travelling through the length of the microchannel.

44

As shown in Fig. 3.6, after the cell has fully entered the channel, the curve will follow a linear region. This indicates that the deformed cell was moving at almost constant velocity along the microchannel. Thus, the transit velocity will be equivalent to the gradient of the trend line, which is 131.85µm/sec.

From Fig. 3.7, it can be observed that once the cell is deformed inside the channel, it will maintain the elongated shape throughout as it transverse across the microchannel.
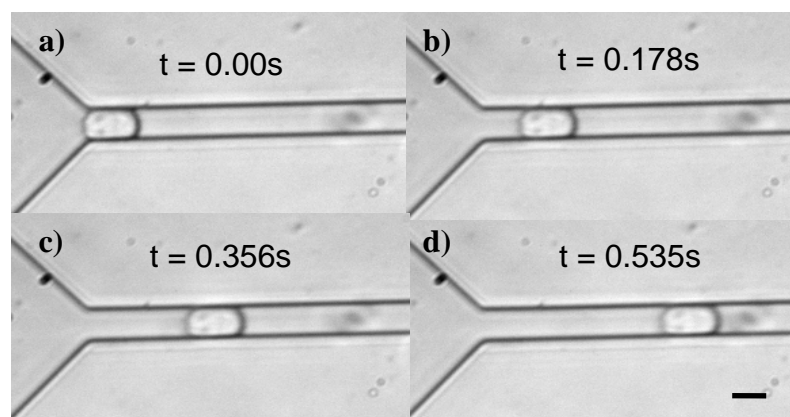
Fig. 3.7 Optical images showing the position of a typical deformed MCF-7 cell in the microchannel at different frames (Scale bar represents 10 µm).

3.3.1.3 Comparison of distance-to-origin profiles between MCF-7 and MCF-10A
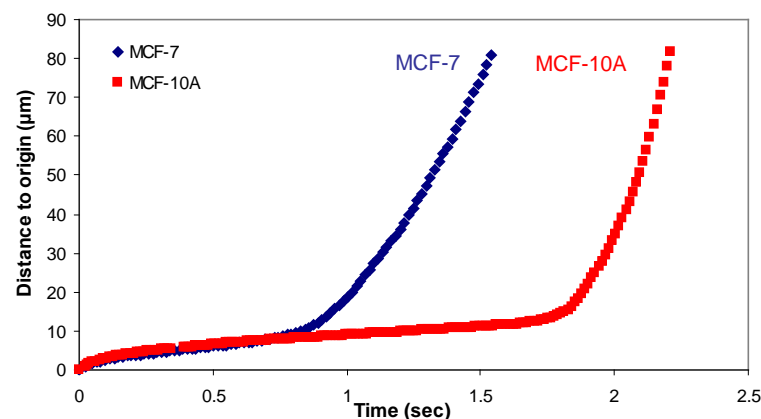
Fig. 3.8 Plot showing the comparison of distance-to-origin profile of MCF-7 and MCF-10A. The cells are chosen such that their sizes are approximately similar as this will give a better comparison.

45

From Fig. 3.8, the general shape of the profiles of the two types of cells is similar. It will always begin with a long entry region, followed by a steep linear transit region. The long entry region can also be further subdivided into 3 distinct portions as mentioned in 3.1.1, characterized by a long linear slope at the centre.

As shown in Fig. 3.8, the entry region for MCF-10A is much longer, which means that the cell takes a longer time to deform completely into the channel. As the cell sizes are roughly the same for both cell types, this may indicate that MCF-10A is less deformable than MCF-7. This is consistent with the results shown by Guck et al. who performed an experiment using the optical stretcher and found that cancerous MCF-7 breast epithelial cells deformed more than the benign MCF-10 breast epithelial cells with the same laser intensity (Guck, Schinkinger et al. 2005). Hence, cancerous MCF-7 cells are more deformable than benign MCF-10A cells.

However, the linear portion of the graph in the transit region for MCF-10A has similar gradients as compared with MCF-7. Hence, this may suggest that the transit velocities of the two types of cells may be similar, even though their entry time varies greatly. This will be discussed in more details in section 3.3.4.

3.3.1.4 Quantitative analysis of parameters

A sample size of 50 cells from MCF-7 and MCF-10A were collected for analysis. The experimental conditions used are pressure height difference of 5cm PBS and temperature at $22^{o}C - 24^{o}C$. To validate the defined parameters as mentioned earlier, their distribution was employed as a means of studying the deformability between MCF-7 and MCF-10A. The distributions of these parameters such as entry time, transit velocity and the elongation index were measured and summarized in Table 3.1.

Statistical analysis was performed using the Student's independent t-test for the entry time, the elongation index and the transit velocity. Statistical significance was accepted at p <0.05. Evaluation shows that the entry time and elongation index for the MCF-7 and MCF-10A cell lines were statistically different but transit velocity between these two cell lines were statistically the same. This shows that there is actually a difference in entry time and elongation index between these two cell types which may be due to the differences in their cell stiffness.

Table 3.1 Evaluation of cell deformability by Entry time, Elongation index, Transit velocity using t-tests

	Entry time (±SE) (sec)	Elongation index (±SE)	Transit velocity (±SE) (µm/sec)
MCF -7	0.433 (±0.045)	1.281(±0.01505)	177.3(±9.836)
MCF-10A	1.698(±0.201)	1.231(±0.01191)	187.0(±7.920)
P(<0.05) , N=50 cells	1.07364E-07	0.01917	0.4441

3.3.2 Cell elongation
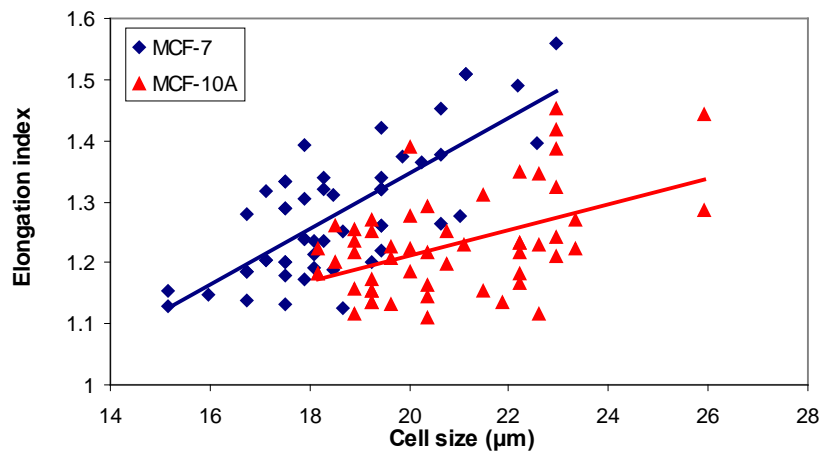
Fig. 3.9 Plot showing the scatter plot of elongation index against cell size.

From Fig. 3.9, it was observed that MCF-7 cells generally have higher elongation indices as compared with MCF-10A for the same cell sizes. As the elongation index provides information on the elasticity and stiffness of cell in the direction of the stretch, this indicates that cancerous MCF-7 cells elongate more in the microchannel as compared to benign MCF-10A cells. This result is also consistent with findings by Lincoln et al. who have used the optical stretcher to stretch both MCF-7 and MCF-10A cell lines. They have found that MCF-7 cells can stretch five times more than normal cells (Lincoln, Erickson et al. 2004).

3.3.3 Entry time

The entry time was also plotted against the elongation index as shown below. Elongation index was used as it will normalize the size of the cell and this allows us to make a fair comparison of the entry time between MCF-10A and MCF-7.
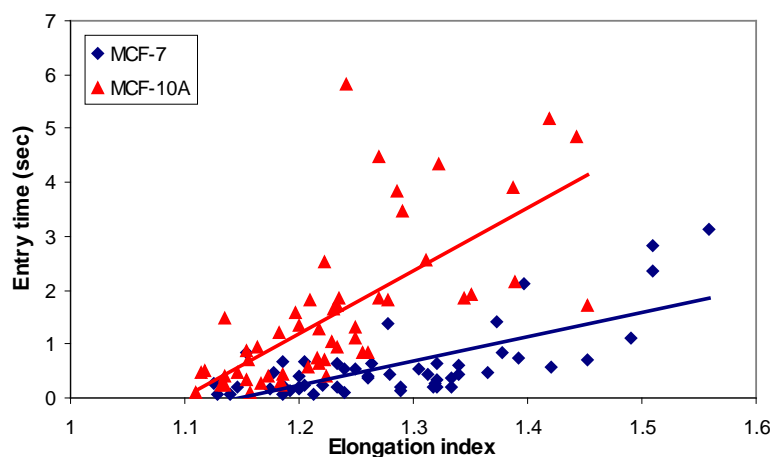
Fig. 3.10 Plot showing the scatter plot of the entry time against elongation index.

In Fig. 3.10, it was observed that the entry time increases as elongation index increases. This means that the bigger the cell, the longer time it will require to squeeze into the microchannel. It is also observed that the trend line for MCF-10A is

steeper than MCF-7. This indicates that MCF-10A on average has a longer entry time as compared to MCF-7. This is consistent as benign MCF-10A cells were known to be stiffer than cancerous MCF-7 cells and will therefore take a longer time to squeeze into the microchannel.

However, it is important to note that the parameter entry time depends on both the cell deformability and the friction encountered by the cell during its entry into the microchannel. Hence, transit velocity was measured and analyzed between these two cell lines in the following section which acts as a control and provide information on the friction encountered by these cells.

3.3.4 Transit velocity
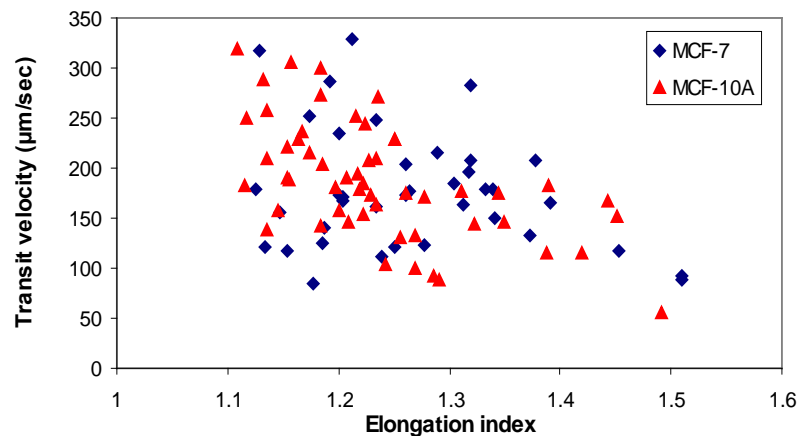
Fig. 3.11 Plot showing the scatter plot of transit velocity against elongation index.

Fig. 3.11 shows a plot of transit velocity against elongation index for MCF-7 and MCF-10A cell lines. From the graph, most of the points are actually randomly scattered in the transit velocity region ranging from 100 to 300 μm/sec. This seems unusual as it is first thought that a bigger cell would have a bigger cell surface area in contact with the channel wall. This would lead to increased friction and may slow

down the transit velocity significantly. However, experimental data shows that cell size and cell type do not actually have a clear relationship with the cell transit velocity across the channel. This result is consistent with the work done by Lee et al. who have also studied the transit velocity of cancerous blood using a microfluidics chip (Lee, Bang et al. 2007). In their work, the transit velocities of the deformed cancerous red blood cells were measured through the microchannel and most of the points were randomly scattered when transit velocity was plotted against elongation index. Hence, this may suggest that transit velocity is independent of cell size when the cells are flowing through the microchannel.

This indicates that the BSA coating of the channel wall was effective. The PDMS reservoirs and microchannel were incubated with BSA (4% wt) for 1 hour before the experiment. This is to prevent any non-specific adsorptions of the cells to the reservoirs so that the cells can flow smoothly. The coating may also help to reduce friction between the deformed cells in the channel with the channel walls, making the effect of friction negligible. Hence, transit velocity will not be affected considerably by the cell size.

As cancerous MCF-7 cells are more deformable, the deformed cells will exert less pressure on the channel wall and there will be less friction between the cell surface and the channel wall. For the stiffer MCF-10A cells, they will exert a higher pressure when deformed inside the channel, leading to a higher friction between the cells and the channel walls. The average transit velocities of MCF-7 and MCF-10A cells were then calculated from the samples and shown in Fig. 3.12. It turned out that the average velocities for MCF-7 and MCF-10A are quite similar even though cancerous MCF-7 cells are more deformable than benign MCF-10A.
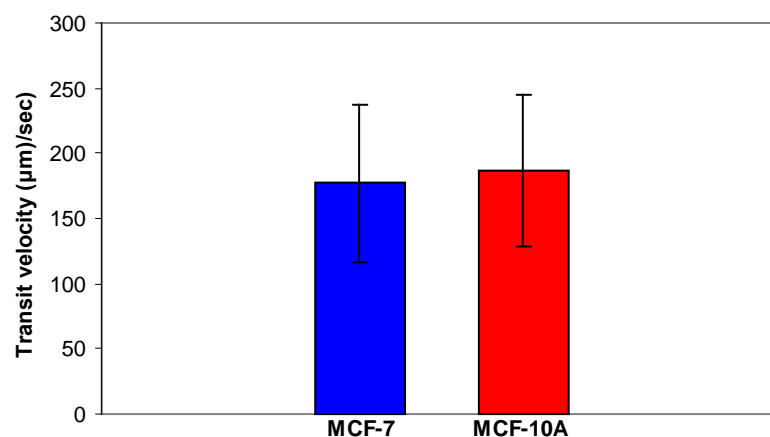
Fig. 3.12 Histogram showing the average transit velocities of MCF-7 and MCF-10A.

The experimental data have shown that the average velocities of these two cell lines are similar despite the difference in cell stiffness. This indicates that the frictions encountered by these two cell linings are actually similar. It may be due to the BSA coating which reduces the friction significantly between the channel walls and the area of the cell in contact with them.

Hence, measurement of the transit velocities of cells across the microchannel serves as a control to study the friction encountered by the cells. From the results, it can be shown that the friction encountered by MCF-7 and MCF-10A are similar as both type of cells have similar transit velocities despite having different stiffness.

This also allows us to eliminate the friction factor in the analysis of entry time. As the entry time of cells depends on the cell deformability and the friction encountered by the cell, it can now be concluded that entry time is affected mostly by the cell stiffness of MCF-7 and MCF-10A. Thus, it can be inferred that MCF-7 cells are more deformable than MCF-10A based on the difference in the entry time. It can also be

concluded that entry time is a useful parameter to distinguish the differences in deformability between these two cell lines.

3.3.5 Role of nuclei in large deformation of cancer cells
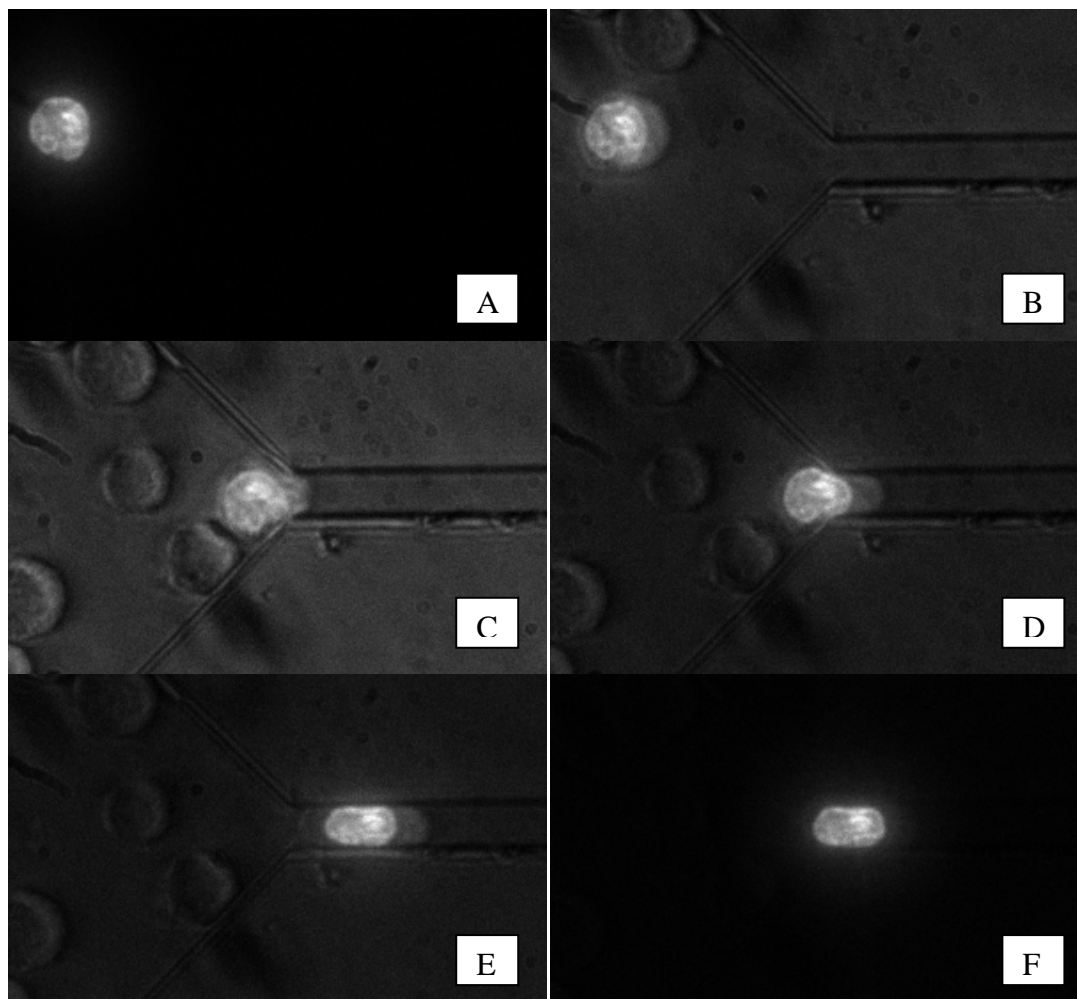
Fig. 3.13 Optical images showing the nucleus undergoing large deformation when the cell (MCF-7) passes through the microchannel (bright region in the center showing the stained nucleus, and the outer boundary showing the cell).

Breast cancer cells with fluorescence labeled nucleus were passed through the same microchannel and the deformation of nucleus was monitored. As shown in Fig. 3.13, the nucleus undergoes extremely large deformation from a round shape (Fig. 3.13 A) to an elongated shape (Fig. 3.13 F) when the cell squeezes into the microchannel. The nucleus is relatively large as it occupies almost half space of the whole cell as seen in

Fig. 3.1.3 B - E. This experiment mimics the cancer cell nucleus undergoing large deformation when the cancer cell traverse small capillaries which is consistent with *in vivo studies* by Yamauchi et. al (Yamauchi, Yang et al. 2005). Most importantly, this experiment demonstrates the importance of nucleus in the overall deformability of cancer cells as how nuclei deform will affect significantly how fast breast cancer cells get squeezed into the channel. The deformability of cancer cell nucleus will be investigated in the later chapter.

3.4 Conclusions

Here, an *in vitro* capillary-like microenvironment was created using microfluidic technology to mimic the cells traversing small capillaries and study the overall deformability of breast cancer cells under large deformation. Benign breast epithelial cells (MCF-10A) and cancerous breast cells (MCF-7A) were driven by static pressure to deform and pass through a micro-fabricated fluidic channel. Quantitative parameters such as entry time, elongation index and transit velocity, which were related to the deformability of the cell, were defined and measured quantitatively using MetaMorph software and a high-speed camera.

The two different cell lines were found to have similar transit velocities. This indicates that transit velocity is not affected by the cell size and cell type. It also suggests that friction encountered by cells of different stiffness may be the same in the microchannel. MCF-10A cells were also found to have higher entry times than MCF-7 cells of similar cell sizes. As friction does not affect the different cell types, it shows that the entry time is only affected by the deformability of the cells. Hence, MCF-10A is stiffer than MCF-7 cells based on the difference in entry times. These

results were consistent with past studies which also investigated the deformability of breast cancer cells using other techniques.

2D graphs using entry time, transit velocity and elongation index were also plotted and showed a synergistic effect as there is a clear distinction between the scattered data points of MCF-7 and MCF-10A. This is useful as it indicates that the simple microfluidic design used is able to distinguish the difference in stiffness between benign MCF-10A cells and cancerous MCF-7 cells with 2D plot involving the defined parameters. Hence, cell deformability as demonstrated in microfluidics can potentially serve as a useful biomarker to identify cancerous cells from a sample population and thus have the potential for use in cancer diagnostic applications.

Especially, the importance of nucleus in the cellular mechanical behavior is demonstrated. However, in this study, cancer cells undergo large deformation and reflect their overall cellular mechanical properties when they pass through the microchannel, which are generally contributed by the whole cellular structure. To further understand structure-property relationship of cancer cells, specifically probing different parts of cancer cells especially nucleus and investigate their underlying structure is needed.

Chapter 4 Micropipette Aspiration Study of Breast Cancer Cells in Suspension

4.1 Introduction

In the previous chapter, microfluidics study, which mimics breast cancer cells traversing capillaries, gives us a good comparison of overall deformability between MCF-7 and MCF-10A at high throughput. However, it is a relative comparison of the overall mechanical behavior under large deformation. And it is an integrated deformability contributed from the whole cell, which cannot be attributed to specific cellular structural components. To better understand the structure-property relationship of breast cancer cells, probing the mechanical property of breast cancer cells in different parts and investigating its corresponding structural components is needed.

Studying the structure-mechanical property relationship of living cells can contribute towards better understanding of cell physiology and pathophysiology as they are known to change during the onset of certain diseases including cancer. As reviewed in the previous chapter, the deformability of normal and cancerous breast epithelial cells was first investigated by Lincoln *et al*. and Guck *et al*. using the optical stretcher (Guck, Ananthakrishnan et al. 2000; Guck, Ananthakrishnan et al. 2001; Lincoln, Erickson et al. 2004; Guck, Schinkinger et al. 2005). However, they only provided a measure of the relative cell stiffness by defining "stiffness" to be in terms of the ratio of the dimensions of major and minor axes of the cell prior to and during stretching. They found that human cancerous breast cell could stretch to about 5 times more than their non-cancerous counterparts (Lincoln, Erickson et al. 2004). In our study presented in the previous chapter, microfluidics study showed consistent results as

theirs. But it still only gives us a relative cellular deformability defined by how fast a cell deform into a microchannel. Moreover, as cells undergo large deformation when they pass through the microchannel, the difference in overall deformability could not be easily attributed to any specific cellular structure.

To better understand cancer cell mechanics and its role in cancer metastasis, it is important to investigate its underlying structural change compared with normal cells. Altered genetic composition and protein expression in cancer are responsible for changes in intracellular structure and cellular deformability (Fuchs and Weber 1994; Suresh, Spatz et al. 2005). This not only affects cell motility, adhesion and interaction but also cell growth and division (Chen, Mrksich et al. 1997; Boudreau and Bissell 1998; Huang and Ingber 1999; Alberts, Johnson et al. 2002; Lodish, Berk et al. 2003).

To better understand structure-mechanical property relationship of cancer cells, the aim of this chapter is to probe the near surface mechanical property of breast cancer cells using micropipette aspiration and investigate its corresponding underlying actin structure. Benign and cancerous breast cells were aspirated into pipettes of different sizes at room and physiological temperatures, while filamentous actins, which are major components of the cytoskeleton, were imaged using confocal microscopy.

4.2 Methods

4.2.1 Preparation of cell samples

Cell culture and sample preparation were the same as that for microfluidics experiment, as details in section 3.2.1. Cells in suspension were then used for the micropipette aspiration experiments.

4.2.2 Confocal fluorescence imaging

For confocal fluorescence imaging, the cells were seeded on 12 mm coverslips and then incubated for half an hour after they had adhered on the coverslips while still preserving their spherical shape. The cells on coverslips were fixed using 4% paraformaldehyde (Sigma-Aldrich, USA) for 15 minutes. After washing the cells three times with PBS, the cells were permeabilized using 0.2% Triton-X 100 (Bio-Rad Laboratories, USA) for 10 minutes. Finally, the filamentous actin (F-actin) was labeled with 0.1 μg/ml TRITC-Phalloidin (Sigma-Aldrich, USA) for 30 minutes and subsequently the nuclei were labeled with 5μg/ml DAPI (Sigma-Aldrich, USA) for 5 minutes. Fluorescence images were taken using a confocal microscope (Nikon TE2000, Japan).

4.2.3 Micropipette aspiration setup

The micropipette aspiration system used in this chapter is, in principle, similar to those used by others (see (Hochmuth 2000) for review). As shown in Fig. 4.1, the apparatus consists essentially of a hydrostatic system with two reservoirs, a precision syringe pump (Cole-Parmer, USA) for adjusting the water level in one of the reservoirs (variable reservoir) to bring about a suction pressure, a pressure transducer and a micropipette holder on a microscope stage. The cell suspension was placed in a glass chamber with side openings, obtained by sandwiching six layers of parafilm between two glass coverslips. The openings allow two micropipettes to enter the chamber from opposite sides. Fine movement of the micropipette was controlled by a micromanipulator (Eppendorf AG, Germany). Suction pressures can then be applied to the surface of a cell through a micropipette by simply adjusting the water level in the variable reservoir. The suction pressure used was measured from a pressure

transducer which has a resolution of 2.5 Pa (Validyne Engineering Corp., USA). The

cells were viewed with an inverted microscope system (Leica, Germany), using a 63

times objective (NA = 0.7). Microscopic images were taken with a digital camera

(Leica, Germany). Image dimensions were analyzed with the IM 1000 Leica imaging

software. Image acquisition was started simultaneously with the aspiration of the cell.

To carry out the tests at physiologic temperature, the glass chamber was filled with a

cell suspension and placed on a heating stage which is connected to a temperature

controller (Leica, Germany).
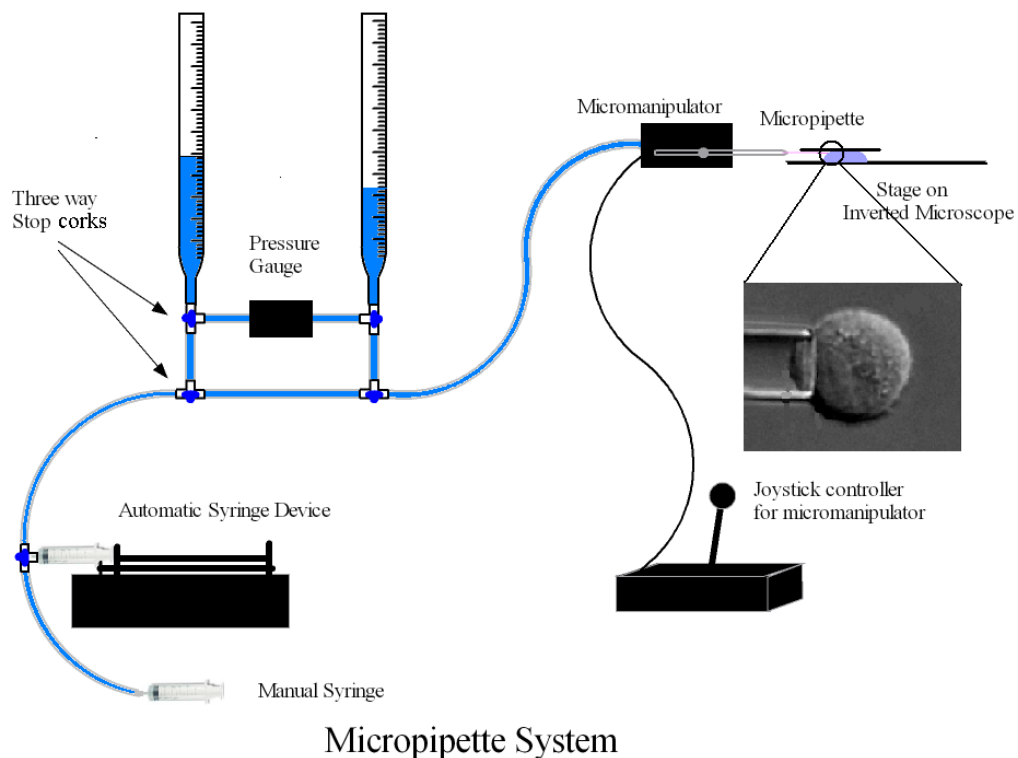
Fig. 4.1 Schematic diagram of the micropipette aspiration system set-up.

Micropipettes with diameters ranging from 6–9 μm were made from borosilicate glass

capillaries with an outer and inner diameters of 1.00 mm and 0.75 mm, respectively

(World Precision Instruments, USA). The glass capillaries were first heated and

pulled with a micropipette puller (Sutter Instrument, USA), and forged in a

microforge (ALA Scientific Instruments Inc., USA). The tips of the glass pipettes were coated with Sigmacote (Sigma Chemical Co., USA), which forms a hydrophobic thin film to prevent cell adhesion.

4.2.4 Data analysis of micropipette aspiration

The mechanical properties of living cells such as erythrocytes, chondrocytes, leukocytes and endothelial cells have been measured using micropipette aspiration (Chien, Sung et al. 1978; Schmid-Schonbein, Sung et al. 1981; Sato, Levesque et al. 1987; Jones, Ting-Beall et al. 1999) and it remains as one of the prevailing experimental techniques used to assess the mechanical properties of cells (Guck, Schinkinger et al. 2005).

(a)

(b)
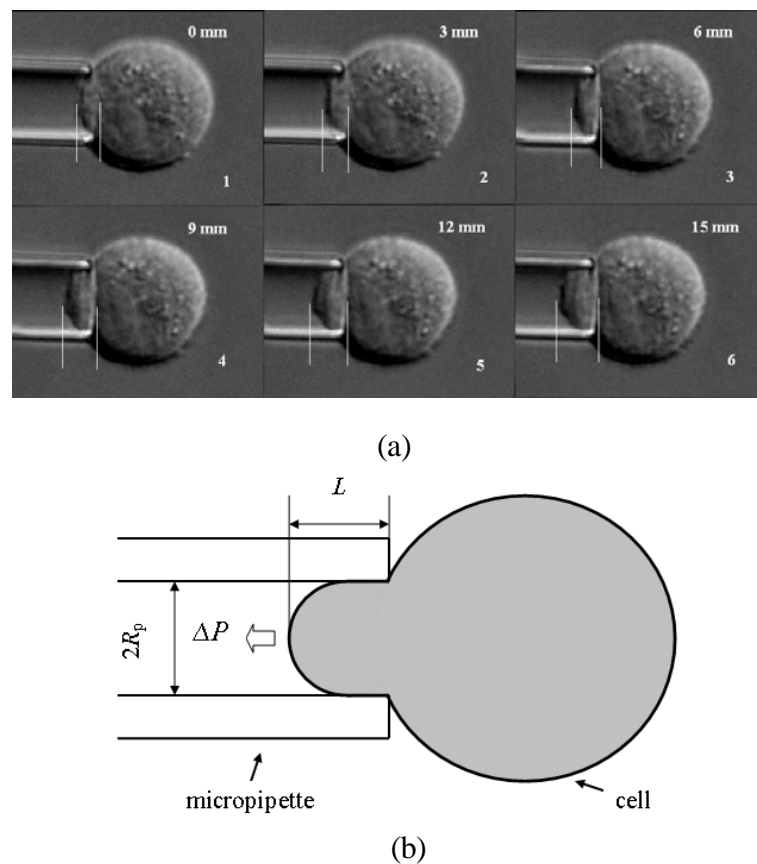
Fig. 4.2 (a) Typical sequential images of a MCF-10A cell undergoing a ramp test at suction pressure rate of 60 ml/hr and (b) a schematic diagram showing the aspiration of a cell using a micropipette.

The technique basically involves exerting a hydrostatic suction pressure, ΔP, on the circular surface of a cell through a glass pipette of radius, R_p, and aspirating the cell into the pipette (Hochmuth 2000) (see Fig. 4.2). By taking note of the aspirated length, L, the suction pressure used, ΔP, and the time taken, the time-dependent pressure-deformation relationship can then be obtained and the mechanical properties of the cell determined (Zhou, Lim et al. 2005; Lim, Zhou et al. 2006 a).

Because we are using large pipettes and small deformation, homogeneity is assumed to be still valid. In micropipette aspiration, the elastic moduli of cells are often derived from experimental results through the use of suitable mechanical models. In our case, the linear elastic half-space model (Theret, Levesque et al. 1988), which assumes that the cell behaves like an incompressible elastic medium with a half-space, was used to determine the apparent shear moduli of both MCF-7 and MCF-10A. In the half-space model (Theret, Levesque et al. 1988), using a pipette of radius R_P, the distance the cell is aspirated or projection length, L_P, is proportional to the aspiration pressure, ΔP, and inversely proportional to the apparent elastic shear modulus, G, of the cell. The model can be written as equation 4.1 or 4.2:

$$\frac{L_p}{R_p} = \frac{\Phi_P}{2\pi}\frac{\Delta P}{G} \approx 0.334 \frac{\Delta P}{G} \text{ , or} \tag{4.1}$$

$$G \approx 0.334 R_P \left(\frac{\Delta P}{L_P} \right) \tag{4.2}$$

where Φ_P is a function of the ratio of pipette wall thickness to pipette radius. Here, Φ_P $\approx$ 2.1 for the pipettes used in this study (Zhou 2006). The half-space model is attractive because the elastic modulus can be easily quantified from the aspiration data

(Theret, Levesque et al. 1988), and its ability to yield a consistent estimation of the modulus during micropipette aspiration tests when comparing between non-adherent cells of a similar geometry and under identical probing conditions (Theret, Levesque et al. 1988; Zhou, Lim et al. 2005; Zhou 2006).

4.3 Results and discussion

Aspiration tests on MCF-10A were carried out at room temperature of 21 °C. Different pipettes, ranging from 6–9 μm in diameter, were used in our study. The mean diameter of the total cell distribution used was 16.80 ± 1.95 μm (mean $\pm$ SD, number of cells used = 201).

4.3.1 Elastic shear modulus and effects of pipette size

A loading rate of 1/30 cm H_2O/s (60 ml/hr) was adapted for the aspiration tests since this value of the loading rate will produce results with higher consistency, and will enable the ramp test to be performed in the shortest time possible. The suction pressure on the cells was linearly ramped up from 0 to 15 mm H_2O in an one minute duration, and an image was captured at every one second interval. For each cell that was aspirated using a pipette of a known diameter, the projection length, L_p, was measured and plotted against the aspiration pressure, ΔP (see Fig. 4.3 (a)). The slope of the L_p–ΔP relation was determined. A mean slope value, S, was subsequently obtained using more than 15 cells. The dependence of S on pipette diameter for MCF-10A is shown in the right panel of Fig. 4.3 (b) with each data point representing an average of 15–20 cells.

(a)

(b)
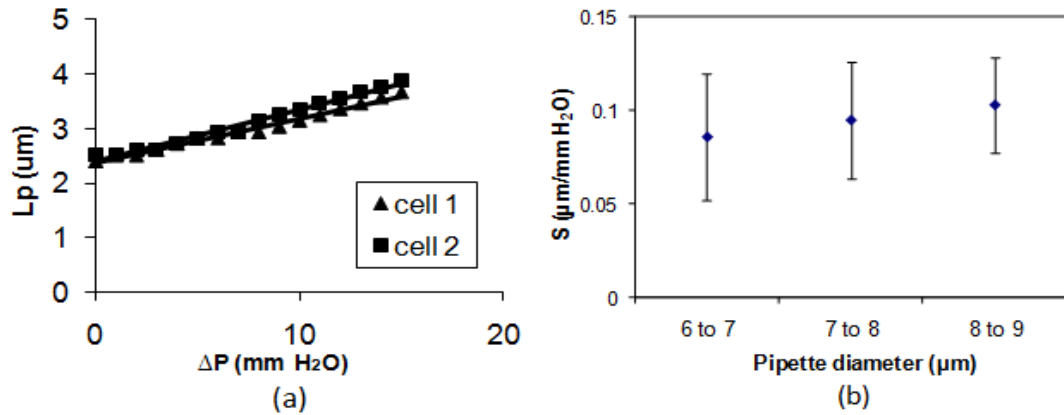
Fig. 4.3 Plots of (a) L_p against ΔP and (b) S against pipette diameter for MCF-10A at room temperature. Error bars indicate standard deviation (n = 20 cells). For illustrative purposes, only the behavior for 2 typical cells are shown in the plot of L_p against ΔP.

Similarly, aspiration tests on MCF-7 were carried out at room temperature of 21 °C using pipettes with diameter 6–9 μm. The mean diameter of the total cell distribution of MCF-7 was 17.90 ± 1.99 μm (mean ± SD, number of cells tested = 172). The slope of the L_p–ΔP relation (see Fig. 4.4 (a)) was subsequently obtained for each of the cell that was aspirated. The dependence of S on pipette diameter for MCF-7 is shown in Fig. 4.4 (b) with each data point representing an average of 15–20 cells.

(a)

(b)
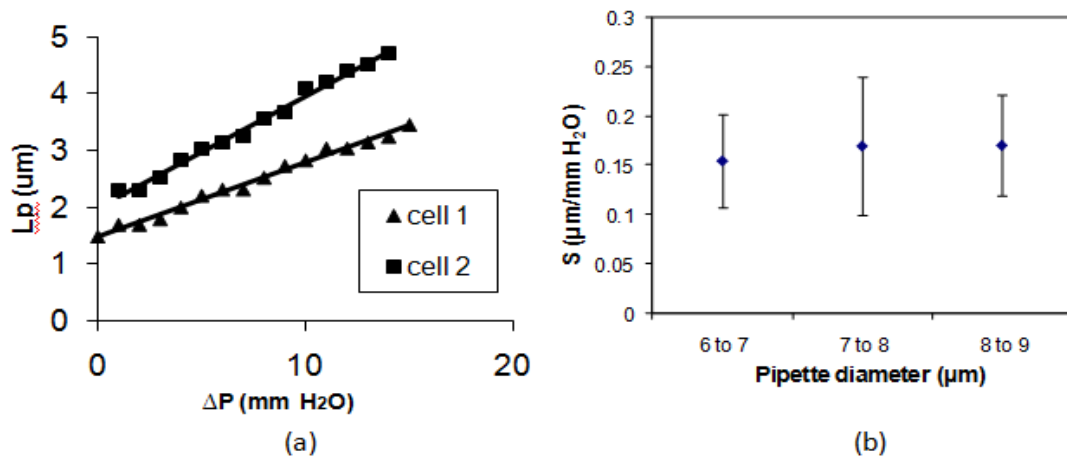
Fig. 4.4 Plots of (a) L_p against ΔP and (b) S against pipette diameter for MCF-7 at room temperature. Error bars indicate standard deviation (n = 20 cells). For illustrative purposes, only the behavior for 2 typical cells is shown in the plot of L_p against ΔP.

The apparent elastic shear modulus was then calculated for both the MCF-7 and MCF-10A cell lines at room temperature for each pipette diameter using the fact that $G = 0.334 R_p/S$ (from the half-space model) where S is the slope of the L_p–ΔP relation

62

obtained at the corresponding pipette diameter in the half-space model. The results are

shown in Fig. 4.5.
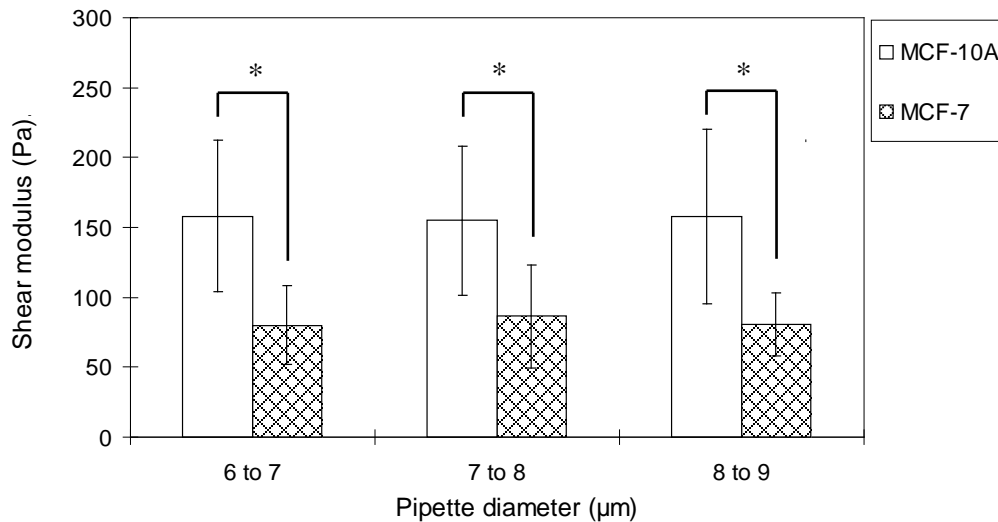
Fig. 4.5 Plot of the apparent elastic shear modulus of MCF-10A and MCF-7 against pipette diameter at room temperature (Error bars indicate standard deviation, *: $p < 0.01$).

It can be observed that the apparent elastic shear modulus of MCF-10A was found to

be between 155–158 Pa while that of MCF-7 was found to be between 80–86 Pa

using pipettes with diameters between 6–9 μm. An analysis of variance (ANOVA)

statistical test was performed to check that the three data sets for these two cell lines

obtained using pipettes of different sizes were distinguishable. The average value of

the apparent elastic shear modulus of MCF-10A determined using pipette size with

diameter 6–9 µm was 157 Pa while that of MCF-7 was 82 Pa. Thus, MCF-7 was

found to be about 2 times more deformable than MCF-10A at room temperature in

terms of the average value of the apparent elastic shear modulus. A Student's t-test

assuming unequal variance was used to check that the differences between MCF-10A

and MCF-7 were indeed significant ($p < 0.01$). These results are consistent with what

we found in chapter 3 that MCF-7 cells are more deformable than MCF-10A cells.

4.3.2 Actin structures

In light of these results and the fact that cancer is a disease which is known to alter the cytoskeleton (Guck, Schinkinger et al. 2005), confocal microscopy was subsequently used to image filamentous actin (F-actin) in MCF-10A and MCF-7 in an attempt to obtain insight into the structure of the cytoskeleton in benign and cancerous cells. For both types of breast cells MCF-10A and MCF-7, F-actin was labeled with TRITC-Phalloidin and the nucleus labeled with DAPI. Images were then taken using a confocal laser scanning microscope (Eclipse C1si, Nikon, Japan) and they are shown in Fig. 4.6. Clearly, the benign MCF-10A (see Fig. 4.6 (b)) has higher concentration of actin network than its malignant counterpart, MCF-7 (see Fig. 4.6 (a)), especially at the peripheral region, which showed a thicker layer of actin cortex. Our results are consistent with other group, which also showed that suspended MCF7 has lower amount of F-actin as compared with MCF-10A (Kim, Park et al. 2008). This change in the cytoskeletal content such as F-actin and structure of a cell will result in a change in its mechanical properties. With the onset of metastasis, the cytoskeleton is known to deteriorate from a regular and ordered structure to become irregular and compliant (Guck, Schinkinger et al. 2005). In this early stage of metastasis process, the cytoskeleton undergoes restructuring and the amount of constituent polymers making up the cytoskeleton, is reduced as well (Benzeev 1984; Rao and Cohen 1991; Cunningham, Gorlin et al. 1992; Katsantonis, Tosca et al. 1994; Moustakas and Stournaras 1999). In addition, both MCF-7 and MCF-10A has a generally large nucleus, which will be studied in the later chapters.

(a)   (b)
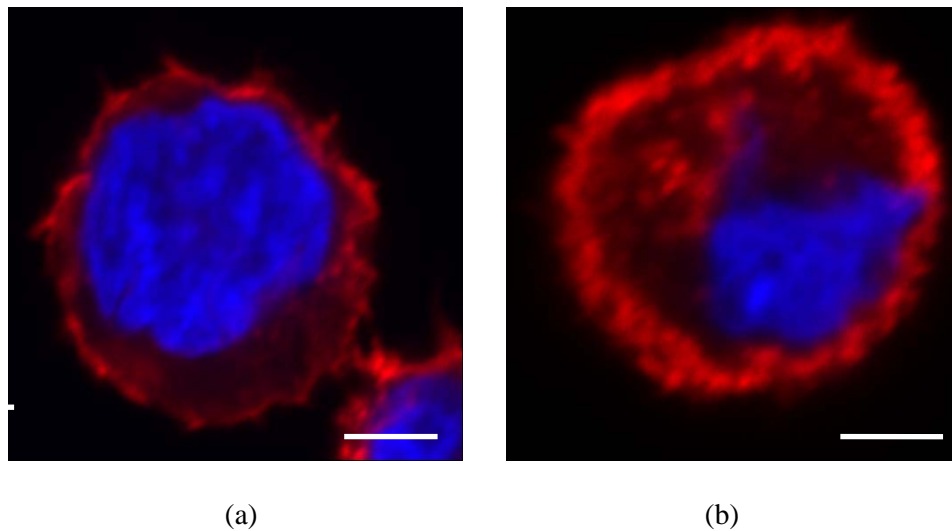
Fig. 4.6 Fluorescence confocal images showing the actin filaments (*red*) and nucleus (*blue*) in (a) cancerous MCF-7 and (b) benign MCF-10A (Scale bar represents 5 µm).

In addition, it was noted that the standard deviation in the shear modulus of MCF-10A at each pipette diameter is larger than that of MCF-7, inferring that the population variance of MCF-10A cells is larger than MCF-7. Nevertheless, MCF-10A is still commonly compared with MCF-7 because MCF-10A expressed many of the characteristics of normal breast epithelial cells and they are easy to culture. More importantly, MCF-10A and MCF-7 have been the standard model cell lines used in the study of breast cancer (Tait, Soule et al. 1990; Johnson, Torri et al. 1999; Wang, Lee et al. 2001).

4.3.3 Temperature effects

To investigate the effect of temperature on the mechanical properties of benign and malignant breast cells, the aspiration experiments were again repeated at physiologic temperature of 37 °C for both MCF-10A and MCF-7. In this case, the mean diameter of the total cell distribution for MCF-10A was 17.9 ± 2.6 µm (number of cells tested = 99) while that for MCF-7 was 18.1 ± 1.96 µm (number of cells tested = 81). The shear elastic modulus results obtained at 37 °C are shown in Fig. 4.7 together with those
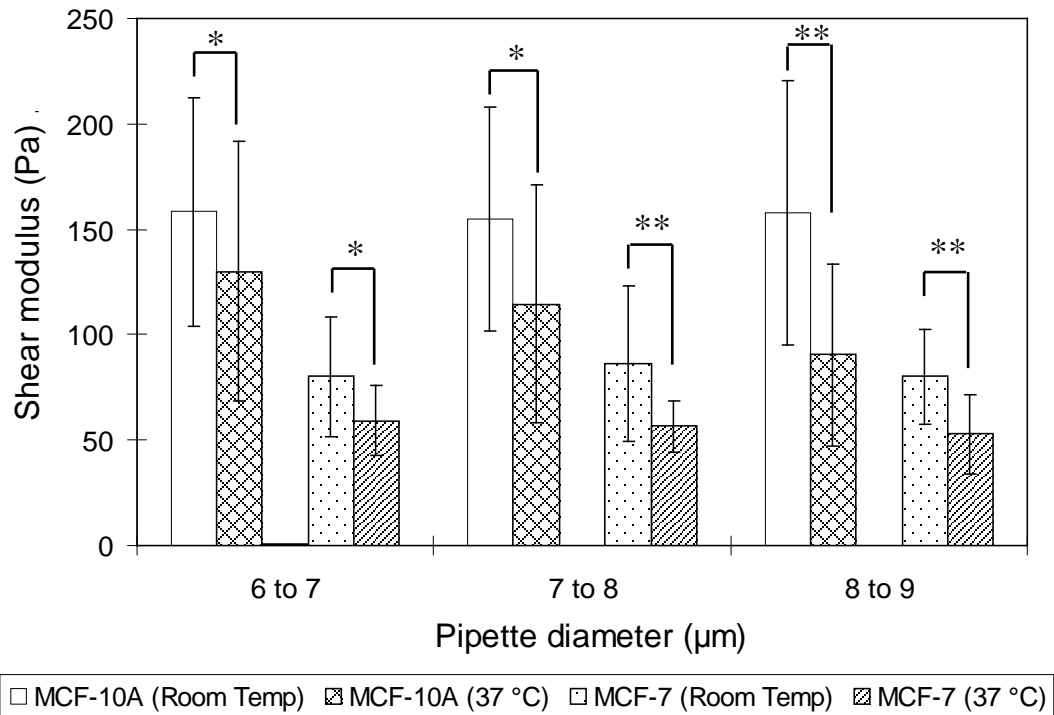
Fig. 4.7 Plot of the apparent elastic shear modulus of MCF-10A (n = 99) and MCF-7 (n = 81) determined using pipettes of various diameters at room and physiologic temperatures (Error bars indicate standard deviation, N=20) (*: $p < 0.05$, **: $p < 0.005$).

obtained at room temperature to facilitate easy comparison.

At 37 °C, the apparent elastic shear modulus of MCF-10A was found to be between 90–130 Pa while that of MCF-7 was found to be between 53–59 Pa using pipettes with diameters between 6–9 µm. Thus, increasing the temperature decreases the apparent elastic shear moduli of both MCF-10A and MCF-7. Therefore our results showed that the apparent elastic shear moduli for both MCF-10A and MCF-7 obtained at 37 °C are lower than those obtained at room temperature. A Student's *t*-test assuming unequal variance was used to check that the differences between the apparent elastic shear modulus at 37 °C and room temperature were indeed distinguishable and significant.

The cytoskeleton is a dynamic structure which is polymerized and is in a state of

constant association and dissociation (Lodish, Berk et al. 2003). At higher temperature, the rate of cytoskeleton association and dissociation may increase, and this may lead to a more active remodeling of the cytoskeleton. Thus, the cytoskeletal structure may become more compliant which results in a change in the overall elasticity of the cell.

Fig. 4.7 also shows that the apparent elastic shear moduli decrease with increasing pipette diameter at 37 °C. However, an ANOVA statistical test was carried out to check this behavior and the differences in the apparent elastic shear modulus were found to be insignificant.

The results obtained might suggest that the increased deformability exhibited by MCF-7 when compared with MCF-10A can facilitate the tumor cells to squeeze more easily into or out of the vasculature or lymphatics and possibly facilitating the intravasation and extravasation processes during metastasis, since circulating tumor cells (CTCS) do move in the blood vessels (Tan, Yobas et al. 2009).

4.4 Conclusions

In this chapter, standard quantification technique micropipette aspiration was utilized to specifically probe the near surface elastic modulus of suspended benign (MCF-10A) and cancerous (MCF-7) breast epithelial cells (n=201) under small deformation. Effects of temperature and using pipettes of different sizes were also investigated. Our results show that malignant breast epithelial cells are more deformable than their non-malignant counterparts and both of them become more compliant as temperature increases from room temperature to physiological temperature.

At room temperature, the increased deformability exhibited by MCF-7 may be attributed to the fact that its underlying cytoskeletal contents and structure are

different from that of MCF-10A, which were brought about by the malignant transformation process (Guck, Schinkinger et al. 2005). The higher temperature might have brought about a remodeling of the cytoskeleton leading to the structure of the cytoskeleton becoming more dynamic, which alters the elasticity of both MCF-10A and MCF-7. Hence, tumor breast epithelial cells are more deformable than normal breast cells at the physiological temperature of 37 °C as compared to that at room temperature.

Currently, there is very little understanding of how changes in the structure and biomechanical properties of cancer cells can contribute to cancer metastasis. A critical step in metastasis is the intravasation process, which involves primarily the migration of malignantly-transformed cells from a primary tumor site into circulation. Results obtained in this study have shown that malignant cells have less concentration and less organized actin structure as benign cells and become more deformable. The acquired increased deformability may then allow them to squeeze through surrounding tissue matrix that restricts their movement, thereby promoting the critical processes such as intravasation and extravasation of the metastatic cascade. This chapter demonstrates the difference in sub-membrane actin structure of breast cancer cells as compared with normal cells, which offers one of the reasons why cancer cells become more deformable and migrate more easily through small capillaries in the process of metastasis.

Chapter 5 AFM Indentation Study of Adherent Breast Cancer Cells

5.1 Introduction

In previous chapters, microfluidics was first utilized to investigate the overall deformability of breast cancer cells in suspension under large deformation condition. Then micropipette aspiration was utilized to specifically probe the near surface mechanical property (shear modulus) of suspended breast cancer cells, which was then attributed to the underlying actin cortex structure. However, both microfluidics study and micropipette aspiration experiment investigate cellular mechanical properties in their suspended state.

Breast cancer cells in suspension are usually in a spherical shape as we saw in previous chapters. However, they need to adhere to a substrate to grow, divide, and migrate. In the context of cancer metastasis, cancer cells which detach from the primary tumor and migrate through extra-cellular matrix and endothelial barriers are in an adherent state, while they are in suspended state when they infiltrate into the blood vessel and get transported in the blood stream. To comprehensively understand mechanical behavior of cancer cells in different physiological conditions, we need to characterize their mechanical properties not only in suspension but also in their adherent state.

With the recent advances in biomechanics and nanotechnology, a variety of experimental techniques have been developed to study single cell mechanics. For example, biophysical tools and techniques such as atomic force microscopy (Lekka, Laidler et al. 1999; Lekka, Laidler et al. 2001; Park, Koch et al. 2005), micropipette aspiration (Ward, Li et al. 1991; Zhang, Long et al. 2002), and the optical stretcher (Lincoln, Erickson et al. 2004; Guck, Schinkinger et al. 2005) have been used to

probe the mechanical property of different types of cells (see (Van Vliet, Bao et al. 2003; Lim, Zhou et al. 2006 a; Lee and Lim 2007) for reviews). Also, mechanical models have been developed to study the mechanical properties of these cells (Lim, Zhou et al. 2006 b). Among them, micropipette aspiration and optical stretcher are designed to study cells in suspension. Here, we chose AFM to study breast cancer cell at adherent condition.

AFM has long been established as a versatile tool for imaging and measuring nanoscale elastic properties of adherent living cells (Radmacher, Fritz et al. 1996; A-Hassan, Heinz et al. 1998). In addition, AFM has been applied to investigate the mechanical properties of *ex vivo* cancer cells obtained from patients (Cross, Jin et al. 2007). Lekka *et al*. used the atomic force microscope (AFM) to study the elasticity of normal human bladder epithelial cells (Hu609 and HCV29) and cancerous ones (Hu456, T24 and BC3726) by AFM indention of these cells (Lekka, Laidler et al. 1999). They found that normal cells are an order of magnitude stiffer than normal cells, which was attributed to the reorganization of the cytoskeleton.

As reviewed earlier, Lincoln *et al*. were the first to investigate the deformability of non-malignant and malignant human breast epithelial cells using the optical stretcher (Lincoln, Erickson et al. 2004; Guck, Schinkinger et al. 2005). However, optical stretcher including our studies in the previous chapters using microfluidics and micropipette aspiration only investigated mechanical properties of cells in suspension. No studies on mechanical properties of adherent breast cancer cells (MCF-10A and MCF-7) have been done.

The objective of this chapter is to investigate the cytoskeletal structure and mechanical properties of non-malignant (MCF-10A) and malignant (MCF-7) human

breast epithelial cells in adherent state using AFM and confocal microscopy. We will quantify and compare the apparent Young's modulus of these cells and investigate their corresponding sub-membrane cytoskeletal structures. In addition, the effects of different loading rates during indentation will be presented.

5.2 Methods

5.2.1 Cell culture and sample preparation

Cell culture was the same as that for microfluidics and micropipette aspiration experiments as details in section 3.2.1. For the indentation studies, cells harvested from the subculture were seeded on sterilized 12 mm coverslips (Heinz glass, Germany) and kept in a 6-well microplate (IWAKI, Japan) which would stay in the incubator for 2–3 days prior to indentation. The medium was changed one day after seeding to clear any dead cells on the coverslip.

5.2.2 Confocal fluorescence imaging

For confocal fluorescence imaging, the coverslips with cells seeded on them were prepared using a protocol which is similar to the protocol adapted for indentation studies (5.2.1). The staining protocol was the same as described in section 4.2.2.

5.2.3 AFM indentation

A Nanoscope IV multimode AFM with a picoforce scanner (Digital Instruments Inc., USA) was used to carry out the experiments. For AFM contact mode imaging, a silicon nitride AFM tip with a spring constant of 0.01 N/m was used. For AFM indentation, a modified silicon nitride AFM cantilever (NovaScan, USA) having a spring constant of 0.01 N/m with a 4.5 μm diameter polystyrene bead adhered to the

tip was used to indent the cells. A spherical bead indenter was used here instead of a sharp tip to get better assessment of cell elasticity by averaging over a larger cell surface area with a well-defined contact geometry (Mahaffy, Park et al. 2004; Smith, Tolloczko et al. 2005). In addition, smaller local strains applied arising from the spherical bead can reduce the possibility of nonlinear or destructive deformation to the cell (Dimitriadis, Horkay et al. 2002). During the experiment, the glass coverslip was mounted on the AFM stage and the cells were kept in their culture medium using a standard fluid cell (Digital Instruments Inc., USA). A heater (Digital Instruments Inc., USA) was used to maintain the sample at physiological temperature (37 ºC) during indentation.

Indentation was carried out at the cell centre using different loading rates from 0.03 to 1 Hz. The ramp size used in this study was 3 µm (Costa 2003) and an indentation force of 0.2 nN was applied during the tests in order to ensure that a small deformation was exerted on the cell and minimize any substrate contributions.

5.2.4 Data analysis

Fig. 5.1 schematically depicts the indentation carried out on the centre of a cell using a 4.5 µm diameter bead attached to an AFM cantilever. The relationship between the indentation depth and Z stage position is also illustrated (Indentation depth = Z – cantilever deflection). Fig. 5.2 shows the relative deflection versus indentation depth curve.
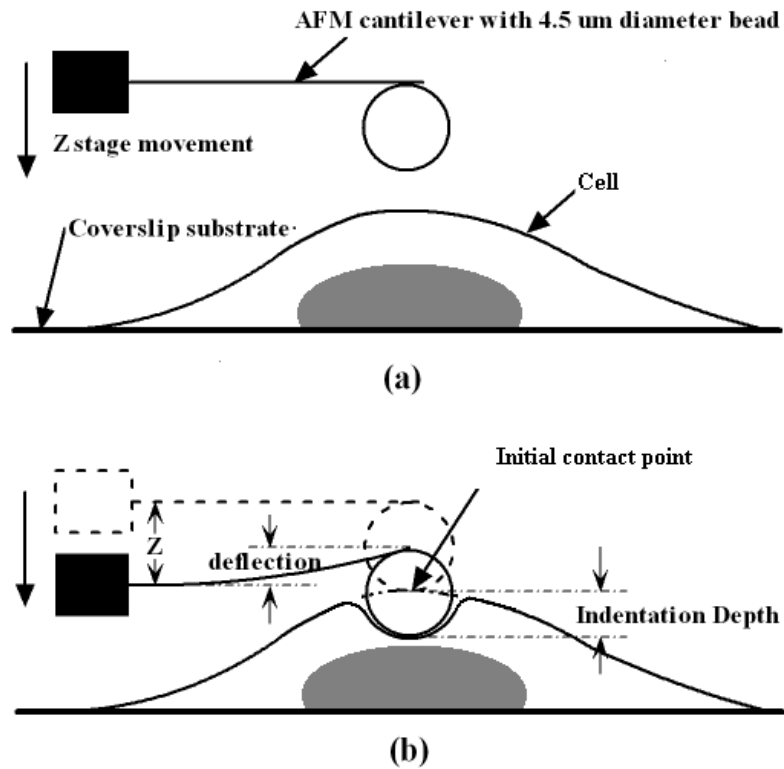
Fig. 5.1 (a) Schematic of the indentation of a cell using a 4.5 µm diameter spherical probe. (b) An illustration showing that the indentation depth is given by the difference between the z stage position and the cantilever deflection.
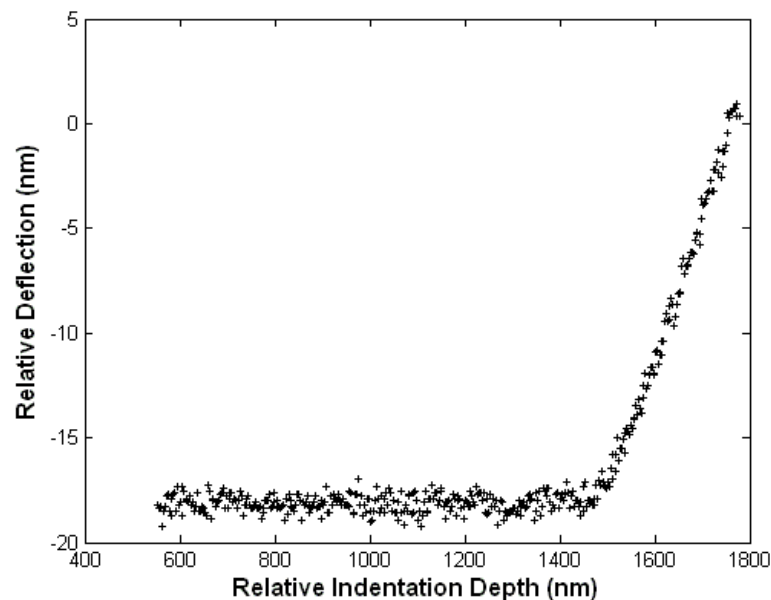
Fig. 5.2 Plot of relative cantilever deflection versus indentation depth curve obtained from the approaching curve of the AFM indentation experiment.

The Young's modulus was subsequently determined using Hertz's contact model, since this model is able to account for the geometry of the spherical probe (Costa 2003; Smith, Tolloczko et al. 2005) used in this present study and it has been used extensively in other AFM studies to evaluate the Young's modulus of cells (Rotsch, Jacobson et al. 1999; Costa 2003). Here, Hertz's model is used to study the small deformation behavior of a cell being indented by a hard axisymmetric indenter (Mahaffy, Park et al. 2004):

$$F = \frac{4}{3} \frac{E}{\left(1 - v^2\right)} \sqrt{R\delta^3} \qquad (5.1)$$

where F is the indentation force, E is the Young's modulus to be determined, v is the Poisson ratio, R is the radius of the spherical bead, and δ is indentation depth. The cell was assumed incompressible and a Poisson ratio of 0.5 was used (Costa 2003).

Before we use Hertz's model to extract the Young's modulus, we must first determine the contact point. Contact point is defined as the point where the probe first makes contact with the cell surface and the cantilever starts to deflect. As the initial deflection after the contact point is small and nonlinear for a soft sample, it will be difficult to determine the contact point (Dimitriadis, Horkay et al. 2002). Accurate identification of the contact point is very crucial in correctly calculating the Young's modulus using Hertz's model (Costa 2003; Crick and Yin 2007). As we can see in the relative deflection versus indentation depth curve, the noise level is also a factor which will affect the accurate determination of the contact point and possibly give rise to any error in the calculation of the Young's modulus. So we develop a method to fit the experiment data to get the contact point and obtain Young's modulus at the same time while reducing the native noise effect.

From the principle of AFM indentation, we know that:

$$F = CD \cdot k \tag{5.2}$$

$$CD = RD - RD_0 \tag{5.3}$$

$$\delta = RID - RID_0 \tag{5.4}$$

where CD is the AFM cantilever deflection, k is the spring constant of the cantilever, RD is the relative deflection of the cantilever, RID is the relative indentation depth, and (RID_0, RD_0) is the coordinates of the contact point. Substituting (5.2), (5.3), (5.4) into (5.1), we can get:

$$RD = \frac{4E\sqrt{R}}{3(1-v^2)k}\left(RID - RID_0\right)^{1.5} + RD_0 \tag{5.5}$$

$$\begin{cases} RD = \dfrac{4E\sqrt{R}}{3(1-v^2)k}\left(RID - RID_0\right)^{1.5} + RD_0 & RID \geq RID_0 \\ RD = a(RID - RID_0) + RD_0 & RID < RID_0 \end{cases} \tag{5.6}$$

A straight line is used to fit the region before the contact point as theoretically, there is no cantilever deflection in that region. Combining this with (5.5), we have (5.6) which can be used to fit the data and get parameters including the contact point (RID, RD_0) and Young's modulus E as shown in Fig. 5.3.
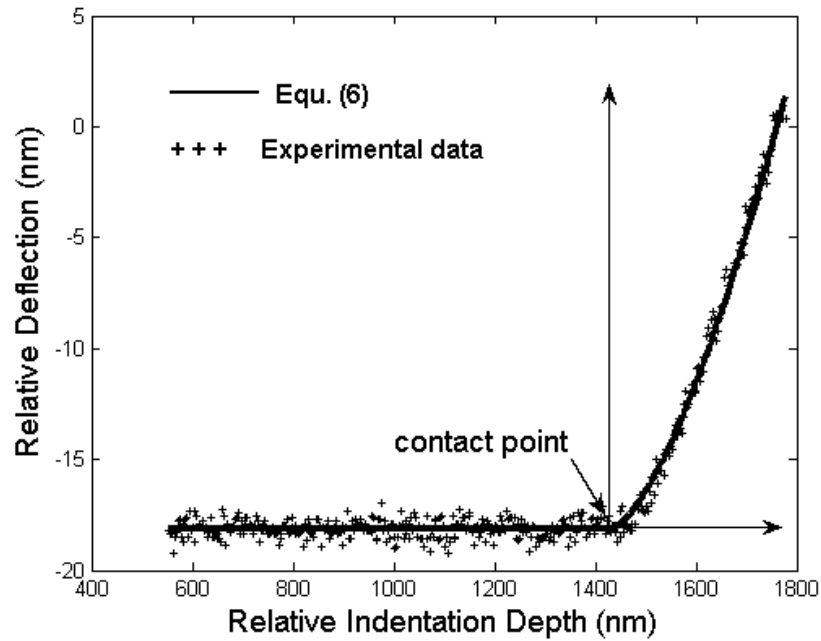
Fig. 5.3 Graph illustrating curve fitting using a theoretical line to detect he contact point.

This method provides a very good fit to the experimental data and it also allows for the systematic determination of the contact point. Moreover, noise is reduced significantly based on the theoretical model and no possible filter induced error is introduced (Nyland and Maughan 2000).

5.3 Results and discussion

This section presents the results obtained from the AFM indentation carried out on two human breast cell lines MCF-10A (benign) and MCF-7 (malignant), using different loading rates. Also, the sub-membrane structures of these cells were investigated using both AFM and confocal fluorescence microscopy. The effect of using different loading rates on the apparent elasticity of these cells and the structure-mechanical property correlation will be subsequently discussed.

5.3.1 Apparent Young's modulus and effects of loading rates

As the contact point has been identified using the method described in section 2.2, the relative deflection versus relative indentation depth curve can be converted to a plot of indentation force against indentation depth. Fig. 5.4 shows the force versus indentation depth curves at different loading rates (from 0.03 Hz to 1Hz). These curves describe the apparent elasticity of the cell according to the loading rate in a qualitative way. For the same amount of force applied, the indentation depth decreases as the loading rate was increased from 0.03 to 1 Hz. This suggests that cells appear to be stiffer at a higher loading rate, which will be described in detail later.
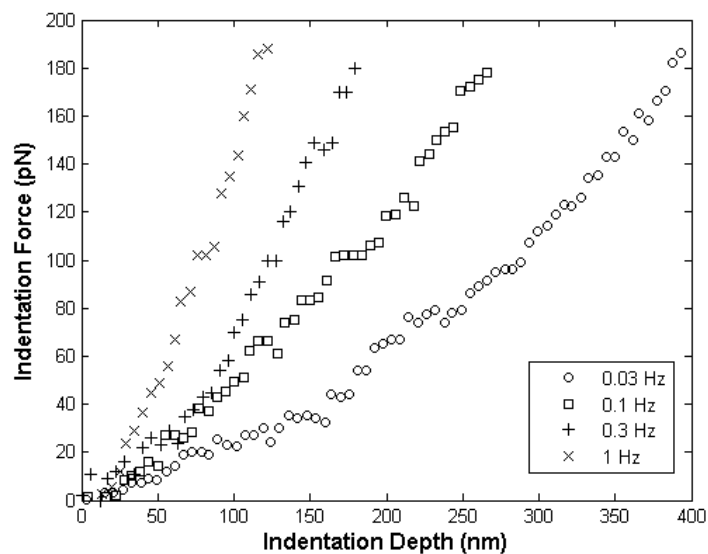
Fig. 5.4 Indentation force versus indentation depth curves of MCF-10A cells at different loading rates.

To investigate the loading rate effect, the apparent Young's modulus calculated according to the method described in section 2.2 was used to characterize the elasticity of the cells. Apparent Young's modulus at different loading rates is used to characterize cell elasticity due to the viscous contributions of the cellular mechanical response (Costa and Yin 1999; Lieber, Aubry et al. 2004). The dependence between

the apparent Young's modulus and the loading rates used in this present study for both MCF-10A and MCF-7 at the physiological temperature of 37 ºC was shown in Fig. 5.5. It is evident that higher values of the apparent Young's modulus were associated with an increased loading rate for both MCF-10A and MCF-7. The cells appear to be stiffer when probed using a higher loading rate due to the contribution of cell viscosity (Maksym, Fabry et al. 2000; Fabry, Maksym et al. 2001; Alcaraz, Buscemi et al. 2003; Desprat, Richert et al. 2005; Smith, Tolloczko et al. 2005; Trepat, Grabulosa et al. 2005; Roca-Cusachs, Almendros et al. 2006). Previous indentation works (see (Lekka, Laidler et al. 1999; Lekka, Lekki et al. 1999; Park, Koch et al. 2005)) carried out on other types of cancerous cells and fibroblasts did not take into account this dependence of the apparent Young's modulus on the loading rate. Our study shows that the loading rate used needs to be carefully considered when characterizing cell elasticity using AFM indentation, because the apparent Young's modulus characterized in different studies may not be comparable due to this effect. At the physiological temperature of 37 ºC, the apparent Young's modulus of MCF-10A is about 1.5 times higher than that of MCF-7 at the same value of the loading rate.
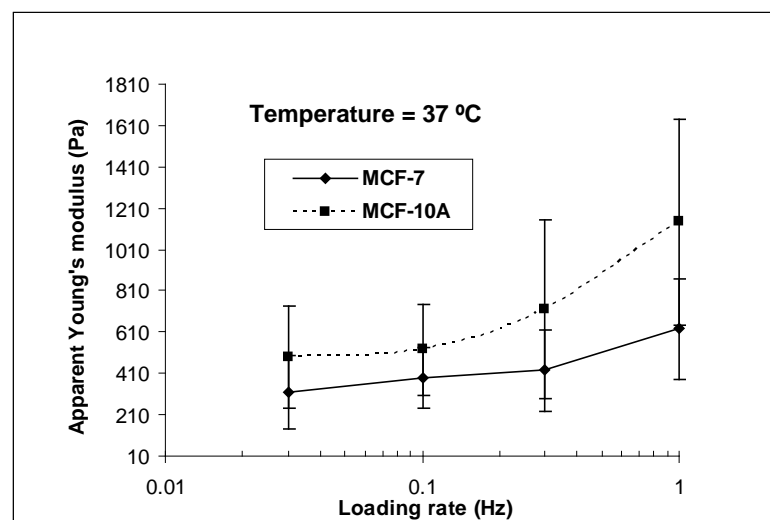
Fig. 5.5 Plot of the apparent elastic modulus against loading rate for MCF-10A and MCF-7 at 37 ºC (Error bars indicate standard deviations).

5.3.2 Temperature effect
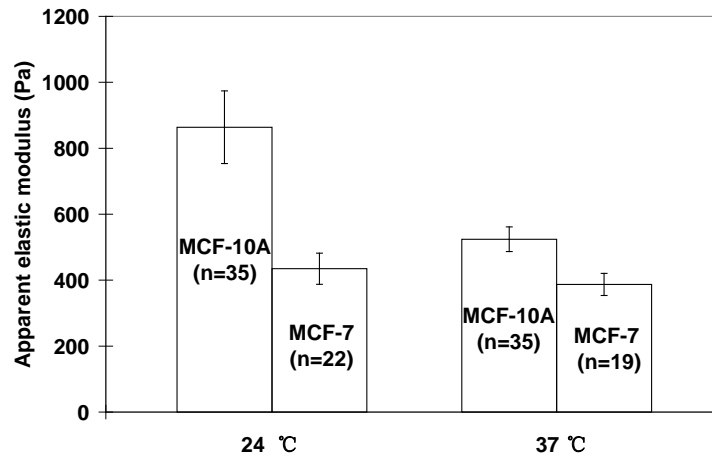
Fig. 5.6 Apparent elastic modulus of MCF-10A and MCF-7 cells tested at different temperatures and at a loading rate of 0.1 Hz. Error bars indicate standard error and n denotes the number of samples tested.

Fig. 5.6 shows the stiffness of cells, determined using indentation, at both room temperature and 37°C. It can be observed that the apparent elastic modulus is smaller at a higher temperature. For MCF-10A at 37 °C, the apparent elastic modulus is about 1.6 times smaller than the corresponding value at room temperature. In addition, we can also observe that MCF-7 is more deformable than MCF-10A at both 24 °C and 37 °C. Thus it is evident that temperature does have an effect on the mechanical properties of cells and it needs to be taken into account during probing cell elasticity. The temperature effect is consistent with what we observed in our micropipette aspiration experiments, which means temperature has an effect on cell mechanics whether they are in suspended state or adherent state.

Actin is a major component of the cellular cytoskeleton system (actin filament, intermediate filament, microtubule) and contributes significantly to the mechanical properties of the cell. In addition, actin structure is a highly dynamic structure and is strongly correlated with dynamic events such as migration and proliferation (McGrath

and Dewey 2006). The reduced stiffness of both benign and cancerous cells as temperature increases may be attributed to the remodeling of the actin structure and a change occurring in its dynamic state due to the temperature change.

5.3.3 Structure-property relationship

In this section, we seek to establish a structure-mechanical property-disease correlation in the context of malignant transformation of breast epithelial cells. Cell mechanics can indicate the state of the cellular cytoskeletal structure and dictates its function (Elson 1988; Lekka, Laidler et al. 2001). Organization of the cytoskeleton is also an important reflection of cellular mechanical organization (Heidemann, Lamoureaux et al. 2000; Ingber 2000). Actin filaments, microtubules and intermediate filaments are three major components of the cellular cytoskeleton. In particular, actin filaments can form contractile bundles called stress fibers with one end inserted into the plasma membrane forming focal adhesion points. Hence, there is a close relation between cell mechanics and cellular cytoskeleton. The cytoskeletal structure just beneath the cell surface membrane forms the region of interest which we would like to study, as our indentation imposed is minute with force in the pico-newton range (200 pico-newtons) and deformation in the nanometer level (below 500nm in depth).

5.3.3.1 AFM imaging

Contact mode AFM imaging was used to investigate the central region of a typical live MCF-7 and MCF-10A cell (Fig. 5.7). AFM can be used as an indenter and also a powerful high resolution imaging tool. Basically AFM is a mechanically sensitive surface probe, and local mechanical property differences on the sample can lead to differential surface deformation and contribute to image contrast. During the raster

scan of the AFM imaging, the AFM tip will press against the soft cell membrane into the cytosol until the membrane is supported by the underlying stiffer structures, which results in the sub-membrane structures appearing elevated and showing up in the deflection images (Hofmann, Rotsch et al. 1997; Rotsch, Jacobson et al. 1999). Hence AFM images of live cells can reveal the sub-membranous structure, in particular the stiffer filamentous structures that may be present.

(a)   (b)

(c)   (d)
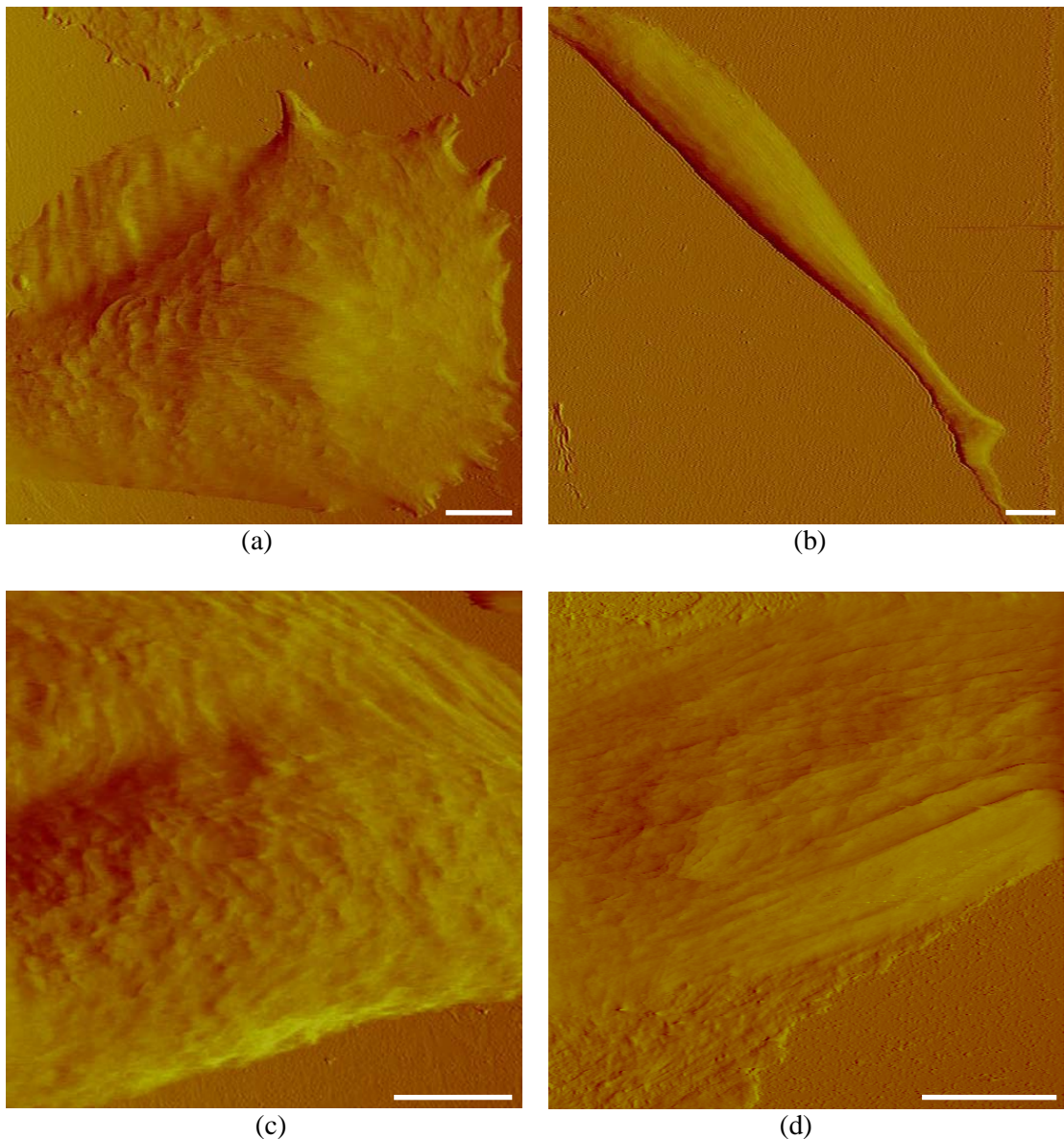
Fig. 5.7 AFM deflection image (mechanically based contrast) of a (a) MCF-7 and (b) MCF-10A cell and the central region of a (c) MCF-7 and (d) MCF-10A cell (Scale bar represents 5 µm).

The AFM deflection images shown in Fig. 5.7 provide a picture of the cellular mechanical organization of the sub-membrane structure. Cancerous MCF-7 cells have a rounded morphology (Fig. 5.7 (a)), while benign MCF-10A cells have an elongated shape (Fig. 5.7 (b)). We can see in Fig. 5.7 (d) which shows the AFM image of MCF-10A that there are well aligned stiffer filamentous structures protruding below the membrane. While in MCF-7 (Fig. 5.7 (c)), we cannot see such filamentous structures but only disorganized ridges can be observed. This may explain why MCF-10A is stiffer than MCF-7 as there is an enhanced filamentous structure organized under the cell membrane to support the MCF-10A cells but not for MCF-7. Presumably, the observed filamentous structures are actin stress fibers as actin structure is the major component of cytoskeleton which localizes underneath the cellular membrane (Lekka, Laidler et al. 1999).

5.3.3.2 Confocal fluorescence imaging

In this section, we chose to further investigate the actin structure of cytoskeleton as the structures observed in AFM image (Fig. 5.7 (d)) are most possibly stress fibers. The observed filamentous structure in MCF-10A which composed of long filaments across the whole cell possesses the feature of stress fibers. In addition, actin filamentous structure is a major component of the cellular cytoskeleton system which contributes significantly to the mechanical properties of the cell (Janmey 1998). Studies have shown that the actin network formed by actin filaments or stress fibers plays a crucial role in the mechanical stability of live cells (Rotsch, Braet et al. 1997; Rotsch and Radmacher 2000). Also it is localized at the periphery of the cell near the membrane, which is the region of interest of our nanometer level deformation on the cell surface. In order to have a better insight of the actin structure of these two cell

lines, we studied the fluorescence confocal images of MCF-10A and MCF-7 in which

F-actin was labeled with TRITC-Phalloidin (red) and the nucleus labeled with DAPI

(blue).

(a)   (b)

(c)   (d)

(e)   (f)
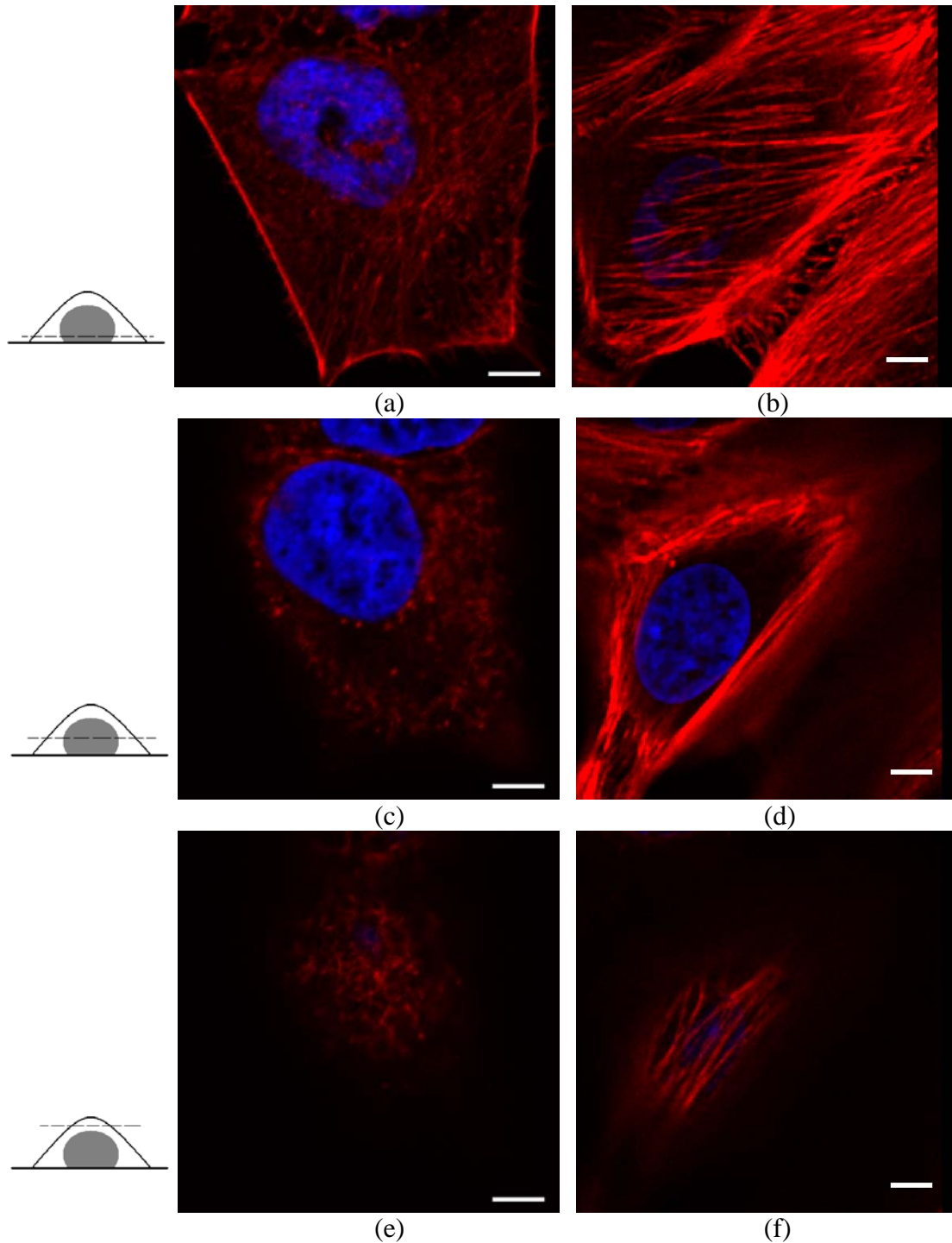
Fig. 5.8 Confocal microscopy planes of F-actin (red) in fixed (a, c, e) MCF-7 and (b, d, f) MCF-10A cells at different section, (a) (b): basal section, (c) (d): medium section, (e) (f): apical section (Scale bar represents 10 µm).

From the confocal fluorescence images of F-actins from the basal section to the apical section in MCF-7 and MCF-10A (see Fig. 5.8), it can be seen that generally MCF-10A possesses a more pronounced network of actin filaments than MCF-7. In MCF-10A, F-actin is more localized on the peripheral region (see Fig. 5.8 (d)) and form organized parallel filamentous structure. On the contrary, the actin structure in MCF-7 is a more disorganized and cross-linked network with no striations although there are fewer actin filaments existing at the basal plane of the cell. This may imply that malignant cells are generally in a more 'relaxed' state while non-malignant cells tend to be in a more pre-stressed state (Kumar, Maxwell et al. 2006). Our fluorescence images showed that there is a reduction in the organized actin filaments in MCF-7 and it may be one reason that MCF-7 is more deformable than MCF-10A.

In addition, there is a well-aligned actin filamentous structure at the apical plane of the MCF-10A cell (Fig. 5.8 (f)), while in the MCF-7 cell, F-actin seems to be a randomly organized network (Fig. 5.8 (e)). In particular, we can see in Fig. 5.8 (b) that the actin filaments on the basal section are not parallel to the actin filaments on the apical section shown in Fig. 5.8 (f). However, the actin filaments on the apical section (Fig. 5.8 (f)) are parallel to the long axis of the spreaded cell which is the same as those filamentous structures shown in AFM image (Fig. 5.7 (d)). This is an indication that for MCF-10A the sub-membrane filamentous structures observed in AFM images are stress fibers composed of actin filaments. We can also see similar features for MCF-7 as the disorganized actin network in the apical section in Fig. 5.8 (e) manifest in AFM image (Fig. 5.7 (c)) in terms of random ridges. By comparing apical plane images in Fig. 5.8 (e) (f) with the AFM images in Fig. 5.7, we can see quite similar features for both MCF-7 and MCF-10A, which is another indication that sub-membranous structures can be revealed by AFM. This finding is also consistent

with other studies, which show that in adherent cells such as fibroblasts, chicken cardiocytes and glial cells, the filamentous structure visualized by AFM corresponds to actin stress fibers (Henderson, Haydon et al. 1992; Hofmann, Rotsch et al. 1997; Rotsch and Radmacher 2000). Our AFM images and confocal fluorescence images show that MCF-10A cells have more well-defined stress fibers than MCF-7 cells, which exhibits a stronger actin filamentous network in MCF-10A. This is a significant change in cellular structural feature as benign human MCF-10A breast epithelial cells transform to malignant MCF7 cells, which may be one of the reasons for the corresponding change in the mechanical property.

Interestingly, AFM images of more motile cells like rat liver macrophages show that such filamentous structures cannot be found (Rotsch, Braet et al. 1997), and more motile fibroblasts have a less pronounced network of stress fibers (Rotsch, Jacobson et al. 1999; Rotsch and Radmacher 2000). The presence of less filamentous structures in MCF-7 suggests that malignant human breast epithelial MCF-7 cells have a high potency to migrate like the findings for other motile cells, which is also an important difference between cancer cells and normal cells.

5.4 Conclusions

In this chapter, atomic force microscopy (AFM) indentation was carried out to characterize the elasticity of benign (MCF-10A) and cancerous (MCF-7) human breast epithelial cells at their adherent condition. In addition, AFM imaging and confocal fluorescence imaging were used to further investigate their corresponding sub-membrane cytoskeletal structure. Our results show that malignant (MCF-7) breast cells have an apparent Young's modulus about twice lower than that of their non-malignant (MCF-10A) counterparts at physiological temperature (37 ℃), and their

apparent Young's modulus increase with loading rate. The confocal and AFM images both show a significant difference in the organization of their sub-membrane actin structures, which might contribute to their difference in mechanical properties.

Moreover, an improved method was developed to analyze the indentation curves of MCF-10A and MCF-7 cells based on Hertz's model. Although assumptions like homogeneous, isotropic, linear elastic material cannot be exactly fulfilled when applying the Hertz's model to analyze data obtained from the AFM indentation experiments carried out on cells, it is currently the most accepted model and many studies showed that it is able to describe the experimental data sufficiently under small deformation (Kuznetsova, Starodubtseva et al. 2007). Also in our study, we found that Hertz's model can fit our experimental data very well and this model is sufficient to give us a relatively good comparison between the apparent elasticity of MCF-7 and MCF-10A cells at the same loading rate.

In addition, loading rate effect is an important factor which needs to be considered during AFM indentation test. Apparent Young's modulus instead of "absolute" Young's modulus is used to characterize and compare the relative elasticity of the cells at different loading rates. Our indentation results which were obtained using different loading rates, continued to show that cancerous MCF-7 is more deformable than benign MCF-10A at different loading rate.

Cancerous MCF-7 cells are more deformable than non-malignant MCF-10A cells due to the oncogenic transformation process causing a change in cellular structure. The reduced stiffness of these cancer cells compared with benign ones may be partially contributed by a significant reduction in the amount of well-defined actin filaments or their bundles (stress fibers), which results in a weaker cytoskeletal structure. The

combination of AFM (both as indenter and high resolution imaging tool) and fluorescence microscopy has proven to be very useful in studying the mechanical property and corresponding structures. In particular, AFM image which is force-based in nature can be used to investigate the cellular sub-membrane structure like stress fibers.

Our work demonstrates that there is a structural change in the actin network of cancer cells in adherent condition, which is also seen in previous chapter as they are in suspension. This change may aid in facilitating easy migration and invasion during metastasis. However, the difference in cytoskeletal structure may only be one of the reasons causing the change in cellular mechanical property and internal cellular components such as the nucleus will be further studied.

Chapter 6 AFM Indentation Study of Isolated Nuclei of Breast Cancer Cells

6.1 Introduction

As shown in previous chapters, near surface mechanical properties of breast cancer cells both in suspension and in adherent condition have been probed using micropipette aspiration and AFM, respectively. The underlying cytoskeletal structures (actin cortex) have been investigated using confocal microscopy, and the difference in actin structure contributes to the difference in the mechanical properties probed. However, as we discussed in the introduction and microfluidic study chapters, nucleus is also an important contributor to the overall mechanical behavior of cancer cells. So we first characterize the mechanical properties of isolated nucleus and compare that with the whole cell.

Nucleus is known to be the most important organelle inside the cell as it contains the 'secret of life' (DNA) and it is a site of major metabolic activities, including DNA replication, gene transcription, RNA processing and ribosome subunit maturation and assembly. More than its functional role, nucleus has gradually been found also to be important as a structural component inside the cell. Consequently, nuclear mechanics has attracted more and more attention in recent years (Lammerding J 2007; Dahl, Ribeiro et al. 2008). Nucleus has been found to play an important role in contributing to the whole cell mechanical behavior (Caille, Thoumine et al. 2002; Sugitate, Kihara et al. 2009). Moreover, experimental findings suggest that nucleus is directly involved in mechanotransduction (Dahl, Ribeiro et al. 2008). As evidence already show that there are physical connections from the surface adhesion molecule (integrin receptor) to the cytoskeleton (actin filament) and finally the nucleus (Maniotis, Chen et al.

1997). This physical connection may serve as a channel to transmit the mechanical signals (stress or strain) received by the adhesion molecule, from outside of the cell directly to the nucleus and regulate gene expression. Therefore, any change in the nuclear structure can cause impaired nuclear mechanics and alter the mechanotransduction pathway leading to certain diseases. One typical example is laminopathies, which are a group of diseases caused by the mutation of the nuclear lamin A/C gene leading to impaired mechanical integrity of nucleus.

Understanding the nuclear mechanics and its contribution to cell mechanics, of course, will be the first step in revealing the role of nucleus in mechanotransduction and the pathology of certain disease related to malfunction of nucleus.

As reviewed in chapter 1, nucleus is separated from cytoplasm by a nuclear envelope. The nuclear envelope consists of an inner nuclear membrane (INM), an outer nuclear membrane (ONM, an extension of rough endoplasmic reticulum (ER)) and nuclear lamina (Prokocimer, Margalit et al. 2006). The nuclear lamina, which is the major structural component of nuclear envelope, is a dense network of lamins plus lamin-associated proteins lying beneath the INM. Lamins are part of the intermediate filament (IF) gene family and are thought to be the evolutionary progenitors of IF proteins. The IF gene super family comprises five groups with about 60 members. Group I-IV are cytoplasmic IF, and lamins belongs to the group V IF family. Lamins are classified into types A and B according to their difference in biochemical properties, expression pattern and behavior during mitosis (Stuurman, Heins et al. 1998). A-type lamins, which include lamin A and C, are products of alternative splicing from the *LMNA* gene, and B-type lamins are encoded by 2 separate genes, *LMNB1* and *LMNB2*. Type B lamins are present in all mammalian cells as they are

essential for cell viability, but type A lamins are developmentally regulated. Type A lamins are absent in human embryonic stem cells, but are expressed only after cells differentiate and generally increased during terminal differentiation and grow arrest (Prokocimer, Margalit et al. 2006).

Lamins are very important in their contribution to nuclear structure. They not only determine nuclear integrity, but are also involved in numerous nuclear functions. Especially, A-type lamins play a major role in maintenance of nuclear shape (Dahl, Scaffidi et al. 2006; Lammerding, Fong et al. 2006; Scaffidi and Misteli 2006), stability (Dahl, Kahn et al. 2004; Lammerding, Schulze et al. 2004; Broers, Kuijpers et al. 2005) and structural integrity (Broers, Kuijpers et al. 2005; Lammerding, Fong et al. 2006; Stewart, Roux et al. 2007). Moreover, lamins regulate and support protein complexes involved in gene expression, nuclear positioning (Meaburn and Misteli 2007), DNA replication, transcription and repair (Parnaik and Manju 2006), and aging (Scaffidi and Misteli 2006).

In the context of cancer, the nuclear lamina is involved in many nuclear activities which are implicated in tumor formation including transcriptional activation, heterochromatin organization, senescence and apoptosis (Moss, Krivosheyev et al. 1999). It has been found that there are dramatic changes in nuclear architecture including nuclear size and shape, numbers and sizes of nucleoli, and chromatin texture, during malignant transformation (Zink, Fischer et al. 2004). In fact, the irregularity of cancer nucleus was observed long time ago and it was quite a common feature for many types of cancer. Nuclear morphology analysis has been used to detect certain type of cancer since the 19th century (Zink, Fischer et al. 2004). Deviation of the nuclear lamins and their associated proteins are thought to be an

additional event involved in malignant transformation and tumor progression, which can be a potential novel target for anti-cancer drug development (Prokocimer, Margalit et al. 2006).

The absence or low levels of type A lamins are often observed in many types of human hematological malignancies. For non-hematological malignancies, the main changes are aberrant localization and reduction in expression of lamins A/C, which are frequently correlated with aggressiveness of cancer, proliferation rate and differentiation state. Lamin A/C has been found to be reduced in some skin cancers (basal cell and squamous cell) (Venables, McLean et al. 2001; Oguchi, Sagara et al. 2002), gastrointestinal tract neoplasms including adenocarcinoma of stomach and colon, lung cancer (Kaufmann, Mabry et al. 1991; Broers, Raymond et al. 1993), testicular germ cell tumors (Machiels, Ramaekers et al. 1997), cancerous prostate tissues (Coradeghini, Barboro et al. 2006). And it is also reduced in breast cancer (Moss, Krivosheyev et al. 1999). However, they are not sufficiently specific to be used in histopathological diagnosis (Bosman 1999).

Based on these studies, we hypothesize that there is a corresponding change in mechanical properties of nuclei of cancer cells when compared to normal cells.

Another common feature in cancer cell nuclei is their enlarged size compared to those of normal cell (Mihailovic, Dordevic et al. 1999). Studies have shown that the nucleus plays an import role in the mechanical properties of the whole cell (Caille, Thoumine et al. 2002; Zink, Fischer et al. 2004; Deguchi, Maeda et al. 2005). While in the context of cancer metastasis, cancer cells migrate and traverse in blood vessels and small capillaries, the whole cell and its nucleus undergoes extremely large deformation, as shown in the *in vivo* study (Yamauchi, Yang et al. 2005) and also our

microfluidic study which mimics the process of cancer cells traversing small capillaries (Hou, Li et al. 2009). Therefore for cancer cells, their enlarged and structurally modified nuclei could play a more significant role in contribution to their mechanical behavior and subsequently the outcome of metastasis.

Therefore it is important to characterize the mechanical properties of cancer cell nucleus, as it will contribute not only towards understanding of the structural change of nuclei in malignant transformation and subsequent cancer detection, but also shed light on their contribution to cell mechanics and its role in cancer metastasis.

However, as reviewed in chapter 2, so far no studies have been done to investigate the nuclear mechanics in the context of cancer cells. In this chapter, AFM indentation was used to characterize the elasticity of isolated nuclei of benign (MCF-10A) and cancerous (MCF-7) human breast epithelial cells. The underlying lamina (lamin A/C) structure of both cell types was also investigated by confocal microscopy to understand its possible contribution to the mechanical property of nucleus. The decrease in elasticity of nuclei of malignant cells compared with non-malignant cells gives us a quantitative biomarker to assist cancer detection. Also it provides us with a better insight in terms of contribution of nucleus to cell mechanics.

6.2 Materials and methods

6.2.1 Cell culture

Cell culture was the same as that described in section 3.2.1. Cells harvested from the subculture were seeded and kept in a 6-well microplate which was then placed in the incubator for 2–3 days until confluent before nuclear isolation. The medium was changed one day after seeding to clear any dead cells.

6.2.2 Nuclear isolation

The procedure is adapted from (Thoumine, Ott et al. 1999; Caille, Thoumine et al. 2002):

1. Confluent MCF-7 (or MCF-10A) cells grown in 6-well chamber are rinsed once with PBS.

2. Cells are treated for 5 min with 1 ml of a 0.01% Igepal CA-630 (a non-ionic detergent, Sigma), 1% citric acid solution in water. Nuclei are expelled while the cytomatrix remains adherent.

3. The medium is collected, mixed with 5 ml PBS, and centrifuged at 300 *g* for 5 min.

4. The nuclei-rich pellet is resuspended in PBS, 60 to 100 μl suspended nuclei solution was dropped onto a 12 mm coverslip for 1h and the nuclei will stick to the coverslip.

(A)   (B)
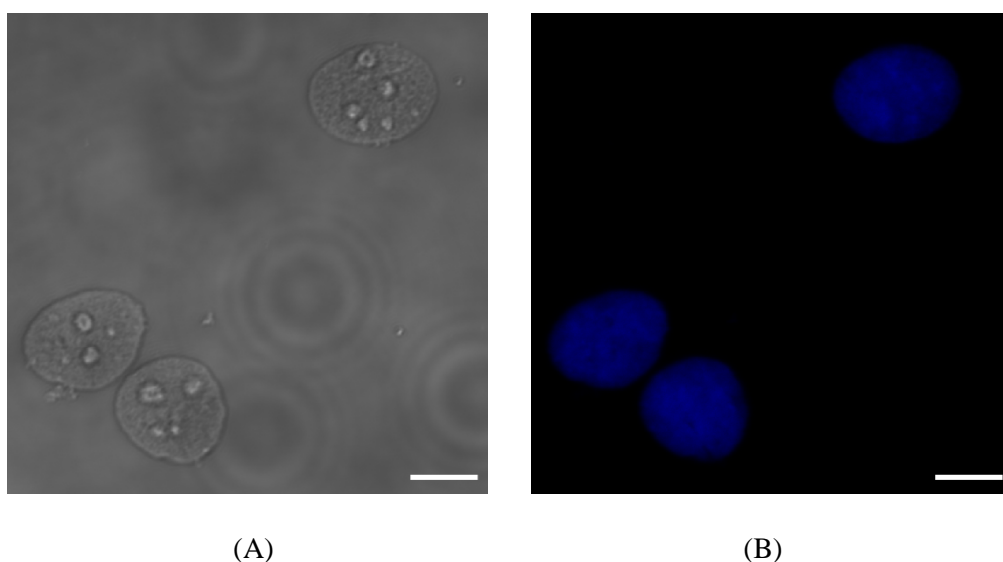
Fig. 6.1 (A) Bright field and (B) fluorescence image (DNA stained with DAPI) of isolated nuclei (MCF-7).

As shown in Fig. 6.1, isolated nuclei with DNA stained using DAPI showed that the nuclear isolation procedure is reliable to get clean and intact isolated nuclei.

6.2.3 Confocal fluorescence imaging

For fluorescence staining, coverslips with isolated nucleus seeded on them were fixed by cold methonal for ten minutes at -20°C. After washing with PBS, the samples were incubated with Image-iT FX signal enhancer (Invitrogen) for 30 minutes at room temperature, and followed by incubation with 10% goat serum for 1 h at room temperature. Then samples were incubated with primary antibody rabbit polyclonal lamin A/C (H-110) (Santa Cruz, USA) for 1 h at room temperature, and followed by incubation with secondary antibody Alexa Fluor 488 goat anti-rabbit IgG for 1 h at room temperature. Finally samples were labeled with 5μg/ml DAPI (Sigma-Aldrich, USA) for 5 minutes. Fluorescence images were taken using a confocal microscope (Nikon TE2000, Japan).

6.2.4 AFM indentation and data analysis

For indentation studies, isolated nuclei were seeded onto a 12mm coverslip and incubated at room temperature for 1 hour for the nuclei to adhere to the substrate. For AFM indentation on isolated nuclei (as shown in Fig. 6.2), the same protocol as AFM indentation on cells was used, as details in section 5.2.3. For indentation data analysis, refer to section 5.2.4.
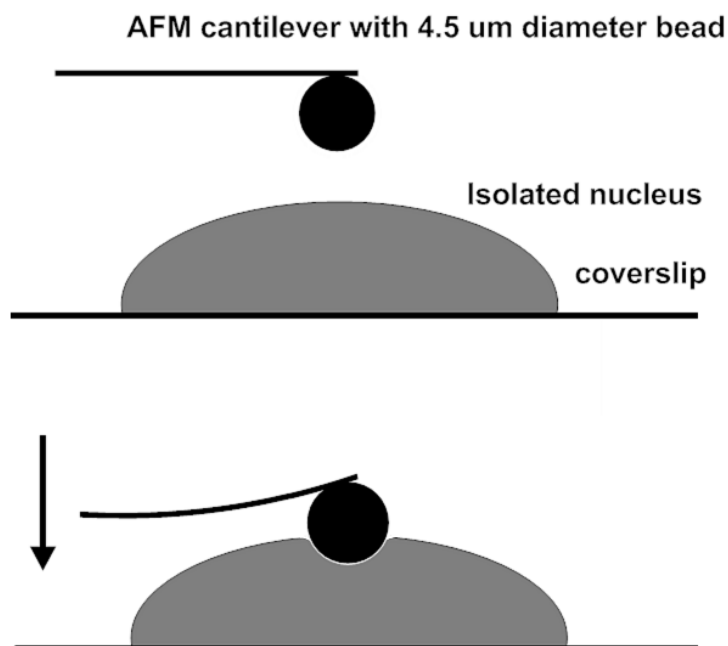
Fig. 6.2 Schematic of AFM indentation on an isolated nucleus using a 4.5 µm diameter spherical probe.

6.3 Results and discussion

6.3.1 Consistency of AFM indentation on isolated nucleus

To test the consistency of our AFM indentation on nucleus, we repeatedly indent the same location of the nucleus and see whether there is any change in the force-indentation depth curve. Fig. 6.3 shows that the force-indentation depth curves for both MCF-10A and MCF-7 highly overlap with each other after repeatedly indentation at 0.3Hz for more than fifteen times. These results suggest that our experiment is highly reproducible and that there is no permanent damage or plastic deformations induced by the AFM probe. Also these results suggest that nuclei behave generally in an elastic manner within the condition of our test, which is consistent with other studies (Guilak, Tedrow et al. 2000). Interestingly, the reproducibility was still maintained even when we used very large force (0.8 nN indetation force with about 1µm indentation depth). However, the current Hertz's

model that we have used will not apply to large deformation (the large deformation region deviate from Hertz's model prediction). So for better comparison, we chose to extract the apparent elastic modulus based on the region below 200 pN, which is the same as that for the whole cell indentation.
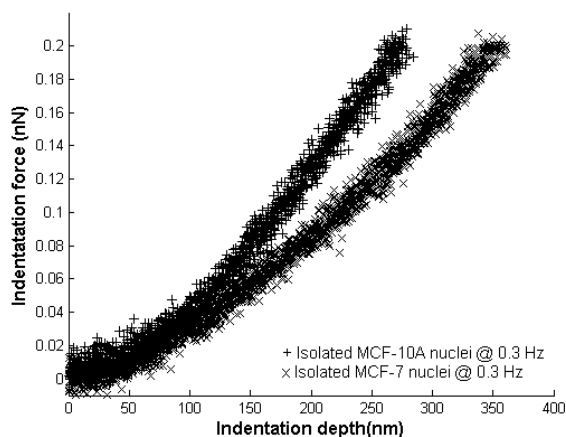
Fig. 6.3 Indentation force versus depth curve of repeated indentations (n=20) at the same location of an isolated nucleus using the same force (0.2 nN).
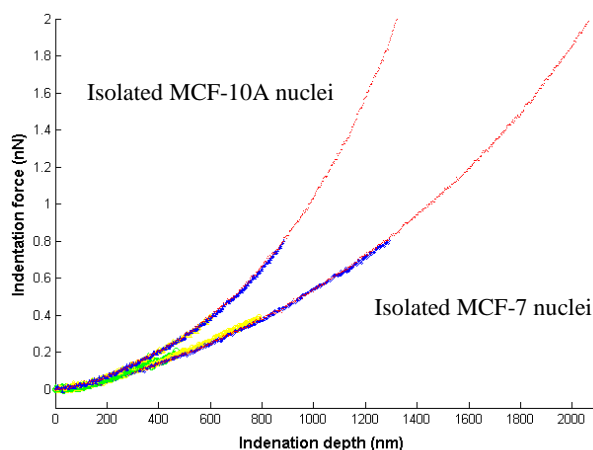
Fig. 6.4 Indentation force versus depth curve of repeated indentations (n=20) at the same location of a isolated MCF-7 nucleus using increasing force (0.2, 0.4, 0.8, 2 nN) and at 0.3 Hz.

As shown in Fig. 6.4 repeated indentation using increasing force again confirmed the reproducibility of AFM indentation as there is no hysteresis in force-depth curves. We can also see that isolated nuclei of MCF-7 appear more deformable than that of MCF-

10A, as less deformation of the formers compared with the later using the same indentation force.

6.3.2 Apparent Young's modulus of isolated nucleus of MCF-7 and MCF-10A

Based on the above analysis, we extracted the apparent Young's modulus and compare between MCF-10A and MCF-7. As shown in Fig. 6.5, we can see that at different loading rates, MCF-10A nuclei appear twice stiffer than MCF-7 nuclei. A Student's t-test assuming unequal variance was used to check that the differences between MCF-10A and MCF-7 nuclei were indeed significant ($p < 0.01$). Also apparent Young's modulus increases with the loading rate due to the viscoelastic nature of nucleus, which is also reported in other studies (Guilak, Tedrow et al. 2000; Dahl, Engler et al. 2005). The distinct difference in deformability of isolated nucleus of MCF-10A and MCF-7 can serve as an indicator to differentiate cancer cells from normal cells.
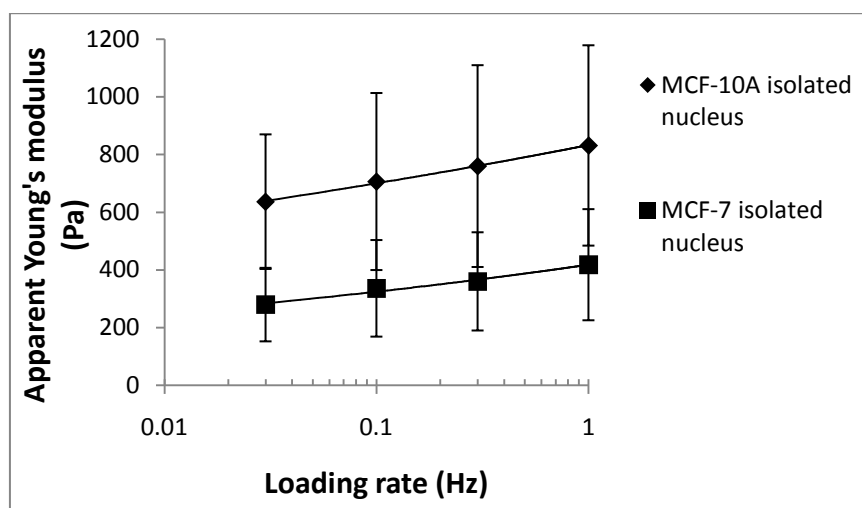
Fig. 6.5 Comparison between apparent Young's modulus of isolated nucleus of MCF-10A and MCF-7.

6.3.3 Lamin A/C structure of nucleus

To understand the possible reason underlying the difference in the mechanical property of nucleus of MCF-10A and MCF-7, we stained and investigated the lamin A/C structure of isolated nucleus of both types of cells. Lamin A/C was chosen as studies have shown that they play an important role in determining nuclear mechanics (Lammerding, Fong et al. 2006). Aberrant localization and reduction in expression of lamins A/C were observed in many malignancies (Prokocimer, Margalit et al. 2006). Many studies have reported that there is reduction in lamin A/C expression during malignant transformation of different types of cells (Kaufmann, Mabry et al. 1991; Broers, Raymond et al. 1993; Machiels, Ramaekers et al. 1997; Venables, McLean et al. 2001; Oguchi, Sagara et al. 2002; Coradeghini, Barboro et al. 2006) including breast cancer (Moss, Krivosheyev et al. 1999). All these reasons make lamin A/C a most promising target structure which might contribute to the difference that we have observed between the stiffness of isolated nuclei of MCF-10A and MCF-7. As shown in Fig. 6.6, lamin A/C is uniformly distributed at the peripheral region of isolated nucleus of MCF-10A, while not for MCF-7. Especially, we have also analyzed the intensity profile of one typical section of the fluorescence image. In isolated nucleus of MCF-10A, there is high concentration of lamin A/C at the peripheral region than inside. While in isolated nucleus of MCF-7, the level of intensity is lower compared with that of MCF-10A and it is not highly concentrated at the peripheral. Generally, lamin A/C of isolated nucleus of MCF-10A has higher intensity and higher concentration at the peripheral region than that of MCF-7, which might contribute to their difference in stiffness.

(A)   (B)
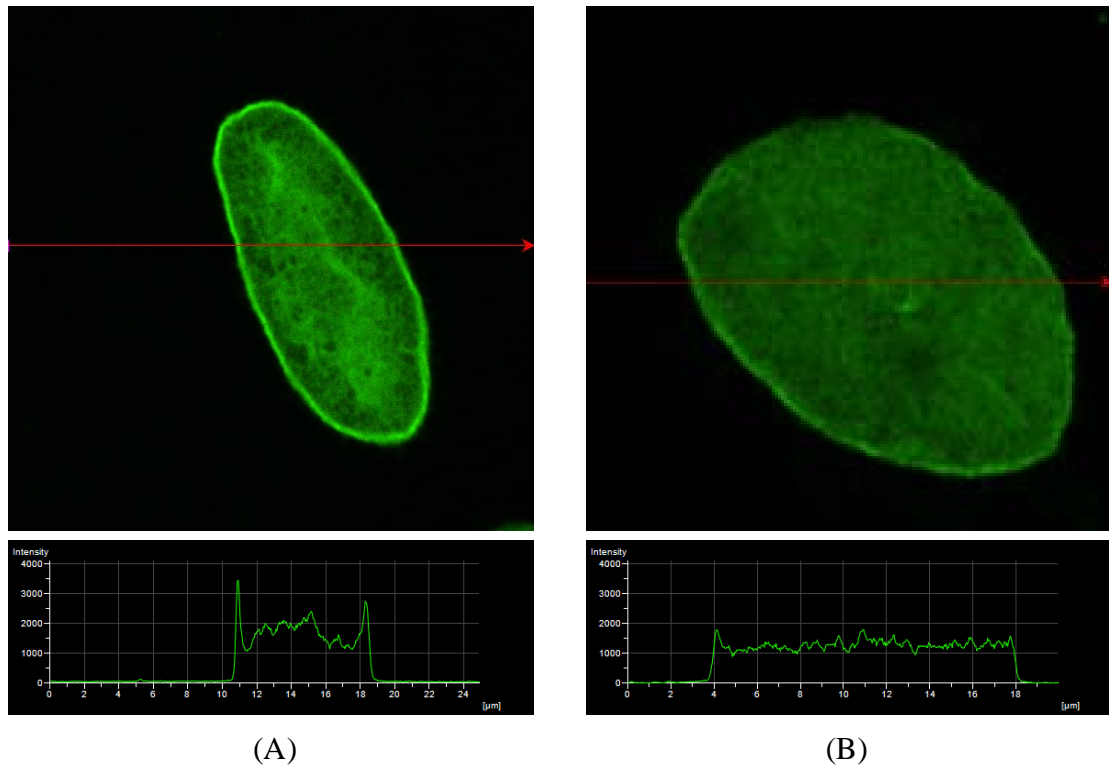
Fig. 6.6 Lamin A/C structure of isolated nucleus of (A) MCF-10A and (B) MCF-7 (intensity profile corresponds to the line section of fluorescence image).

However, another possible reason is the chromatin inside the nucleus as studies have shown that it is a force-bearing element inside the nucleus (Dahl, Engler et al. 2005). Therefore, the internal structural change including chromatin and associated proteins during malignant transformation might also contribute to the observed difference in deformability, which needs further studies.

6.3.4 Comparison with whole cell indentation

Most interestingly, as we compare apparent Young's modulus of isolated nuclei with our previous results on that of the cells in chapter 5, we found that the stiffness we characterized for the nuclei was very close to the cell. As shown in Fig. 6.7, apparent Young's modulus of isolated nuclei is, in general, statistically insignificant compared to that of the cell for both MCF-10A and MCF-7, except for one isolated case of MCF-10A at 0.1 Hz. While most studies showed that stiffness of isolated nuclei is 4

to 10 times stiffer than the whole cell (cytoplasm) (Dong, Skalak et al. 1991; Maniotis, Chen et al. 1997; Guilak, Tedrow et al. 2000; Caille, Thoumine et al. 2002). So we believe in our previous cell indentation experiments, the nuclei inside the cell also contribute significantly to the mechanical property although it was measured under small deformation. However, the cytoskeleton (including cytoplasm) does contribute to cell mechanics in different aspects. As we can see the trend of increased apparent Young's modulus is higher in cell than in nucleus, which suggests that the cell is more viscous than the nucleus. Higher viscosity of the whole cells compared with the nuclei might contribute from cytoskeleton or cytoplasm. However, further studies including computational modeling is needed.
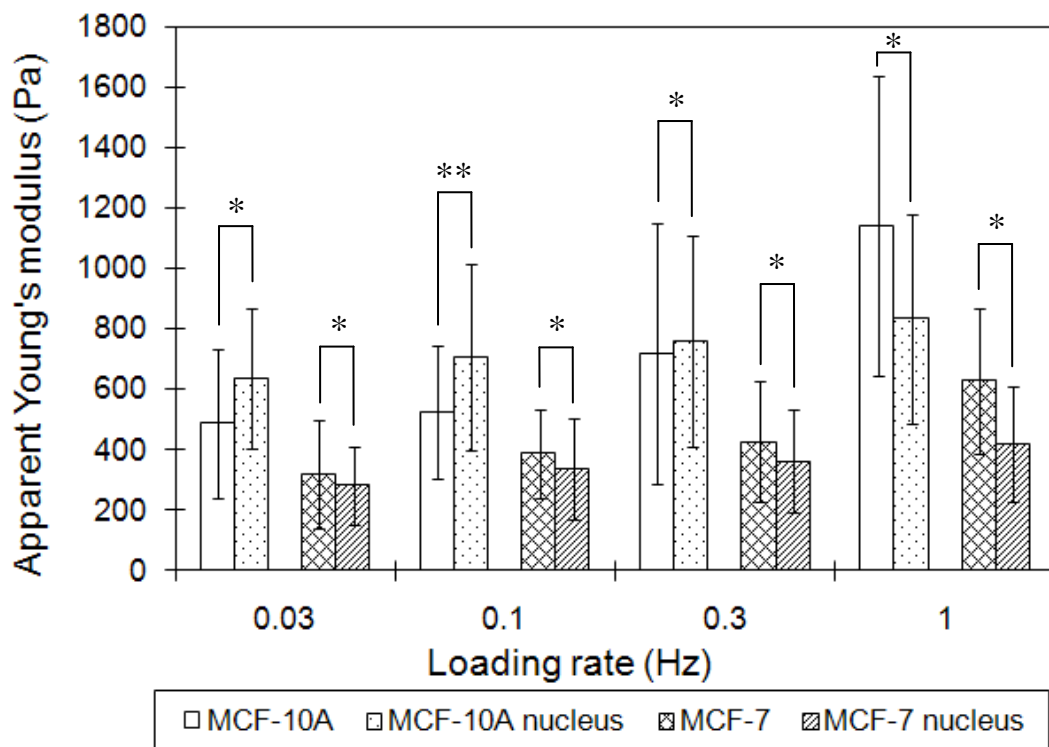
Fig. 6.7 Comparison between apparent Young's modulus of isolated nuclei and cells of both MCF-10A and MCF-7 (*: $p > 0.1$, **: $p < 0.05$, $N \approx 20$).

6.4 Conclusions

In the chapter, mechanical property of isolated nucleus of cancer cells was characterized using AFM indentation based on previous established protocol.

We reported for the first time that there is a decrease in elasticity of isolated nuclei of malignant breast cells compared with that of non-malignant ones. Considering the fact that absence or low levels of type A lamins are often observed in many types of human hematological malignancies, the related decrease of nuclear stiffness can be quite promising as a distinct feature of malignancy. Our study showed that characterization of mechanical properties of cancer nucleus using AFM is a robust method to distinguish malignant breast cells from nonmalignant ones. A method established by Beale in 1860 and used as a "gold standard" for detecting cancer is to examine unstained cell structure and look out for any variations in nuclear size and shape (Zink, Fischer et al. 2004). In our case, the possible change in mechanical properties of the nucleus can be a quantitative and more accurate method to help detect cancer. The application of this study for clinical samples has a high potential. Alteration in the composition of nuclear lamins and nuclear mechanics are potential novel targets for future anti-cancer therapy, which also provides a basis for development of new diagnostic tools.

In addition, more detailed information on the mechanical properties of the nucleus is needed to understand its role in mechanotransduction and its role in mechanical behavior of cancer cells may provide insight on the process of malignant transformation and metastasis.

It is interesting to see that the stiffness of the isolated nuclei is very close to the stiffness of the cells characterized using the same technique. However, there is a notable difference in their viscosity evident by their different response to the loading rates. In our previous study we have monitored the change in actin structure comparing two cell lines which contributes to their difference in mechanical property. But this study gives us a more comprehensive understanding about the contribution of underlying cellular structures to cell mechanics. Both nucleus and cytoskeleton (actin) contribute to cell mechanics but probably in different aspects. The nucleus might contribute more to the cell elasticity while the cytoskeleton (or cytoplasm) contributes to the viscous response of the cell. However, a more thorough understanding requires computational modeling.

Chapter 7 Conclusions and Future Work

This thesis focused on probing the structure-mechanical property relationship of breast cancer cells (MCF-7 and MCF-10A). These cancer cells at different physiological conditions including suspension and adherent condition were studied using different techniques including microfluidics, micropipette aspiration and AFM. Besides actin structure, which is considered as a major contributor to cell mechanics, the importance of another internal cellular component nucleus, which also contributes to cancer cell mechanical behavior especially in the context of cancer metastasis, was proposed and investigated.

7.1 Conclusions

Malignant breast epithelial cells (MCF-7) were found almost twice more deformable than non-malignant breast epithelial cells (MCF-10A) both at suspended and adherent state, which might facilitate easier migration through tissues and endothelial barrier and traversing through small capillaries.

There is a distinct difference in the actin structure of MCF-10A and MCF-7, both at suspended and adherent conditions. In suspended condition, MCF-10A has a thicker and concentrated actin cortex than MCF-7. While in adherent condition, MCF-10A was found to have significantly more actin stress fibers than MCF-7 especially on the top layer of the cell.

Temperature was found to have a significant effect on cellular mechanical properties. As temperature increase from room temperature to physiological temperature (37 ºC), both MCF-7 and MCF-10A become more deformable.

Isolated nuclei of MCF-7 were found twice more deformable than that of MCF-10A and there is corresponding change in the lamin A/C distribution, which might be used as another quantitative biomarker for cancer detection.

Both the whole cell and isolated nucleus of MCF-7 were found to be twice more deformable than that of MCF-10A, and apparent elastic modulus of nucleus characterized by AFM indentation was very close to that of the whole cell, which is different from other reports. Both these facts suggest that nucleus also play a significant role in contributing to the overall cancer cell mechanics.

As breast epithelial cells become malignant, both cytoskeletal structure (actin) and nuclear structure (lamin A/C) undergoes significant changes, and both contribute to the overall deformability of cancer cells.

7.2 Future work

The work in this thesis points to better understanding about structure-mechanical property relationship of cancer cell mechanics, which is the contribution of internal organelle nucleus to overall cellular mechanical behavior in the context of cancer metastasis. Moreover, it also gives potential applications in cancer detection and diagnosis. Future work can include the following:

1. Computational modeling to systematically study the contribution of different cellular components, especially the nucleus to overall cell mechanics. To understand how the cytoskeleton and nucleus contribute specifically to cellular mechanical behavior in terms of elasticity and viscosity.

2. In view of the close connections between the cytoskeleton and nucleus, and that the mechanical property of nucleus is very close to that of the whole cell observed

in this work, how cytoskeleton and nucleus regulate each other and play a role in contributing to the overall cell mechanics and mechanotransduction.

3. We studied how nucleus contributes to the overall cell deformability when they are passively deformed by passing them through the microchannel. The fundamental and interesting question is how the nucleus adapts or deforms and affects migration when cells actively move through the tissues or endothelial barriers in the context of cancer metastasis.

4. Clinical studies on the mechanical properties of nuclei of cancer cells will further confirm the potential application of this study as a biomarker to help cancer detection and diagnosis.

References

A-Hassan, E., W. F. Heinz, M. D. Antonik, N. P. D'Costa, S. Nageswaran, C. A. Schoenenberger and J. H. Hoh (1998). "Relative microelastic mapping of living cells by atomic force microscopy." Biophys. J. **74**(3): 1564-1578.

Alberts, B., A. Johnson, J. Lewis, M. Raff, K. Roberts and P. Walter (2002). Molecular biology of the cell New York, Garland Science.

Alcaraz, J., L. Buscemi, M. Grabulosa, X. Trepat, B. Fabry, R. Farre and D. Navajas (2003). "Microrheology of human lung epithelial cells measured by atomic force microscopy." Biophysical Journal **84**(3): 2071-2079.

Ananthakrishnan, R., J. Guck, F. Wottawah, S. Schinkinger, B. Lincoln, M. Romeyke, T. Moon and J. Kas (2006). "Quantifying the contribution of actin networks to the elastic strength of fibroblasts." Journal of Theoretical Biology **242**(2): 502-516.

Barberaguillem, E., A. Alonsovarona and F. Vidalvanaclocha (1989). "Selective Implantation and Growth in Rats and Mice of Experimental Liver Metastasis in Acinar Zone-One." Cancer Research **49**(14): 4003-4010.

Benzeev, A. (1984). "The Cytoskeleton in cancer cells." Biochimica Et Biophysica Acta **780**(3): 197-212.

Bosman, F. T. (1999). "The nuclear matrix in pathology." Virchows Arch **435**(4): 391-9.

Boudreau, N. and M. J. Bissell (1998). "Extracellular matrix signaling: integration of form and function in normal and malignant cells." Current Opinion in Cell Biology **10**(5): 640-646.

Braet, F., C. Seynaeve, R. De Zanger and E. Wisse (1998). "Imaging surface and submembranous structures with the atomic force microscope: a study on living cancer cells, fibroblasts and macrophages." J Microsc **190**(Pt 3): 328-38.

Braet, F. and E. Wisse (2004). "Imaging surface and submembranous structures in living cells with the atomic force microscope: notes and tricks." Methods Mol Biol **242**: 201-16.

Broers, J. L., H. J. Kuijpers, C. Ostlund, H. J. Worman, J. Endert and F. C. Ramaekers (2005). "Both lamin A and lamin C mutations cause lamina instability as well as loss of internal nuclear lamin organization." Exp Cell Res **304**(2): 582-92.

Broers, J. L., Y. Raymond, M. K. Rot, H. Kuijpers, S. S. Wagenaar and F. C. Ramaekers (1993). "Nuclear A-type lamins are differentially expressed in human lung cancer subtypes." Am J Pathol **143**(1): 211-20.

Broers, J. L. V., E. A. G. Peeters, H. J. H. Kuijpers, J. Endert, C. V. C. Bouten, C. W. J. Oomens, F. P. T. Baaijens and F. C. S. Ramaekers (2004). "Decreased mechanical stiffness in LMNA-/- cells is caused by defective nucleo-cytoskeletal integrity: implications for the development of laminopathies." Human Molecular Genetics **13**(21): 2567-2580.

Bushell, G. R., C. Cahill, F. M. Clarke, C. T. Gibson, S. Myhra and G. S. Watson (1999). "Imaging and force-distance analysis of human fibroblasts in vitro by atomic force microscopy." Cytometry **36**(3): 254-264.

Caille, N., O. Thoumine, Y. Tardy and J. J. Meister (2002). "Contribution of the nucleus to the mechanical properties of endothelial cells." J Biomech **35**(2): 177-87.

Cameron, M. D., E. E. Schmidt, N. Kerkvliet, K. V. Nadkarni, V. L. Morris, A. C. Groom, A. F. Chambers and I. C. MacDonald (2000). "Temporal progression

of metastasis in lung: Cell survival, dormancy, and location dependence of metastatic inefficiency." Cancer Research **60**(9): 2541-2546.

Canetta, E., A. Duperray, A. Leyrat and C. Verdier (2005). "Measuring cell viscoelastic properties using a force-spectrometer: Influence of protein-cytoplasm interactions." Biorheology **42**(5): 321-333.

Chambers, A. F., A. C. Groom and I. C. MacDonald (2002). "Dissemination and growth of cancer cells in metastatic sites." Nature Reviews Cancer **2**(8): 563-572.

Chaw, K. C., M. Manimaran, F. E. H. Tay and S. Swaminathan (2006). "A quantitative observation and imaging of single tumor cell migration and deformation using a multi-gap microfluidic device representing the blood vessel." Microvascular Research **72**(3): 153-160.

Chen, B., Q. Wang and L. Han (2004). "Using the atomic force microscope to observe and study the ultrastructure of the living BIU-87 cells of the human bladder cancer." Scanning **26**(4): 162-166.

Chen, C. S., M. Mrksich, S. Huang, G. M. Whitesides and D. E. Ingber (1997). "Geometric control of cell life and death." Science **276**(5317): 1425-1428.

Chen, Z. Z., S. Y. Zhang, Z. M. Tang, P. F. Xiao, X. Y. Guo and Z. H. Lu (2006). "Pool-dam structure based microfluidic devices for filtering tumor cells from blood mixtures." Surface and Interface Analysis **38**(6): 996-1003.

Chien, S., K. L. Sung, R. Skalak, S. Usami and A. Tozeren (1978). "Theoretical and experimental studies on viscoelastic properties of erythrocyte membrane." Biophysical Journal **24**(2): 463-487.

Coradeghini, R., P. Barboro, A. Rubagotti, F. Boccardo, S. Parodi, G. Carmignani, C. D'Arrigo, E. Patrone and C. Balbi (2006). "Differential expression of nuclear lamins in normal and cancerous prostate tissues." Oncol Rep **15**(3): 609-13.

Costa, K. D. (2003). "Single-cell elastography: Probing for disease with the atomic force microscope." Dis. Markers **19**(2-3): 139-154.

Costa, K. D. (2006). "Imaging and probing cell mechanical properties with the atomic force microscope." Methods Mol Biol **319**: 331-61.

Costa, K. D., A. J. Sim and F. C. P. Yin (2006). "Non-Hertzian approach to analyzing mechanical properties of endothelial cells probed by atomic force microscopy." J. Biomech. Eng.-Trans. ASME **128**(2): 176-184.

Costa, K. D. and F. C. P. Yin (1999). "Analysis of indentation: Implications for measuring mechanical properties with atomic force microscopy." Journal of Biomechanical Engineering-Transactions of the Asme **121**(5): 462-471.

Crick, S. L. and F. C. P. Yin (2007). "Assessing micromechanical properties of cells with atomic force microscopy: importance of the contact point." Biomech. Model. Mechanobiol. **6**(3): 199-210.

Cross, S. E., Y.-S. Jin, J. Rao and J. K. Gimzewski (2007). "Nanomechanical analysis of cells from cancer patients." Nat. Nano. **2**(12): 780-783.

Cunningham, C. C., J. B. Gorlin, D. J. Kwiatkowski, J. H. Hartwig, P. A. Janmey, H. R. Byers and T. P. Stossel (1992). "Actin-binding protein requirement for cortical stability and efficient locomotion." Science **255**(5042): 325-327.

Dahl, K. N., A. J. Engler, J. D. Pajerowski and D. E. Discher (2005). "Power-law rheology of isolated nuclei with deformation mapping of nuclear substructures." Biophys. J. **89**(4): 2855-2864.

Dahl, K. N., S. M. Kahn, K. L. Wilson and D. E. Discher (2004). "The nuclear envelope lamina network has elasticity and a compressibility limit suggestive of a molecular shock absorber." J Cell Sci **117**(Pt 20): 4779-86.

Dahl, K. N., A. J. Ribeiro and J. Lammerding (2008). "Nuclear shape, mechanics, and mechanotransduction." Circ Res **102**(11): 1307-18.

Dahl, K. N., P. Scaffidi, M. F. Islam, A. G. Yodh, K. L. Wilson and T. Misteli (2006). "Distinct structural and mechanical properties of the nuclear lamina in Hutchinson-Gilford progeria syndrome." Proceedings of the National Academy of Sciences of the United States of America **103**(27): 10271-10276.

Davie, J. R., S. K. Samuel, V. A. Spencer, L. T. Holth, D. N. Chadee, C. P. Peltier, J. M. Sun, H. Y. Chen and J. A. Wright (1999). "Organization of chromatin in cancer cells: role of signalling pathways." Biochem Cell Biol **77**(4): 265-75.

Deguchi, S., K. Maeda, T. Ohashi and M. Sato (2005). "Flow-induced hardening of endothelial nucleus as an intracellular stress-bearing organelle." J Biomech **38**(9): 1751-1759.

Desprat, N., A. Richert, J. Simeon and A. Asnacios (2005). "Creep function of a single living cell." Biophysical Journal **88**(3): 2224-2233.

Dimitriadis, E. K., F. Horkay, J. Maresca, B. Kachar and R. S. Chadwick (2002). "Determination of elastic moduli of thin layers of soft material using the atomic force microscope." Biophys. J. **82**(5): 2798-810.

Ding, L., M. Sunamura, T. Kodama, J. Yamauchi, D. G. Duda, H. Shimamura, K. Shibuya, K. Takeda and S. Matsuno (2001). "In vivo evaluation of the early events associated with liver metastasis of circulating cancer cells." British Journal of Cancer **85**(3): 431-438.

Dong, C., R. Skalak and K. L. P. Sung (1991). "Cytoplasmic Rheology of Passive Neutrophils." Biorheology **28**(6): 557-567.

Du, Z., K. H. Cheng, M. W. Vaughn, N. L. Collie and L. S. Gollahon (2007). "Recognition and capture of breast cancer cells using an antibody-based platform in a microelectromechanical systems device." Biomedical Microdevices **9**(1): 35-42.

Elson, E. L. (1988). "Cellular mechanics as an indicator of cytoskeletal structure and function." Annu. Rev. Biophys. Biophys. Chem. **17**: 397-430.

Enns, A. E., P. Gassmann, K. Schluter, T. Korb, H. U. Spiegel, N. Senninger and J. Haier (2004). "Integrins can directly mediate metastatic tumor cell adhesion within the liver sinusoids." Journal of Gastrointestinal Surgery **8**(8): 1049-1059.

Fabry, B., G. N. Maksym, J. P. Butler, M. Glogauer, D. Navajas and J. J. Fredberg (2001). "Scaling the microrheology of living cells." Physical Review Letters **8714**(14).

Faivre, M., M. Abkarian, K. Bickraj and H. A. Stone (2006). "Geometrical focusing of cells in a microfluidic device: An approach to separate blood plasma." Biorheology **43**(2): 147-159.

Fuchs, E. and K. Weber (1994). "Intermediate filaments - structure, dynamics, function, and disease." Annual Review of Biochemistry **63**: 345-382.

Gabor, H. and L. Weiss (1985). "Mechanically induced trauma suffered by cancer cells in passing through pores in polycarbonate membranes." Invasion Metastasis **5**(2): 71-83.

Gassmann, P., A. Enns and J. Haier (2004). "Role of tumor cell adhesion and migration in organ-specific metastasis formation." Onkologie **27**(6): 577-582.

Guck, J., R. Ananthakrishnan, H. Mahmood, T. J. Moon, C. C. Cunningham and J. Kas (2001). "The optical stretcher: a novel laser tool to micromanipulate cells." Biophysical Journal **81**(2): 767-784.

Guck, J., R. Ananthakrishnan, T. J. Moon, C. C. Cunningham and J. Kas (2000). "Optical deformability of soft biological dielectrics." Physical Review Letters **84**(23): 5451-5454.

Guck, J., S. Schinkinger, B. Lincoln, F. Wottawah, S. Ebert, M. Romeyke, D. Lenz, H. M. Erickson, R. Ananthakrishnan, D. Mitchell, J. Kas, S. Ulvick and C. Bilby (2005). "Optical deformability as an inherent cell marker for testing malignant transformation and metastatic competence." Biophys. J. **88**(5): 3689-3698.

Guilak, F. (2000). "The deformation behavior and viscoelastic properties of chondrocytes in articular cartilage." Biorheology **37**(1-2): 27-44.

Guilak, F., J. R. Tedrow and R. Burgkart (2000). "Viscoelastic properties of the cell nucleus." Biochemical and Biophysical Research Communications **269**(3): 781-786.

Gupta, G. P. and J. Massague (2006). "Cancer metastasis: Building a framework." Cell **127**(4): 679-695.

Hart, I. R. (1982). "'Seed and soil' revisited: mechanisms of site-specific metastasis." Cancer Metastasis Rev **1**(1): 5-16.

Heidemann, S. R., P. Lamoureaux and R. E. Buxbaum (2000). "Opposing views on tensegrity as a structural framework for understanding cell mechanics." J. Appl. Physiol. **89**(4): 1670-1678.

Henderson, E. (1994). "Imaging of Living Cells by Atomic-Force Microscopy." Progress in Surface Science **46**(1): 39-60.

Henderson, E., P. G. Haydon and D. S. Sakaguchi (1992). "Actin filament dynamics in living glial cells imaged by atomic force microscopy." Science **257**(5078): 1944-6.

Hochmuth, R. M. (2000). "Micropipette aspiration of living cells." Journal of Biomechanics **33**(1): 15-22.

Hofmann, U. G., C. Rotsch, W. J. Parak and M. Radmacher (1997). "Investigating the cytoskeleton of chicken cardiocytes with the atomic force microscope." J. Struct. Biol. **119**(2): 84-91.

Hoh, J. H. and C. A. Schoenenberger (1994). "Surface-Morphology and Mechanical-Properties of Mdck Monolayers by Atomic-Force Microscopy." J Cell Sci **107**: 1105-1114.

Holth, L. T., D. N. Chadee, V. A. Spencer, S. K. Samuel, J. R. Safneck and J. R. Davie (1998). "Chromatin, nuclear matrix and the cytoskeleton: role of cell structure in neoplastic transformation (review)." Int J Oncol **13**(4): 827-37.

Hou, H. W., Q. S. Li, G. Y. H. Lee, A. P. Kumar, C. N. Ong and C. T. Lim (2009). "Deformability study of breast cancer cells using microfluidics." Biomedical Microdevices **11**(3): 557-564.

Houben, F., F. C. Ramaekers, L. H. Snoeckx and J. L. Broers (2007). "Role of nuclear lamina-cytoskeleton interactions in the maintenance of cellular strength." Biochim Biophys Acta **1773**(5): 675-86.

Huang, S. and D. E. Ingber (1999). "The structural and mechanical complexity of cell-growth control." Nature Cell Biology **1**(5): E131-E138.

Ingber, D. E. (2000). "Opposing views on tensegrity as a structural framework for understanding cell mechanics." J. Appl. Physiol. **89**(4): 1663-70.

Janmey, P. A. (1998). "The cytoskeleton and cell signaling: Component localization and mechanical coupling." Physiological Reviews **78**(3): 763-781.

Jemal, A., T. Murray, E. Ward, A. Samuels, R. C. Tiwari, A. Ghafoor, E. J. Feuer and M. J. Thun (2005). "Cancer statistics, 2005." CA Cancer J. Clin. **55**(1): 10-30.

Johnson, M. D., J. A. Torri, M. E. Lippman and R. B. Dickson (1999). "Regulation of motility and protease expression in PKC-mediated induction of MCF-7 breast cancer cell invasiveness." Experimental Cell Research **247**(1): 105-113.

Jones, W. R., H. P. Ting-Beall, G. M. Lee, S. S. Kelley, R. M. Hochmuth and F. Guilak (1999). "Alterations in the Young's modulus and volumetric properties of chondrocytes isolated from normal and osteoarthritic human cartilage." Journal of Biomechanics **32**(2): 119-127.

Katsantonis, J., A. Tosca, S. B. Koukouritaki, P. A. Theodoropoulos, A. Gravanis and C. Stournaras (1994). "Differences in the G/total actin ratio and microfilament stability between normal and malignant human keratinocytes." Cell Biochemistry and Function **12**(4): 267-274.

Kaufmann, S. H., M. Mabry, R. Jasti and J. H. Shaper (1991). "Differential expression of nuclear envelope lamins A and C in human lung cancer cell lines." Cancer Res **51**(2): 581-6.

Kieran, M. W. and B. M. Longenecker (1983). "Organ specific metastasis with special reference to avian systems." Cancer Metastasis Rev **2**(2): 165-82.

Kim, Y. C., S. J. Park and J. K. Park (2008). "Biomechanical analysis of cancerous and normal cells based on bulge generation in a microfluidic device." Analyst **133**(10): 1432-9.

Knight, M. M., J. Bravenboer, D. A. Lee, G. van Osch, H. Weinans and D. L. Bader (2002). "Cell and nucleus deformation in compressed chondrocyte-alginate constructs: temporal changes and calculation of cell modulus." Biochimica Et Biophysica Acta-General Subjects **1570**(1): 1-8.

Konety, B. R. and R. H. Getzenberg (1999). "Nuclear structural proteins as biomarkers of cancer." J Cell Biochem **Suppl 32-33**: 183-91.

Krishnan, V., S. M. Bane, P. D. Kawle, K. N. Naresh and R. D. Kalraiya (2005). "Altered melanoma cell surface glycosylation mediates organ specific adhesion and metastasis via lectin receptors on the lung vascular endothelium." Clinical & Experimental Metastasis **22**(1): 11-24.

Kumar, S., I. Z. Maxwell, A. Heisterkamp, T. R. Polte, T. P. Lele, M. Salanga, E. Mazur and D. E. Ingber (2006). "Viscoelastic retraction of single living stress fibers and its impact on cell shape, cytoskeletal organization, and extracellular matrix mechanics." Biophysical Journal **90**(10): 3762-3773.

Kuznetsova, T. G., M. N. Starodubtseva, N. I. Yegorenkov, S. A. Chizhik and R. I. Zhdanov (2007). "Atomic force microscopy probing of cell elasticity." Micron **38**(8): 824-33.

Lammerding J, D. K., Discher, DE, and Kamm RD. (2007). "Nuclear Mechanics and Methods." Methods in Cell Biology **83**: 269-294.

Lammerding, J., L. G. Fong, J. Y. Ji, K. Reue, C. L. Stewart, S. G. Young and R. T. Lee (2006). "Lamins A and C but not lamin B1 regulate nuclear mechanics." J Biol Chem **281**(35): 25768-80.

Lammerding, J. and R. T. Lee (2005). "The nuclear membrane and mechanotransduction: impaired nuclear mechanics and mechanotransduction in lamin A/C deficient cells." Novartis Found Symp **264**: 264-73; discussion 273-8.

Lammerding, J., P. C. Schulze, T. Takahashi, S. Kozlov, T. Sullivan, R. D. Kamm, C. L. Stewart and R. T. Lee (2004). "Lamin A/C deficiency causes defective nuclear mechanics and mechanotransduction." Journal of Clinical Investigation **113**(3): 370-378.

Le Grimellec, C., E. Lesniewska, M. C. Giocondi, E. Finot, V. Vie and J. P. Goudonnet (1998). "Imaging of the surface of living cells by low-force contact-mode atomic force microscopy." Biophys. J. **75**(2): 695-703.

Lee, G. Y. H. and C. T. Lim (2007). "Biomechanics approaches to studying human diseases." Trends Biotechnol. **25**(3): 111-8.

Lee, W. G., H. Bang, H. Yun, J. Lee, J. Park, J. K. Kim, S. Chung, K. Cho, C. Chung, D. C. Han and J. K. Chang (2007). "On-chip erythrocyte deformability test under optical pressure." Lab on a Chip **7**(4): 516-519.

Legrimellec, C., E. Lesniewska, C. Cachia, J. P. Schreiber, F. Defornel and J. P. Goudonnet (1994). "Imaging of the Membrane-Surface of Mdck Cells by Atomic-Force Microscopy." Biophys. J. **67**(1): 36-41.

Lekka, M., P. Laidler, D. Gil, J. Lekki, Z. Stachura and A. Z. Hrynkiewicz (1999). "Elasticity of normal and cancerous human bladder cells studied by scanning force microscopy." Eur. Biophys. J. **28**(4): 312-6.

Lekka, M., P. Laidler, J. Ignacak, M. Labedz, J. Lekki, H. Struszczyk, Z. Stachura and A. Z. Hrynkiewicz (2001). "The effect of chitosan on stiffness and glycolytic activity of human bladder cells." Biochim. Biophys. Acta **1540**(2): 127-36.

Lekka, M., J. Lekki, M. Marszalek, P. Golonka, Z. Stachura, B. Cleff and A. Z. Hrynkiewicz (1999). "Local elastic properties of cells studied by SFM." Appl. Surf. Sci. **141**(3-4): 345-349.

Lieber, S. C., N. Aubry, J. Pain, G. Diaz, S. J. Kim and S. F. Vatner (2004). "Aging increases stiffness of cardiac myocytes measured by atomic force microscopy nanoindentation." Am. J. Physiol.-Heart Circul. Physiol. **287**(2): H645-H651.

Lim, C. T., E. H. Zhou, A. Li, S. R. K. Vedula and H. X. Fu (2006 a). "Experimental techniques for single cell and single molecule biomechanics." Mater. Sci. Eng. C-Biomimetic Supramol. Syst. **26**(8): 1278-1288.

Lim, C. T., E. H. Zhou and S. T. Quek (2006 b). "Mechanical models for living cells - A review." J. Biomech. **39**(2): 195-216.

Lincoln, B., H. M. Erickson, S. Schinkinger, F. Wottawah, D. Mitchell, S. Ulvick, C. Bilby and J. Guck (2004). "Deformability-based flow cytometry." Cytometry Part A **59A**(2): 203-209.

Lincoln, B., S. Schinkinger, K. Travis, F. Wottawah, S. Ebert, F. Sauer and J. Guck (2007). "Reconfigurable microfluidic integration of a dual-beam laser trap with biomedical applications." Biomedical Microdevices **9**(5): 703-710.

Lodish, H., A. Berk, S. L. Zipurksy, P. Matsudaira, D. Baltimore and J. E. Darnell (2003). Molecular cell biology. New York, W.H. Freeman and Company.

Lulevich, V., T. Zink, H. Y. Chen, F. T. Liu and G. Y. Liu (2006). "Cell mechanics using atomic force microscopy-based single-cell compression." Langmuir **22**(19): 8151-8155.

Machiels, B. M., F. C. Ramaekers, H. J. Kuijpers, J. S. Groenewoud, J. W. Oosterhuis and L. H. Looijenga (1997). "Nuclear lamin expression in normal testis and testicular germ cell tumours of adolescents and adults." J Pathol **182**(2): 197-204.

Mahaffy, R. E., S. Park, E. Gerde, J. Kas and C. K. Shih (2004). "Quantitative analysis of the viscoelastic properties of thin regions of fibroblasts using atomic force microscopy." Biophys. J. **86**(3): 1777-93.

Maksym, G. N., B. Fabry, J. P. Butler, D. Navajas, D. J. Tschumperlin, J. D. Laporte and J. J. Fredberg (2000). "Mechanical properties of cultured human airway smooth muscle cells from 0.05 to 0.4 Hz." Journal of Applied Physiology **89**(4): 1619-1632.

Maniotis, A. J., C. S. Chen and D. E. Ingber (1997). "Demonstration of mechanical connections between integrins cytoskeletal filaments, and nucleoplasm that stabilize nuclear structure." Proceedings of the National Academy of Sciences of the United States of America **94**(3): 849-854.

McGrath, J. L. and C. F. Dewey (2006). Cell dynamics and the actin cytoskeleton, Cambridge University Press.

McNally, H. A. and R. Ben Borgens (2004). "Three-dimensional imaging of living and dying neurons with atomic force microscopy." Journal of Neurocytology **33**(2): 251-258.

Meaburn, K. J. and T. Misteli (2007). "Cell biology: Chromosome territories." Nature **445**(7126): 379-381.

Mihailovic, D., B. Dordevic and V. Mihailovic (1999). "Nuclear volume in type I gastric intestinal metaplasia." Anal Quant Cytol Histol **21**(2): 143-4.

Moloney, M., L. McDonnell and H. O'Shea (2004). "Atomic force microscopy of BHK-21 cells: an investigation of cell fixation techniques." Ultramicroscopy **100**(3-4): 153-161.

Mook, O. R. F., J. Van Marle, H. Vreeling-Sindelarova, R. Jonges, W. M. Frederiks and C. J. F. Van Noorden (2003). "Visualization of early events in tumor formation of eGFP-transfected rat colon cancer cells in liver." Hepatology **38**(2): 295-304.

Morris, V. L., I. C. Macdonald, S. Koop, E. E. Schmidt, A. F. Chambers and A. C. Groom (1993). "Early Interactions of Cancer-Cells with the Microvasculature in Mouse-Liver and Muscle During Hematogenous Metastasis - Videomicroscopic Analysis." Clinical & Experimental Metastasis **11**(5): 377-390.

Moss, S. F., V. Krivosheyev, A. de Souza, K. Chin, H. P. Gaetz, N. Chaudhary, H. J. Worman and P. R. Holt (1999). "Decreased and aberrant nuclear lamin expression in gastrointestinal tract neoplasms." Gut **45**(5): 723-9.

Moustakas, A. and C. Stournaras (1999). "Regulation of actin organisation by TGF-beta in H-ras-transformed fibroblasts." Journal of Cell Science **112**(8): 1169-1179.

Muys, J., M. Alkaisi, D. Melville, J. Nagase, P. Sykes, G. Parguez and J. Evans (2006). "Cellular transfer and AFM imaging of cancer cells using Bioimprint." J Nanobiotechnology **4**: 1.

Nagayama, K. and T. Matsumoto (2008). "Contribution of actin filaments and microtubules to quasi-in situ tensile properties and internal force balance of cultured smooth muscle cells on a substrate." Am J Physiol Cell Physiol **295**(6): C1569-1578.

Nyland, L. R. and D. W. Maughan (2000). "Morphology and transverse stiffness of Drosophila myofibrils measured by atomic force microscopy." Biophys. J. **78**(3): 1490-7.

Oguchi, M., J. Sagara, K. Matsumoto, T. Saida and S. Taniguchi (2002). "Expression of lamins depends on epidermal differentiation and transformation." Br J Dermatol **147**(5): 853-8.

Ohashi, T., M. Hagiwara, D. L. Bader and M. M. Knight (2006). "Intracellular mechanics and mechanotransduction associated with chondrocyte deformation during pipette aspiration." Biorheology **43**(3-4): 201-214.

Park, S., D. Koch, R. Cardenas, J. Kas and C. K. Shih (2005). "Cell motility and local viscoelasticity of fibroblasts." Biophys. J. **89**(6): 4330-4342.

Parnaik, V. K. and K. Manju (2006). "Laminopathies: multiple disorders arising from defects in nuclear architecture." J Biosci **31**(3): 405-21.

Pesen, D. and J. H. Hoh (2005). "Micromechanical architecture of the endothelial cell cortex." Biophys J **88**(1): 670-9.

Pietrasanta, L. I., A. Schaper and T. M. Jovin (1994). "Imaging subcellular structures of rat mammary carcinoma cells by scanning force microscopy." J Cell Sci **107 (Pt 9)**: 2427-37.

Prokocimer, M., A. Margalit and Y. Gruenbaum (2006). "The nuclear lamina and its proposed roles in tumorigenesis: projection on the hematologic malignancies and future targeted therapy." J. Struct. Biol. **155**(2): 351-60.

Radmacher, M., M. Fritz, C. M. Kacher, J. P. Cleveland and P. K. Hansma (1996). "Measuring the viscoelastic properties of human platelets with the atomic force microscope." Biophys. J. **70**(1): 556-67.

Rao, K. M. and H. J. Cohen (1991). "Actin cytoskeletal network in aging and cancer." Mutation Research **256**: 139-148.

Roca-Cusachs, P., I. Almendros, R. Sunyer, N. Gavara, R. Farre and D. Navajas (2006). "Rheology of passive and adhesion-activated neutrophils probed by atomic force microscopy." Biophysical Journal **91**(9): 3508-3518.

Rosenbluth, M. J., W. A. Lam and D. A. Fletcher (2006). "Force microscopy of nonadherent cells: a comparison of leukemia cell deformability." Biophys. J. **90**(8): 2994-3003.

Rotsch, C., F. Braet, E. Wisse and M. Radmacher (1997). "AFM imaging and elasticity measurements on living rat liver macrophages." Cell Biol. Int. **21**(11): 685-696.

Rotsch, C., K. Jacobson and M. Radmacher (1999). "Dimensional and mechanical dynamics of active and stable edges in motile fibroblasts investigated by using atomic force microscopy." Proc. Natl. Acad. Sci. U. S. A. **96**(3): 921-926.

Rotsch, C. and M. Radmacher (2000). "Drug-induced changes of cytoskeletal structure and mechanics in fibroblasts: an atomic force microscopy study." Biophys. J. **78**(1): 520-35.

Rowat, A. C., J. Lammerding and J. H. Ipsen (2006). "Mechanical properties of the cell nucleus and the effect of emerin deficiency." Biophys. J. **91**(12): 4649-4664.

Sato, M., M. J. Levesque and R. M. Nerem (1987). "An application of the micropipette technique to the measurement of the mechanical properties of cultured bovine aortic endothelial cells." Journal of Biomechanical Engineering **109**(1): 27-34.

Scaffidi, P. and T. Misteli (2006). "Lamin A-dependent nuclear defects in human aging." Science **312**(5776): 1059-63.

Schmid-Schonbein, G. W., K. L. Sung, H. Tozeren, R. Skalak and S. Chien (1981). "Passive mechanical properties of human leukocytes." Biophysical Journal **36**(1): 243-256.

Shelby, J. P., J. White, K. Ganesan, P. K. Rathod and D. T. Chiu (2003). "A microfluidic model for single-cell capillary obstruction by Plasmodium falciparum infected erythrocytes." Proceedings of the National Academy of Sciences of the United States of America **100**(25): 14618-14622.

Shevkoplyas, S. S., T. Yoshida, S. C. Gifford and M. W. Bitensky (2006). "Direct measurement of the impact of impaired erythrocyte deformability on microvascular network perfusion in a microfluidic device." Lab on a Chip **6**(7): 914-920.

Simon, M. S., D. Ibrahim, L. Newman and M. Stano (2002). "Efficacy and economics of hormonal therapies for advanced breast cancer." <u>Drugs & Aging</u> **19**(6): 453-463.

Sinniah, K., J. Paauw and J. Ubels (2002). "Investigating live and fixed epithelial and fibroblast cells by atomic force microscopy." <u>Current Eye Research</u> **25**(1): 61-68.

Smith, B. A., B. Tolloczko, J. G. Martin and P. Grutter (2005). "Probing the viscoelastic behavior of cultured airway smooth muscle cells with atomic force microscopy: Stiffening induced by contractile agonist." <u>Biophysical Journal</u> **88**(4): 2994-3007.

Smith, B. A., B. Tolloczko, J. G. Martin and P. Grutter (2005). "Probing the viscoelastic behavior of cultured airway smooth muscle cells with atomic force microscopy: Stiffening induced by contractile agonist." <u>Biophys. J.</u> **88**(4): 2994-3007.

Sommoggy, S., H. J. Wiendl, M. Schwabe and G. Blumel (1975). "Electronic volume analysis of cell nuclei in the gastric mucosa." <u>Langenbecks Arch Chir</u> **Suppl**: 239-43.

Spencer, V. A. and J. R. Davie (2000). "Signal transduction pathways and chromatin structure in cancer cells." <u>J Cell Biochem Suppl</u> **Suppl 35**: 27-35.

Stewart, C. L., K. J. Roux and B. Burke (2007). "Blurring the boundary: the nuclear envelope extends its reach." <u>Science</u> **318**(5855): 1408-12.

Stuurman, N., S. Heins and U. Aebi (1998). "Nuclear lamins: their structure, assembly, and interactions." <u>J Struct Biol</u> **122**(1-2): 42-66.

Sugarbaker, E. (1981). "Patterns of metastasis in human malignancies." <u>Cancer Biol Rev</u> **2**: 385-390.

Sugitate, T., T. Kihara, X.-Y. Liu and J. Miyake (2009). "Mechanical role of the nucleus in a cell in terms of elastic modulus." <u>Current Applied Physics</u> **In Press, Corrected Proof**.

Sun, D. G., J. H. Wang, W. J. Yao, L. Gu, Z. Y. Wen and C. Shu (2004). "Tumorigenesis of murine erythroleukemia cell line transfected with exogenous p53 gene." <u>Clinical Hemorheology and Microcirculation</u> **30**(2): 117-126.

Suresh, S. (2007). "Biomechanics and biophysics of cancer cells." <u>Acta Biomater</u> **3**(4): 413-38.

Suresh, S., J. Spatz, J. P. Mills, A. Micoulet, M. Dao, C. T. Lim, M. Beil and T. Seufferlein (2005). "Connections between single-cell biomechanics and human disease states: gastrointestinal cancer and malaria." <u>Acta Biomaterialia</u> **1**(1): 15-30.

Sutton, N., M. C. Tracey, I. D. Johnston, R. S. Greenaway and M. W. Rampling (1997). "A novel instrument for studying the flow behaviour of erythrocytes through microchannels simulating human blood capillaries." <u>Microvascular Research</u> **53**(3): 272-281.

Tait, L., H. D. Soule and J. Russo (1990). "Ultrastructural and Immunocytochemical Characterization of an Immortalized Human Breast Epithelial-Cell Line, Mcf-10." <u>Cancer Research</u> **50**(18): 6087-6094.

Tan, S. J., L. Yobas, G. Y. Lee, C. N. Ong and C. T. Lim (2009). "Microdevice for the isolation and enumeration of cancer cells from blood." <u>Biomed Microdevices</u>.

Tatsuo Ushiki, S. Y., Jiro Hitomi, Shigeaki Ogura, Takeshi Umemoto and Masatsugu Shigeno2 (2000). "Atomic force microscopy of living cells." Jpn. J. Appl. Phys. : 4.

Theret, D. P., M. J. Levesque, M. Sato, R. M. Nerem and L. T. Wheeler (1988). "The Application of a homogeneous half-space model in the analysis of endothelial-cell micropipette measurements." Journal of Biomechanical Engineering - Transactions of the ASME **110**(3): 190-199.

Thoumine, O. and A. Ott (1997). "Comparison of the mechanical properties of normal and transformed fibroblasts." Biorheology **34**(4-5): 309-326.

Thoumine, O., A. Ott, O. Cardoso and J. J. Meister (1999). "Microplates: a new tool for manipulation and mechanical perturbation of individual cells." Journal of Biochemical and Biophysical Methods **39**(1-2): 47-62.

Trepat, X., M. Grabulosa, L. Buscemi, F. Rico, R. Farre and D. Navajas (2005). "Thrombin and histamine induce stiffening of alveolar epithelial cells." Journal of Applied Physiology **98**(4): 1567-1574.

Trickey, W. R., F. P. T. Baaijens, T. A. Laursen, L. G. Alexopoulos and F. Guilak (2006). "Determination of the Poisson's ratio of the cell: recovery properties of chondrocytes after release from complete micropipette aspiration." J Biomech **39**(1): 78-87.

Tseng, Y., J. S. H. Lee, T. P. Kole, I. Jiang and D. Wirtz (2004). "Micro-organization and visco-elasticity of the interphase nucleus revealed by particle nanotracking." J Cell Sci **117**(10): 2159-2167.

Ushiki, T., J. Hitomi, T. Umemoto, S. Yamamoto, H. Kanazawa and M. Shigeno (1999). "Imaging of living cultured cells of an epithelial nature by atomic force microscopy." Arch Histol Cytol **62**(1): 47-55.

Van Vliet, K. J., G. Bao and S. Suresh (2003). "The biomechanics toolbox: experimental approaches for living cells and biomolecules." Acta Materialia **51**(19): 5881-5905.

Vaziri, A., H. Lee and M. R. K. Mofrad (2006). "Deformation of the cell nucleus under indentation: Mechanics and mechanisms." Journal of Materials Research **21**(8): 2126-2135.

Vaziri, A. and M. R. K. Mofrad (2007). "Mechanics and deformation of the nucleus in micropipette aspiration experiment." Journal of Biomechanics **40**(9): 2053-2062.

Venables, R. S., S. McLean, D. Luny, E. Moteleb, S. Morley, R. A. Quinlan, E. B. Lane and C. J. Hutchison (2001). "Expression of individual lamins in basal cell carcinomas of the skin." Br J Cancer **84**(4): 512-9.

Wang, Q., D. Lee, V. Sysounthone, R. A. S. Chandraratna, S. Christakos, R. Korah and R. Wieder (2001). "1,25-dihydroxyvitamin D-3 and retonic acid analogues induce differentiation in breast cancer cells with function- and cell-specific additive effects." Breast Cancer Research and Treatment **67**(2): 157-168.

Ward, K. A., W. I. Li, S. Zimmer and T. Davis (1991). "Viscoelastic properties of transformed cells: role in tumor cell progression and metastasis formation." Biorheology **28**(3-4): 301-13.

Weyn, B., W. Kalle, S. Kumar-Singh, E. Van Marck, H. Tanke and W. Jacob (1998). "Atomic force microscopy: influence of air drying and fixation on the morphology and viscoelasticity of cultured cells." Journal of Microscopy-Oxford **189**: 172-180.

Wottawah, F., S. Schinkinger, B. Lincoln, S. Ebert, K. Muller, F. Sauer, K. Travis and J. Guck (2005). "Characterizing single suspended cells by optorheology." <u>Acta Biomater</u> **1**(3): 263-71.

Wu, Z., G. Zhang, K. Shao, M. Long, H. Wang, G. Song, B. Wang and S. Cai (2001). "Investigation on the rheological properties of hepatocellular carcinoma cells and their relevance to cytoskeleton structure." **9**(1): 25-7.

Wu, Z., G. Zhang, X. Wang, G. Song, H. Wang, M. Long, S. Cai and Y. Wu (1997). "Investigation on the viscoelastic properties of hepatocytes and their relavances to cytoskeleton structure." <u>Sheng Wu Yi Xue Gong Cheng Xue Za Zhi</u> **14**(2): 111-4.

Wu, Z. Z., G. Zhang, M. Long, H. B. Wang, G. B. Song and S. X. Cai (2000). "Comparison of the viscoelastic properties of normal hepatocytes and hepatocellular carcinoma cells under cytoskeletal perturbation." <u>Biorheology</u> **37**(4): 279-290.

Yamauchi, K., M. Yang, P. Jiang, N. Yamamoto, M. X. Xu, Y. Amoh, K. Tsuji, M. Bouvet, H. Tsuchiya, K. Tomita, A. R. Moossa and R. M. Hoffman (2005). "Real-time in vivo dual-color imaging of intracapillary cancer cell and nucleus deformation and migration." <u>Cancer Research</u> **65**(10): 4246-4252.

Yao, W. J., L. Gu, D. G. Sun, W. B. Ka, Z. Y. Wen and S. Chien (2003). "Wild type p53 gene causes reorganization of cytoskeleton and, therefore, the impaired deformability and difficult migration of murine erythroleukemia cells." <u>Cell Motility and the Cytoskeleton</u> **56**(1): 1-12.

Zhang, G., M. Long, Z. Z. Wu and W. Q. Yu (2002). "Mechanical properties of hepatocellular carcinoma cells." <u>World J. Gastroenterol.</u> **8**(2): 243-246.

Zhao, R., J. F. Antaki, T. Naik, T. N. Bachman, M. V. Kameneva and Z. J. J. Wu (2006). "Microscopic investigation of erythrocyte deformation dynamics." <u>Biorheology</u> **43**(6): 747-765.

Zhou, E. H. (2006). "Experimental and numerical studies on the viscoelastic behavior of living cells." <u>PhD Thesis</u>: National University of Singapore.

Zhou, E. H., C. T. Lim and S. T. Quek (2005). "Finite element simulation of the micropipette aspiration of a living cell undergoing large viscoelastic deformation." Mechanics of Advanced Materials and Structures 12(6): 501-512.

Zink, D., A. H. Fischer and J. A. Nickerson (2004). "Nuclear structure in cancer cells." Nat Rev Cancer 4(9): 677-87.

Appendix Curriculum Vitae

Li Qingsen

PhD Candidate in Department of Mechanical Engineering and

Nano Biomechanics Lab, Department of Bioengineering

National University of Singapore, 1 Engineering Drive 2, Singapore 117576

Email: qingsen@nus.edu.sg

Profile

Trained as an Engineer, passion in Biology. Expertise in Atomic Force Microscopy, confocal microscopy, micropipette aspiration, design and fabrication of microfluidic device. With strong interest in nuclear mechanics and related mechanotransduction. Ready to communicate and collaborate with multidiscipline researchers. Passionate in creative ideas with deep analytical and thinking ability.

CURRENT RESEARCH INTERESTS

Understand nuclear structure and its role in mechanotrasduction in the context of whole cell, to bridge the mechanical signal pathway from the cellular level to the nucleus, down to molecular level in effect of gene regulation.

Education

➢ **Sept. 1999 to June 2003**

 B.Sc in Engineering Mechanics, Huazhong University of Science & Technology (HUST), China

 Excellent Graduate of HUST

➢ **Sept. 2001 to January 2002**

Bioengineering (elective course), Wuhan University, China

- **Sept. 2003 to June 2005**

  M.Sc in Solid Mechanics, Huazhong University of Science & Technology, China

  Thesis: Finite element modeling on molecular structure of carbon nanospring

- **Sept. 2005 to present**

  Ph.D. in Mechanical Engineering, National University of Singapore, Singapore

  - ✓ *In vitro* study of breast cancer cells transversing through capillary-like microenvironment using microfluidics (developed an auto balanced static pressure system with better precision).
  - ✓ Characterization of mechanical properties of suspended breast cancer cells using micropipette aspiration.
  - ✓ Investigation on mechanical properties of adherent breast cancer cells and their underlying cytoskeletal structure using AFM and confocal microscopy.
  - ✓ Isolation of breast cancer nucleus and investigation on its structure and mechanical properties and its contribution to cell mechanics.

Awards

- **December 2002** First-Class National Scholarship of China
- **June 2003**   Excellent Graduate of HUST
- **February 2008**   Best Poster Award, 3rd MRS-S Conference on Advanced Materials

Publications

1. Li, Q.S., G.Y. Lee, C.N. Ong, and C.T. Lim, AFM indentation study of breast cancer cells. Biochem Biophys Res Commun, 2008. 374(4): p. 609-13.

2. Hou, H.W., Q.S. Li, G.Y.H. Lee, A.P. Kumar, C.N. Ong, and C.T. Lim, Deformability study of breast cancer cells using microfluidics. Biomedical Microdevices, 2009. 11(3): p. 557-564.

3. Fong Yew Leong, Qingsen Li, Chwee Teck Lim, K.-H. Chiam, Modeling of cell entry into a micro-channel. (Submitted)

4. Li, Q.S., B.P. Ting, G.Y. Lee, C.N. Ong, and C.T. Lim, Micropipette aspiration of tumor breast cells. (Prepared for submission)

5. Li, Q.S., C.N. Ong, and C.T. Lim, Nuclear mechanics as a biomarker for cancer detection. (In preparation)

6. Q. S. Li, G.Y.H.L., C. N. Ong and C. T. Lim, Probing the Elasticity of Breast Cancer Cells Using AFM. 13th International Conference on Biomedical Engineering, 2009. 23: p. 2122-2125.

7. S.R.K. Vedula, E. Mendoz, Sun Wei, T.S. Lim, A. Li, Q.S. Li, and C.T. Lim, Human cell as a structure and machine – An engineering perspective, IES Journal Part A: Civil and Structural Engineering, 2009.